ELS HEINSALU

Normal and anomalously slow diffusion under external fields

The study was carried out at the Institute of Theoretical Physics, University of Tartu, Institut of Physics, University of Augsburg, and Department of Physics, University of Camerino.

The Dissertation was admitted on May 2, 2008 in partial fulfilment of the requirements for the degree of Doctor of Philosophy (theoretical physics), and allowed for defence by the Council of the Insitute of Physics, University of Tartu.

Contents

List of publications

The thesis is based on the following papers:

I   E. Heinsalu, R. Tammelo, T. Örd, *Diffusion and current of Brownian particles in tilted piecewise linear potentials: Amplification and coherence*, Phys. Rev. E **69**, 021111 (2004).

II E. Heinsalu, R. Tammelo, T. Örd, *Correlation between diffusion and coherence in the Brownian motion on tilted periodic potential*, Physica A **340**, 292 (2004).

III E. Heinsalu, T. Örd, R. Tammelo, *Diffusion and coherence in tilted piecewise linear double-periodic potentials*, Phys. Rev. E **70**, 041104 (2004).

IV E. Heinsalu, T. Örd, R. Tammelo, *Peculiarities of Brownian motion depending on the structure of the periodic potentials*, Acta Physica Polonica B **36**, 1613 (2005).

V   M. Patriarca, P. Szelestey, E. Heinsalu, *Brownian model of dissociated dislocations*, Acta Physica Polonica B **36**, 1745 (2005).

VI T. Örd, E. Heinsalu, R. Tammelo, *Suppression of diffusion by a weak external field in periodic potentials*, Eur. Phys. J. B **47**, 275 (2005).

VII I. Goychuk, E. Heinsalu, M. Patriarca, G. Schmid, P. Hänggi, *Current and universal scaling in anomalous transport*, Phys. Rev. E **73**, 020101(R) (2006).

VIII E. Heinsalu, M. Patriarca, I. Goychuk, G. Schmid, P. Hänggi, *Fractional Fokker-Planck dynamics: Numerical algorithm and simulations*, Phys. Rev. E **73**, 046133 (2006).

IX E. Heinsalu, M. Patriarca, I. Goychuk, P. Hänggi, *Fractional diffusion in periodic potentials*, J. Phys.: Condens. Matter **19**, 065114 (2007).

X   E. Heinsalu, M. Patriarca, I. Goychuk, P. Hänggi, *Use and Abuse of a Fractional Fokker-Planck Dynamics for Time-Dependent Driving*, Phys. Rev. Lett. **99**, 120602 (2007).

XI E. Heinsalu, M. Patriarca, F. Marchesoni, *Dimer diffusion in a washboard potential*, Phys. Rev. E **77**, 021129 (2008).

List of other publications:

1. M. Patriarca, A. Chakraborti, E. Heinsalu, G. Germano, *Relaxation in statistical many-agent economy models*, Eur. Phys. J. B **57**, 219 (2007).

Invited talks:

1. *Anomalously slow diffusion in force fields*, 10 April 2008, University of Perugia, Department of Physics, Perugia, Italy.

Presentations at international conferences:

1. E. Heinsalu, R. Tammelo, T. Örd, *Correlation between diffusion and coherence in the Brownian motion in tilted periodic potential* (poster-presentation), NEXT2003, Second Sardinian International Conference on News and Expectations in Thermostatistics, 21-28 September, 2003, Villasimius, Italy.

2. E. Heinsalu, T. Örd, R. Tammelo, *Pecularities of Brownian motion in tilted double-periodic potentials* (poster-presentation), 17th Marian Smoluchowski Symposium on Statistical Physics, 4-9 September 2004, Zakopane, Poland.

3. M. Patriarca, P. Szelestey, E. Heinsalu, *Langevin description of dislocation dynamics* (poster-presentation), 17th Marian Smoluchowski Symposium on Statistical Physics, 4-9 September 2004, Zakopane, Poland.

4. E. Heinsalu, I. Goychuk, M. Patriarca, P. Hänggi, *Fractional diffusion in periodic potentials* (poster-presentation), XX Sitges Conference on Statistical Mechanics, Physical Biology: from Molecular Interactions to Cellular Behavior, 5-9 June 2006, Sitges, Spain.

5. E. Heinsalu, M. Patriarca, I. Goychuk, G. Schmid, P. Hänggi, *Recent results on fractional diffusion in space-periodic force fields* (oral and poster-presentations), XXXVI Winter Meeting on Statistical Physics, 9-12 January 2007, Taxco, Guerrero, Mexico.

6. E. Heinsalu, M. Patriarca, *Motion in washboard potentials: Dimer versus monomoer* (poster-presentation), XXXVI Winter Meeting on Statistical Physics, 9-12 January 2007, Taxco, Guerrero, Mexico.

3

7. E. Heinsalu, M. Patriarca, I. Goychuk, P. Hänggi, *Anomalously slow processes in alternating force fields* (poster-presentation), XXIII IU-PAP International Conferenc on Statistical Physics, 9-13 July, 2007, Genova, Italy.

8. E. Heinsalu, M. Patriarca, F. Marchesoni, *Diffusion of dimers in washboard potentials* (poster-presentation), XXIII IUPAP International Conferenc on Statistical Physics, 9-13 July, 2007, Genova, Italy.

9. E. Heinsalu, M. Patriarca, I. Goychuk, P. Hänggi, *Anomalously slow diffusion in time-dependent force fields* (poster-presentation), ISF-IAS Workshop 2008, Modeling Anomalous Diffusion and Relaxation: From Single Molecules to the Flight of the Albatross, 23-28 March, 2008, Jerusalem, Israel.

10. E. Heinsalu, M. Patriarca, I. Goychuk, P. Hänggi, *Anomalously slow diffusion in periodic potentials* (poster-presentation), ISF-IAS Workshop 2008, Modeling Anomalous Diffusion and Relaxation: From Single Molecules to the Flight of the Albatross, 23-28 March, 2008, Jerusalem, Israel.

Contributions to presentations at international conferences:

1. I. Goychuk, E. Heinsalu, M. Patriarca, G. Schmid, P. Hänggi, *Universal scaling in anomalous transport* (oral-presentation), German Physical Society Meeting, 27-31 March 2006, Dresden, Germany.

2. M. Patriarca, E. Heinsalu, A. Chakraborti, *Statistical Models of social systems* (oral-presentation), Third Annual Meeting COST ACTION P10 Physics of Risk, 13-16 May 2006, Vilnius, Lithuania.

3. M. Patriarca, A. Chakraborti, E. Heinsalu, G. Germano, *Many-agent models in economic and social sciences* (oral-presentation), APFA5, V Conference on the Applications of Physics in Financial Analysis, 29 June - 1 July 2006, Torino, Italy,

4. M. Patriarca, E. Heinsalu, A. Chakraborti, *Generalized Many-agent models of social systems* (oral-presentation), II Conference on Management of Risk Factors in economically relevant human activities, 31 August - 2 September 2006, Rome, Italy.

5. M. Patriarca, E. Heinsalu, *Influence of geography on language competition* (oral-presentation), GIACS-workshop, Languge Competition, 11-14 September 2006, Warsaw, Poland.

6. I. Goychuk, E. Heinsalu, M. Patriarca, G. Schmid, P. Hänggi, *Current, diffusion, and universal scaling in anomalous transport* (oral-presentation), Workshop on Nonlinear Physics of the German Physical Society, October 2006, Bayreuth, Germany.

Author's contribution to the papers on which the presented thesis is based, is the following:

Papers I-II: The author performed the analytical calculations, carried out the numerical study of the quantities of interest and participated in writing the paper.

Papers III-IV: The author performed the analytical calculations and carried out the numerical study of the quantities of interest; main person responsible for writing the paper.

Papers V-VI: The author contributed to the development of the model and participated in writing the paper.

Paper VII: The author contributed to the development of the numerical code, performed the numerical simulations and the analysis of the results and participated in writing the paper.

Paper VIII: The author contributed to the development of the numerical code and performed the numerical simulations and the analysis of the results; main person responsible for writing the paper.

Paper IX: The author suggested the problem investigated, performed the analytical calculations and the numerical simulations and the analysis of the results; main person responsible for writing the paper.

Paper X: The author suggested the problem investigated, contributed to the analytical calculations and to the development of the numerical code, performed the numerical simulations and the analysis of the results and participated in writing the paper.

Paper XI: The author contributed to the development of the numerical code and performed the numerical simulations and the analysis of the results; main person responsible for writing the paper.

1 Introduction

The first person to address the problem of diffusion was probably the German physiologist Adolf Fick, who was interested in the way water and nutrients travel through membranes in living organisms. In 1855 Fick published his diffusion laws [1,2]. He also showed that the mean-squared displacement of an object undergoing diffusion grows linearly in time. However, Fick's approach was purely phenomenological, based on an analogy with Fourier's heat equation. It took 50 years until Einstein derived the diffusion equation from first principles as a part of his work on Brownian motion [3,4].

In many systems, however, the mean square displacement of the Brownian particle does not grow linearly in time, but as t^α with $\alpha \neq 1$ [5]. Depending on the value of the anomalous diffusion exponent α the motion can be subdiffusive, i.e., slower than the normal diffusion, or superdiffusive, i.e., faster than the normal diffusion [6].

In the present thesis we study normal and anomalously slow diffusion on periodic substrates and subdiffusion under the action of a force alternating periodically in time. The original study consists of four parts, the first two focused on normal diffusion and the other two focused on processes with anomalously slow relaxation. In the first part we investigate the motion of non interacting Brownian particles in spatially periodic substrates in the presence and in the absence of an external bias (papers [I-IV, VI]) and in the second part the motion of dimers, consisting of two interacting Brownian particles, in washboard potentials (papers [V, XI]). In the third part we study processes with anomalously slow relaxation under the influence of forces that are periodic in space (papers [VII-IX]) and in the fourth part subdiffusion processes in the presence of time-dependent forces (paper [X]).

The problems investigated are of importance for various applications in physics, chemistry, nanotechnology, as well as molecular biology [7–11]. In particular, the problems involving normal diffusion on a periodic potential, besides describing a real Brownian particle, are of relevance in numerous other contexts such as superionic conductors [12–14] and the motion of fluxons in superconductors [15], Josephson junctions [16,17], weakly pinned charge-density-wave condensates [18], diffusion of atoms and molecules on crystal surfaces [19–23], particle separation by electrophoresis [24], rotating dipoles in external fields [25], rotation of molecules in solids [26], mode locking in laser gyroscopes [27], plasma accelerators [28], as well as biophysical processes such as neural activity and intracellular transport [29,30].

In a variety of processes involving transport in constrained geometries such as nanoporous materials and ion-channels, a subdiffusive behavior was observed on a finite time scale [31–34]. Anomalously slow transport can occur also due to the disordered character of the medium [5]; the prototype example is the movement of charge carriers in amorphous semiconductors.

Similarly, many biological systems, such as RNA polymerases, exonuclease and DNA polymerases, helicases, the motion of ribosomes along mRNA, the translocation of RNA or DNA through a pore, are advantageously described as particles moving along a disordered substrate, and are characterized by anomalously slow diffusion [5, 35, 36]. Furthermore, during the hydration process of macromolecules water is experimentally observed to undergo subdiffusion. At the same time, many biological systems as well as various condensed matter and artificial nanosystems exhibit (as an approximation) a periodic structure, thus requiring a study of anomalously slow transport processes in periodic force fields and the response to applied external fields.

For the investigation of the normal diffusion, the Langevin and Fokker-Planck equations are used. The anomalously slow diffusion is studied through the fractional Fokker-Planck dynamics and the continuous time random walk, i.e., within our approach we model the subdiffusive dynamics in terms of a suitable residence time probability density with a long tail [5, 36, 37] rather than through a random potential [5, 38, 39]. We employ both, analytical as well as numerical methods.

The structure of the thesis is the following: in Sec. 2 the general introduction to the theory of normal diffusion is made; in Sec. 3 Brownian motion in piecewise linear periodic potentials with one and two minima per period is investigated; in Sec. 4 the motion of dimers in a washboard potential is studied; in Sec. 5 the general introduction to the anomalous fractional diffusion is presented as well as a part of the original study on the numerical simulation of the fractional Fokker-Planck equation through the underlying continuous time random walk (paper [VIII]); in Sec. 6 we study subdiffusion under the action of a force periodic in space; in Sec. 7 processes with anomalously slow relaxation in the presence of a time-dependent force are investigated. Possible applications and motivation of the problems studied are presented and discussed more in detail at the beginning of each chapter, and at the end the conclusions are drawn. In Sec. 8 the summary is made.

4

2 Normal diffusion: Basic concepts

2.1 On the history of Brownian motion

The phenomenon known today as Brownian motion was first recorded probably by the Dutch physiologist and botanist Jan Ingenhousz, who in 1765 noted the irregular movement exhibited by motes of carbon dust in ethanol. In 1827 similar observations were made by Adolphe Brongniart and by Robert Brown, a Scottish-born botanist, whom the discovery is generally credited.

Having observed the unceasing motion of the pollen in water, Brown thought at first that the movement must be due to the living nature of the particles under observation. However, repeating the experiment with pollen kept in alcohol for several months and with non-organic particles, he observed the same results for particles of matter that he definitely considered to be non-alive [40, 41]. Thus, the explanation had to lie more on physical than biological grounds.

Brown was never able to adequately explain the nature of his finding: it remained a puzzle for a long time also for other scientists. Many physical hypotheses and explanations for Brownian motion were put forward, including electrical effects, polarity, surface tension, temperature gradients, etc. (see Ref. [42]).

The qualitative explanation of the Brownian motion as a kinetic phenomenon was proposed by several authors. An important experimental step, from which scientists could begin to consider the fundamental implications of Brownian motion, was made by Leon Gouy in the late 1880s. In a series of experiments he convincingly demonstrated that Brownian motion was a fundamental physical property of fluid matter [43–45]. Gouy verified previous reports of qualitative trends, such as the decrease of "vigour" of the observed motion with increasing particle size and increasing solvent viscosity (temperature). Gouy's conclusions may be summarized by the following seven points [46]:

- the motion is very irregular, composed of translations and rotations, and the trajectory appears to have no tangent;

- two particles appear to move independently, even when they approach one another to within a distance less than their diameter;

- the smaller the particle, the more active the motion;

- the composition and density of the particles have no effect on the motion;

- the less viscous the fluid, the more active the motion;

- the higher the temperature, the more active the motion;

- the motion never ceases.

In 1900 F. M. Exner undertook the first quantitative studies, measuring how the motion depends on the particle size and the solvent viscosity.

The first person to elaborate a consistent theory behind Brownian motion was Louis Bachelier, a French mathematician. In his PhD thesis, presented in 1900, Bachelier proposed the random walk as the fundamental model for financial time series [47–49], many decades before this idea became the basis for modern theoretical finance. He was apparently also the first to see the connection between discrete random walks and the continuous diffusion equation.

However, the term "random walk" was originally proposed by Karl Pearson in a letter titled *The Problem of the Random Walk*, sent to *Nature* in 1905 [50]. Pearson was interested in a solution of the following problem [50]:

> *A man starts from a point O and walks l yards in a straight line; he then turns through any angle whatever and walks another l yards in a second straight line. He repeats this process n times. I require the probability that after these n stretches he is at a distance between r and r + dr from his starting point, O.*

The letter was answered by Lord Rayleigh [51], who had already solved a more general form of this problem in 1880, in the context of sound waves in heterogeneous materials (see also [52]).

In the same year 1905, Albert Einstein completed his doctoral thesis, in which he discussed a statistical theory of liquid behavior based on the hypothesis of the existence of molecules. He later applied his kinetic-molecular theory to explain the phenomenon observed by Brown [3, 4, 53]. In particular, Einstein suggested that the random movements of particles suspended in a liquid are an effect of the random thermal agitation of the molecules that compose the surrounding liquid. In fact, in the work published in 1905 [3, 53] Einstein showed that the kinetic theory of heat predicts an unceasing motion of small suspended particles. However, he was not sure that the phenomenon discussed was exactly the Brownian motion, but considered this as a reasonable hypothesis. After publication of the work, Siedentopf and Gouy pointed out that the effect he discussed was really the Brownian motion, since not only the qualitative properties, but also the predicted orders of magnitude of the effect were correct, as discussed in the Einstein's second work in 1906 [4].

Einstein, in his analysis, connected the motion of the suspended particles with diffusion and showed that this diffusive behavior follows from three postulates:

(1) the particles considered do not interact with each other: their trajectories are independent;

(2) the motion of the particles lacks long-time memory: one can choose a time interval such that the displacements of the particle during two subsequent intervals are independent;

(3) the distribution of the particle displacements during the subsequent time intervals possesses at least two moments; moreover, for the force free situation this distribution is symmetric, i.e., it is an even function of the displacements.

The displacement of the particles can thus be considered as a result of many small, independent, equally distributed steps. The further development of his reasoning is very close to what is called now a Kramers-Moyal expansion [54–56]. That line of reasoning was also adopted by Smoluchowski, who, however, assumed a more radical approach based on combinatorics.

Marian von Smoluchowski, who had begun to work on the problem of Brownian motion around 1900 but did not publish until 1906, obtained essentially the same expression for the time dependence of displacement as Einstein, though with a numerically different coefficient [57] (later found by Langevin to be in error). Importantly, Smoluchowski countered one argument against the molecular origin of the irregular motion of large particles, which was that any molecular "impulse" could never give a strong enough push to generate the observed displacements. The error lies basically in assuming that a visible displacement must arise from a single collision. Unlike Einstein in his original paper, Smoluchowski also considered the experimental literature, making a clear unhesitating link between the diffusion theory and Brownian motion. Finally, Smoluchowski obtained an expression that directly predicted an exponential "sedimentation equilibrium" equivalent to the "aerostatic" law describing the variation of atmospheric pressure with height: the same sedimentation equilibrium measured later in the first experiments of Jean Perrin [46].

In 1908, Paul Langevin demonstrated a third derivation of the time dependence of the mean square displacement [58–60]. His derivation was spectacularly simple and direct compared to the others: Langevin equated forces on the colloidal particle, directly introducing a fluctuating random force to represent the impulses of the molecules, and using, as Einstein and Smoluchowski had done, a Stokesian description of the "opposing" frictional force due to the motion of the particle through the liquid. Through the theorem of the equipartition of kinetic energy the mean particle velocity was linked to the temperature and to Avogadro's number. Langevin obtained an expression consisting essentially of Einstein's diffusion term, plus a decaying exponential correction. This last term resolved what had been an

assumption in Einstein's method, that beyond some "Brownian time" (the characteristic decay time in the exponential term) the particle motion could be assumed completely "diffusive".

Early attempts to quantify anything in Brownian motion had met with great difficulties. In fact, before the parallel theoretical treatments of Einstein, Smoluchowski, and Langevin, the real problem was that the experimentalists did not know what to measure. But after 1905, theory guided experimentalists toward more meaningful measurements. The most decisive experiments in support of Einstein's theory on diffusion were carried out by French physicist Jean Perrin, who eventually won the Nobel Prize in physics in 1926. Furthermore, Perrin's published results of his empirical verification of Einstein's model of Brownian motion are widely credited for finally settling the century-long dispute about the atomic theory of John Dalton.

Motivated by the description of Brownian motion different but strongly interconnected approaches were to describe phenomena where the stochastic nature of the system plays a considerable role. The theoretical approaches of Einstein and Smoluchowski from one side and of Langevin from the other side, marked the two leading strategies to model fluctuation phenomena, the former based on the notion of probability densities, the latter based on the notion of stochastic trajectory. These approaches, refined from the physical and mathematical point of view, provide now the theoretical framework for analyzing both equilibrium and non-equilibrium processes on a mesoscopic scale.

2.2   Langevin description: Stochastic differential equations

If a particle of mass m is immersed in a fluid, a friction force will act on the particle. The simplest expression for such a friction or damping force F_f is given by Stoke's law,

$$F_f = -\eta v \,, \tag{2.1}$$

where v is the velocity of the particle and η is the viscous friction coefficient. Stoke's law is valid if the particle is so large that there are many simultaneous collisions of the fluid molecules with it and if the velocity is low enough so that the flow of the fluid around the particle is laminar. For a spherical particle $\eta = 6\pi\gamma R$, where R is the radius of the particle and γ is the fluid viscosity. In the absence of any additional force, according to Newton's law the equation of motion for the particle reads,

$$m \frac{\mathrm{d}v(t)}{\mathrm{d}t} + \eta \, v(t) = 0 \,. \tag{2.2}$$

The physical mechanism underlying friction is the collision process between the molecules of the fluid and the particle. The momentum of the

particle is transferred to the molecules of the fluid and therefore the velocity of the particle decreases to zero. The differential equation (2.2) is a deterministic equation whereas the velocity $v(t)$ at time t is completely determined by the initial value $v(0)$,

$$v(t) = v(0)\, e^{-t/\tau} \; ; \tag{2.3}$$

$\tau = m\eta^{-1}$ is a relaxation time. However, Eq. (2.2) is valid only if the mass of the particle is large so that its velocity induced by thermal fluctuations is negligible.

We now take into account the fact that the environment is a heat bath at thermal equilibrium with temperature T. We also assume that all transients have died out and the particle is in thermal equilibrium with the environment. From the energy equipartition law it is known that in equilibrium the mean kinetic energy of the particle reaches (per spatial degree of freedom) the value

$$\frac{1}{2}\, m\langle v^2 \rangle = \frac{1}{2}\, k_{\mathrm{B}}T \,, \tag{2.4}$$

where k_{B} is Boltzmann constant. For a small enough mass m the thermal velocity $v_{\mathrm{th}} = \sqrt{k_{\mathrm{B}}T/m}$ may be observable and therefore the velocity of the particle can no longer be described exactly by Eq. (2.2) with the solution (2.3). If the mass of the particle is still large compared to the mass of the molecules, one expects Eq. (2.2) to be valid approximately. Therefore, it must be modified so that it leads to the correct thermal energy (2.4). This result is achieved by adding a stochastic force $\xi(t)$ to the right-hand side of Eq. (2.2), i.e., the total force due to the molecules acting on the free Brownian particle is decomposed into a continuous damping force F_d and a fluctuating force $\xi(t)$ [58, 59] (cf. also Ref. [61, 62]): as a result the particle will be in an animated and irregular state of motion. Thus, Brownian motion is the motion of a macroscopically small but microscopically large particle that is subject to the collisional forces exerted by the molecules of a surrounding fluid. The equation of motion of the free Brownian particle is given as

$$m\, \frac{\mathrm{d}v(t)}{\mathrm{d}t} = -\eta\, v(t) + \xi(t) \,. \tag{2.5}$$

The properties of the random force $\xi(t)$, also called Langevin force, are given only on average. Equation (2.5) is called Langevin equation [60] and it is the first example of a stochastic differential equation, i.e., a differential equation which contains a stochastic term $\xi(t)$.

Due to the random force $\xi(t)$, it is natural to introduce a statistical ensemble of the stochastic processes in (2.5), related to independent realizations of the random fluctuations $\xi(t)$ [54]. Because in the Langevin

equation (2.5) the stochastic force $\xi(t)$ varies from system to system in the ensemble, the velocity of the particle will also vary from system to system, i.e., it will become a stochastic quantity too. Therefore, it is natural to ask for the probability to find the velocity in the interval $(v, v + dv)$, i.e., the number of systems of the ensemble whose velocities are in the interval $(v, v + dv)$ divided by the total number of systems in the ensemble. Since v is a continuous variable one introduces the probability density $P(v)$; then, the probability density times the length of the interval dv is the probability of finding the particle in the interval $(v, v + dv)$. This distribution function depends on time t and the initial distribution. The probability density $P(v, t)$ for v at time t follows as an ensemble average of the form

$$P(v, t) = \langle \delta(v - v(t)) \rangle \,, \tag{2.6}$$

where $\delta(v)$ is Dirac's δ-function; by $\langle \ldots \rangle$ we indicate the average over independent realizations of the random process $\xi(t)$. An immediate consequence of Eq. (2.6) is the normalization

$$\int\limits_{-\infty}^{\infty} P(v, t) \, dv = 1 \,, \tag{2.7}$$

and that $P(v, t) \geq 0$ for all values of v and t.

The method of the Langevin equation gives a natural way for a stochastic generalization of the deterministic description. However, an adequate mathematical grounding for the approach of Langevin was not available until more than 40 years later, when Itô published his formulation of stochastic differential equations [63].

2.3 Gaussian white noise

The right hand side of the Langevin equation (2.5) represents the effects of the thermal environment: the energy dissipation, modeled as viscous friction, and random fluctuations in the form of the thermal noise $\xi(t)$. Thermal fluctuations are assumed to be unbiased, that is,

$$\langle \xi(t) \rangle = 0 \tag{2.8}$$

for all times t. The condition (2.8) ensures also that the equation of motion of the average velocity $\langle v(t) \rangle$ is given by the deterministic limit (2.2).

Since the friction force only depends on the present state of the system and not on what happened in the past, also the random fluctuations are assumed to be uncorrelated in time,

$$\langle \xi(t)\xi(t') \rangle = 0 \quad \text{if} \quad t \neq t' \,. \tag{2.9}$$

Furthermore, the fact that the friction involves no explicit time dependence has its counterpart in the time-translation invariance of all statistical properties of the fluctuations, i.e., the noise $\xi(t)$ is a stationary random process, which implies that $\langle \xi(t)\xi(t')\rangle = \langle \xi(t-t')\xi(0)\rangle$. Finally, since the friction force acts permanently in time, the same is valid for the fluctuations. During a small time interval the effect of the environment thus consists of a large number of small and, according to Eq. (2.9), practically independent contributions. Due to the central limit theorem [64] the net effect of all these contributions on the particle coordinate $x(t)$ is Gaussian-distributed. All the discussed features together with (2.4) lead to the fluctuation-dissipation relation [54, 65–68],

$$\langle \xi(t)\xi(t')\rangle = 2\eta k_{\mathrm{B}}T\, \delta(t-t')\,; \tag{2.10}$$

the quantity $\eta k_{\mathrm{B}}T$ is called the intensity of the noise or the noise strength of the Langevin force [54]. The fluctuation-dissipation theorem expresses the fact that the energy dissipation and random fluctuations are not independent of each other since both of them have the same origin, namely the interaction of the particle with a huge number of microscopic degrees of freedom of the environment. Since $\xi(t)$ is a Gaussian random process, all its statistical properties are completely determined by the mean value (2.8) and the autocorrelation function (2.10) [54, 64, 69]. The only particle property which enters the characteristics of the noise is the friction coefficient η, which may thus be viewed as a measure of the strength of its coupling to the environment.

A random force with the δ-correlation (2.10) is called white noise, because the spectral distribution [54], which is given by the Fourier transform of (2.10), is independent of frequency. If the stochastic forces are not δ-correlated, i.e., if the spectral density depends on frequency, one uses the term colored noise and Eq. (2.10) must be modified. Of course, white noise does not exist as a physically realizable process; it is, however, fundamental in a mathematical, and indeed in a physical sense, in that it is an idealization of many processes that do occur. Furthermore, situations in which white noise is not a good approximation can often be indirectly expressed in terms of white noise [63]. In this sense, white noise is the starting point from which a wide range of stochastic models can be derived.

2.4 Einstein relation

Averaging over many realizations of the stochastic process one finds the average particle position $\langle x(t)\rangle$ and the average velocity $\langle v(t)\rangle$. Usually, one is interested in the asymptotic $(t \to \infty)$ behavior of these quantities. For free Brownian motion Eq. (2.5) yields that in the long time limit $(t \to \infty)$

$\langle v \rangle = 0$ and $\langle x \rangle = \langle x(0) \rangle + \langle v(0) \rangle \tau$. The general definition of the particle current is,

$$\langle v \rangle = \lim_{t \to \infty} \frac{\langle x(t) \rangle - \langle x(0) \rangle}{t}. \tag{2.11}$$

Besides the average particle position and current one is usually also interested in the behavior of the mean square displacement,

$$\langle \delta x^2(t) \rangle = \langle [x(t) - \langle x(t) \rangle]^2 \rangle = \langle x^2(t) \rangle - \langle x(t) \rangle^2. \tag{2.12}$$

Dealing with normal diffusion, in the long time limit the mean square displacement grows linearly in time, and the diffusion coefficient is defined in the following way,

$$D = \lim_{t \to \infty} \frac{\langle \delta x^2(t) \rangle - \langle \delta x^2(0) \rangle}{2t}. \tag{2.13}$$

In the absence of an applied force Eq. (2.13) defies the free diffusion coefficient D_0.

Let us find an expression for the coefficient D_0 characterizing the free diffusion. Multiplying the Langevin equation (2.5) by $x(t)$ and averaging over a large number of different particles, one obtains,

$$m \langle \ddot{x}(t) x(t) \rangle = -\eta \langle \dot{x}(t) x(t) \rangle + \langle \xi(t) x(t) \rangle; \tag{2.14}$$

here $\dot{x} \equiv dx/dt$ and $\ddot{x} \equiv d^2x/dt^2$.

A crucial implicit assumption in Eq. (2.5) is the independence of the friction force, and hence also of the fluctuation force $\xi(t)$, from the system coordinate $x(t)$ [63], i.e.,

$$\langle \xi(t) x(t') \rangle = 0 \quad \text{for} \quad t \geq t'. \tag{2.15}$$

This relation reflects the assumption that the environment can be represented as a heat bath so that its properties are practically not influenced by the behavior of the particle [65].

The left hand side of Eq. (2.14) can be written as

$$m \langle \ddot{x} x \rangle = m \frac{d}{dt} \langle \dot{x} x \rangle - m \langle \dot{x}^2 \rangle. \tag{2.16}$$

From Eq. (2.13) with (2.12), we have for asymptotically large times that in the absence of an external force

$$2D_0 t = \langle x^2(t) \rangle, \tag{2.17}$$

as $\langle x(t) \rangle = $ const. for $t \to \infty$. By differentiating (2.17) we have that $\langle \dot{x} x \rangle = D_0$ and hence $d\langle \dot{x} x \rangle/dt = 0$. Observing (2.4) and (2.15) we finally

obtain from (2.14) and (2.16) for the free diffusion coefficient the following expression [3, 4, 53, 63],

$$D_0 = \frac{k_{\mathrm{B}}T}{\eta}\,, \tag{2.18}$$

known as Einstein relation. Equation (2.18) is a special form of the fluctuation-dissipation theorem; it implies that fluctuation and dissipation are intimately related, and that one cannot be present without the other. However, dissipation would also occur if the collisions with the molecules were not randomly distributed, but occurred at regular intervals. In that case the motion of the particle would be damped, but would not fluctuate. The reason for the relation between dissipation and fluctuation is that the time between collisions is a random variable [62].

One can easily verify that the Einstein relation (2.18) is valid also in the presence of a space-independent force; in this case the system is out of equilibrium and instead of (2.4) one has

$$\frac{1}{2}\,m\langle\delta v^2\rangle = \frac{1}{2}\,k_B T\,, \tag{2.19}$$

where $\langle\delta v^2\rangle = \langle v^2\rangle - \langle v\rangle^2$.

2.5   Overdamped dynamics

In the presence of an external force $f(x,t)$ the Langevin equation (2.5) becomes,

$$m\,\frac{\mathrm{d}^2 x(t)}{\mathrm{d}t^2} = f(x,t) - \eta\,\frac{\mathrm{d}x(t)}{\mathrm{d}t} + \xi(t)\,. \tag{2.20}$$

The dynamics of fluctuations of microscopic systems can often be described within a good approximation with the overdamped dynamics [70,71]. In this approximation the inertial term in the equation of motion is neglected [72]. Hence the second order differential equation (2.20) can be replaced by the following first order differential equation,

$$\eta\,\frac{\mathrm{d}x(t)}{\mathrm{d}t} = f(x,t) + \xi(t)\,, \tag{2.21}$$

which defines the overdamped Brownian dynamics.

Importantly, most of the microbiological systems are well modeled by the overdamped approximation. As an example, we consider the kinesin which is one of the biological (molecular) motors [73–75]. The kinesin moves along microtubules inside the cells [76–78] and after its head detaches from the microtubule binding site, it engages in Brownian movement [72]. Microtubules are spatially periodic structures built of tubulin heterodimers

which are arranged in rows called protofilaments which, in turn, are oriented nearly parallel to the microtubule axis. A heterodimer is about 8 nm long and is composed of two different globular subunits, α- and β-tubulin. This leads to the reflection symmetry breaking of the microtubules. As a consequence, the corresponding potential with period 8 nm is asymmetric.

One should note that the velocity $v(t) = \mathrm{d}x(t)/\mathrm{d}t$ in the corresponding Langevin equation is the velocity of the kinesin head during the diffusion phase, which should be distinguished from the overall velocity of the kinesin moving along microtubules. The radius of the kinesin head (the ellipsoidal catalytic core head is often approximated as a sphere) is $R = 2.94\,\mathrm{nm}$, and the mass of the head is approximately $m = 6 \times 10^{-20}$ g. The aqueous medium of the cell around the kinesin head has a viscosity of approximately $\gamma = 0.01\,\mathrm{g/cm\ s}$. Therefore, $\eta = 5.54 \times 10^{-8}$ g/s and the Langevin relaxation time is $\tau = 1.08 \times 10^{-12}$ s, which is so fast that the inertial term in the equation of motion can be neglected [72].

Approximating the second order Langevin equation by the first order equation affects neither the fluctuation-dissipation relation (2.10) nor the Einstein relation (2.18).

2.6   Random walk model and master equation

Brownian motion can be well described also by the random walk model, proposed by Pearson. Let us consider here a one-dimensional random walk. Following the general picture presented by Pearson, we introduce a one-dimensional lattice $\{x_i = i\Delta x\}$ with a lattice Δx and $i = 0, \pm 1, \pm 2, \dots$ We assume that at every time-unit a particle at site i hops to site $i \pm 1$ with a probability $q_i^{\pm}$ (see Fig. 1); $q_i^+ + q_i^- = 1$. Such a random walk corresponds to an overdamped motion and is described by a master equation for the site populations $P_i(t)$ [64, 79],

$$\frac{\partial}{\partial t} P_i(t) = g_{i-1}^+ P_{i-1}(t) + g_{i+1}^- P_{i+1}(t) - (g_i^+ + g_i^-)P_i(t)\,; \qquad (2.22)$$

$P_i(t)$ is normalized as $\sum_i P_i(t) = 1$. The first two terms on the right hand side of Eq. (2.22) present the gain of state i due to the transitions from states $i \pm 1$ and the last term presents the loss due to transitions from i into states $i \pm 1$, i.e., the master equation is a gain-loss equation for the probabilities of the separate states i. The quantities $g_i^+ = q_i^+ \nu_i$ and $g_i^- = q_i^- \nu_i$ are, correspondingly, the forward and backward rates. Using the normalization condition for the splitting probabilities one obtains that $\nu_i = g_i^+ + g_i^-$, i.e., ν_i represents the total rate; in more general terms, ν_i is the time-scaling parameter at site i. In our problem $\nu_i = 1$, as we assume that at every time unit a particle at site i hops to site $i \pm 1$. It is obvious that the random walk described by the master equation (2.22) is a Markov process, i.e., it is not
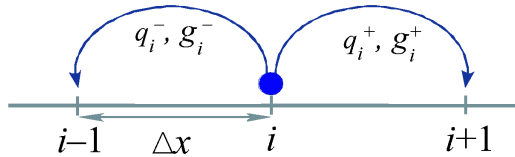
Figure 1: Random walk on a one-dimensional lattice: $q_i^{\pm}$ are the splitting probabilities to jump from site i to site $i \pm 1$; the quantities $g_i^{\pm}$ are the forward and backward rates; Δx is the lattice period.

affected by any knowledge of the process at earlier times: the probability at a later time is determined only by the probability at time $t = t_0$ [54,63,64].

Einstein's explanation of diffusion and Pearson's random walk are both based on the same two assumptions, namely, the existence of a mean free path (the step length in Pearson's model and the distance between the collisions in Einstein's description) and of a mean time (to perform a step in Pearson's model and the time between collisions in the description of Einstein). Therefore, in the limit $\Delta x \to 0$ the random walk model leads to the same results as obtained by Einstein.

2.7 Fokker-Planck equation

Another widely used description of diffusion under an external force field is offered by the Fokker-Planck equation [54], which is just an equation of time evolution for the probability distribution function; it follows as a generalization of the Einstein's approach, based on the discussion of the deterministic equations for the probability densities.

Let us derive the Fokker-Planck equation for the random walk model of Sec. 2.6. Using the notation $P_i(t) = P(x_i, t)$ and $P_{i\pm1}(t) = P(x_i \pm \Delta x, t)$ we introduce the finite difference operator

$$\frac{\Delta P(x_i, t)}{\Delta x} = \frac{P(x_i + \Delta x, t) - P(x_i - \Delta x, t)}{2\,\Delta x}\;; \tag{2.23}$$

for small Δx Eq. (2.23) is equivalent to the operator

$$\frac{\Delta P(x_i, t)}{\Delta x} = \frac{P(x_i + \Delta x/2, t) - P(x_i - \Delta x/2, t)}{\Delta x}\,. \tag{2.24}$$

Applying twice the operator (2.24), we can write,

$$\frac{\Delta}{\Delta x}\left[\frac{\Delta P(x_i, t)}{\Delta x}\right] = \frac{P(x_i + \Delta x, t) + P(x_i - \Delta x, t) - 2P(x_i, t)}{(\Delta x)^2}\,. \tag{2.25}$$

In the continuous limit, $\Delta x \to 0$, the finite difference operator (2.23) yields the partial derivative operator $\partial/\partial x$ and (2.25) gives us $\partial^2/\partial x^2$.

Let us first consider the case when there is no external force applied on the system; natural boundary conditions are assumed. Then the rates to jump to left or right are site-independent and equal, i.e., $g_i^+ = g_i^- \equiv g$. The master equation (2.22) becomes,

$$\frac{\partial}{\partial t} P_i(t) = g \left[P_{i-1}(t) + P_{i+1}(t) - 2P_i(t) \right] . \qquad (2.26)$$

In view of (2.25)

$$\frac{\partial}{\partial t} P_i(t) = \alpha_1 \frac{\Delta}{\Delta x} \left[\frac{\Delta P_i(t)}{\Delta x} \right] , \qquad (2.27)$$

with

$$\alpha_1 = (\Delta x)^2 g = (\Delta x)^2 \nu/2 . \qquad (2.28)$$

Taking in Eq. (2.27) the continuous limit, we obtain,

$$\frac{\partial}{\partial t} P(x,t) = \alpha_1 \frac{\partial^2}{\partial x^2} P(x,t) ; \qquad (2.29)$$

the normalization condition becomes, $\int P(x,t) \mathrm{d}x = 1$. Assuming for the initial distribution the delta-function, $P(x_0, t_0) = \delta(x_0 - X_0)$, the solution of Eq. (2.29) is given by Gaussian distribution,

$$P(x,t) = [4\pi\alpha_1(t - t_0)]^{-1/2} \exp \left[-\frac{(x - X_0)^2}{4\alpha_1(t - t_0)} \right] . \qquad (2.30)$$

Therefore, $\alpha_1 = D_0$ is the free diffusion coefficient and

$$\frac{\partial}{\partial t} P(x,t) = D_0 \frac{\partial^2}{\partial x^2} P(x,t) . \qquad (2.31)$$

The latter equation is the diffusion equation for the probability density $P(x,t)$.

In the case of a space and time dependent force $f(x,t)$, taking into account that $g_i^+(t) + g_i^-(t) = \nu_i(t) \equiv \nu$, the master equation (2.22) can be rewritten,

$$\begin{aligned}
\frac{\partial}{\partial t} P_i(t) = {} & \frac{\nu}{2} \left[P_{i-1}(t) + P_{i+1}(t) - 2P_i(t) \right] \\
& - \frac{1}{2} \left\{ \left[g_{i+1}^+(t) - g_{i+1}^-(t) \right] P_{i+1}(t) \right. \\
& \left. - \left[g_{i-1}^+(t) - g_{i-1}^-(t) \right] P_{i-1}(t) \right\} .
\end{aligned} \qquad (2.32)$$

In view of definitions (2.23) and (2.25), and posing

$$\alpha_1 = (\Delta x)^2 \left[g_i^+(t) + g_i^-(t) \right] /2 = (\Delta x)^2 \nu/2 \qquad (2.33)$$

and

$$\alpha_2 = \Delta x \left[g_i^+(t) - g_i^-(t) \right] , \qquad (2.34)$$

we obtain,

$$\frac{\partial}{\partial t} P_i(t) = \alpha_1 \frac{\Delta}{\Delta x} \left[\frac{\Delta P_i(t)}{\Delta x} \right] - \frac{\Delta}{\Delta x} \left[\alpha_2 P_i(t) \right] . \qquad (2.35)$$

Taking the continuous limit in Eq. (2.35), we can write,

$$\frac{\partial}{\partial t} P(x,t) = \alpha_1 \frac{\partial^2}{\partial x^2} P(x,t) - \frac{\partial}{\partial x} \left[\alpha_2 P(x,t) \right] ; \qquad (2.36)$$

α_2 is a function of space and time. Comparing Eqs. (2.28) and (2.33) one sees that $\alpha_1 = D_0$ also in the presence of an external force. Finding the first moment of Eq. (2.36) one sees that $\partial \langle x \rangle / \partial t = \langle \alpha_2 \rangle$. Comparing this result with the one from the Langevin equation (2.21) corresponding to the master equation (2.32) and therefore also to Eq. (2.36) one see that $\alpha_2 = f(x,t)\eta^{-1}$. Equation (2.36) can be written therefore,

$$\frac{\partial}{\partial t} P(x,t) = -\frac{\partial}{\partial x} \left[\frac{f(x,t)}{\eta} P(x,t) \right] + D_0 \frac{\partial^2}{\partial x^2} P(x,t) . \qquad (2.37)$$

The latter equation is the Fokker-Planck equation corresponding to the Langevin equation (2.21): it describes the overdamped Brownian motion under a force field f that can be space- and time-dependent. The first term on the right hand side of Eq. (2.37) is the drift term and the second one the diffusion term. In the absence of an external force the Fokker-Planck equation (2.37) reduces to the diffusion equation (2.31).

The diffusion-like equation (2.37) was first proposed by A. D. Fokker in his dissertation in 1914 [80], and discussed by M. Planck in 1918 [81]. In fact, Fokker presented an equation for the distribution function of the velocity, $P(v,t)$ [see Eq. (2.41)]. In 1915 Smoluchowski proposed the same equation for the distribution function of the position, $P(x,t)$, [82] and therefore Eq. (2.37) is also known as the Smoluchowski equation.

The Fokker-Planck equation (2.37) can be also written in the form of a continuity equation for the probability density $P(x,t)$:

$$\frac{\partial}{\partial t} P(x,t) = -\frac{\partial}{\partial x} J(x,t) , \qquad (2.38)$$

where $J(x,t)$ is the probability current,

$$J(x,t) = \frac{f(x,t)}{\eta} P(x,t) - D_0 \frac{\partial}{\partial x} P(x,t) . \qquad (2.39)$$

A general Fokker-Planck equation for N macroscopic variables $\zeta_1, \ldots, \zeta_N$ = $\{\zeta\}$ has the form [54]

$$\frac{\partial}{\partial t} P(\{\zeta\}, t) = \left[-\sum_{i=1}^{N} \frac{\partial}{\partial \zeta_i} D_i^{(1)}(\{\zeta\}) + \sum_{i,j=1}^{N} \frac{\partial^2}{\partial \zeta_i \, \partial \zeta_j} D_{ij}^{(2)}(\{\zeta\}) \right] P(\{\zeta\}, t) ; \tag{2.40}$$

the drift vector $D_i^{(1)}$ and the diffusion tensor $D_{ij}^{(2)}$ (see e.g. Ref. [54] for the exact definitions) generally depend on the N variables.

The Fokker-Planck equation for $P(v, t)$ corresponds to the underdamped Brownian motion in the absence of an external force, which may be described also by the Langevin equation (2.5). The Fokker-Planck equation for $P(v, t)$ reads [54],

$$\frac{\partial}{\partial t} P(v, t) = \frac{\eta}{m} \frac{\partial}{\partial v} [v P(v, t)] + \frac{\eta^2}{m^2} D_0 \frac{\partial^2}{\partial v^2} P(v, t) . \tag{2.41}$$

Considering the underdamped Brownian motion in the force field $f(x, t)$, the system is described by the Langevin equation (2.20), or equivalently by the Kramers (Klein-Kramers) equation for $P(x, v, t)$ [54, 55, 83],

$$\frac{\partial}{\partial t} P(x, v, t) = \left\{ -\frac{\partial}{\partial x} v + \frac{\partial}{\partial v} \left[\frac{\eta}{m} v - \frac{f(x, t)}{m} \right] + \frac{\eta^2}{m^2} D_0 \frac{\partial^2}{\partial v^2} \right\} P(x, v, t) . \tag{2.42}$$

3 Brownian motion in periodic potentials

3.1 Motivation and applications

The investigation on Brownian motion in periodic potentials originates from the question, whether it is possible to convert Brownian motion into useful work. The basic idea can be traced back to a talk given by Smoluchowski in 1912 [84], and was later extended by Feynman [85]. The main ingredient of Smoluchowski and Feynman's *Gedankenexperiment* now known as the Smoluchowski-Feynman ratchet is an axle with vanes at one end and at the other end a so-called ratchet, reminiscent of a circular saw with asymmetric saw-teeth (see Fig. 2). The whole device is surrounded by a gas at thermal equilibrium. If the described device could turn freely around, it would perform a rotatory Brownian motion due to random impacts of gas molecules on the paddles. Whereas the pawl blocks the turns of the axle in one direction and allows it to turn in the other one, it seems quite convincing that the whole gadget will perform on the average a systematic rotation in one direction, even if a small load in the opposite direction is applied [65]. However, this would be in contradiction with the second law of thermodynamics (see Refs. [85, 86]).

The Smoluchowski-Feynman ratchet has been experimentally realized on a molecular scale by Kelly, Tellitu, and Sestelo [87, 88]. The predicted absence of a preferential direction of rotation at thermal equilibrium was confirmed in nuclear magnetic resonance experiments.

A bona fide modeling and analysis of the ratchet and pawl device as it stands is rather involved, especially on a microscopic level (see Ref. [65]). However, one can focus on a considerably simplified mathematical model, which retains the basic qualitative features, and is formulated as Brownian motion in a one-dimensional spatially periodic potential.

Brownian motion in periodic structures has now become a relevant problem in several fields of physics, being very interesting from technological, experimental, as well as theoretical point of view, and has been a subject of intense investigations already many years [54, 89–91]. It represents a model that can be applied to numerous systems named already in Sec. 1.

3.2 General model

Brownian motion in a periodic potential $U_0(x) = U_0(x + L)$ under the influence of a constant bias F can be described by the following Langevin equation:

$$m \frac{\mathrm{d}^2 x(t)}{\mathrm{d}t^2} = -\frac{\mathrm{d}U_0(x)}{\mathrm{d}x} + F - \eta \frac{\mathrm{d}x(t)}{\mathrm{d}t} + \xi(t) \,. \tag{3.1}$$
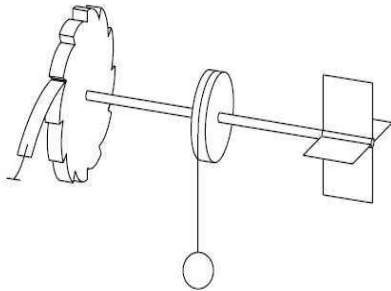
Figure 2: The Smoluchowski-Feynman ratchet and pawl machine.

In Eq. (3.1) the total potential reads,

$$U(x) = U_0(x) - Fx \,, \tag{3.2}$$

and the resulting force

$$f(x) = -\frac{\mathrm{d}U(x)}{\mathrm{d}x} \tag{3.3}$$

when averaged over the period is thus F,

$$\langle f(x) \rangle_L = \frac{1}{L} \int\limits_{x}^{x+L} f(x)\,\mathrm{d}x = F \,. \tag{3.4}$$

The total potential $U(x)$ is referred to tilted periodic potential, or washboard potential.

In the model of the Smoluchowski-Feynman ratchet the periodic potential corresponds to the ratchet (wheel) and the constant force F models the load; in the absence of load $F = 0$. As the symmetry of the ratchet is broken, because of the pawl mechanism (teeth are asymmetrical), also the reflection symmetry of the substrate potential is broken: no real number x' exists such that the relation $U_0(x' - x) = U_0(x' + x)$ is fulfilled for every x. In the remainder of this chapter, however, we concentrate on the more general problem of Brownian motion in spatially periodic force fields and do not assume the broken reflection symmetry by definition.

In the overdamped approximation the Langevin equation (3.1) describing the Brownian motion in a periodic potential reduces to

$$\eta \frac{\mathrm{d}x(t)}{\mathrm{d}t} = -\frac{\mathrm{d}U_0(x)}{\mathrm{d}x} + F + \xi(t) \,. \tag{3.5}$$

3.3 Phenomenology and quantities of interest

If $F = 0$, as long as the fluctuations are zero on average, the average current is zero, i.e., no directed motion occurs. At the same time, because of the excitation due to the Langevin forces the particles may leave the potential well and jump either into the neighboring left or right potential well or they may move in the course of time to other wells which are further away. For long enough time the particles will thus diffuse in both directions of the x-axis. In the long-time limit this diffusion can be described by the effective diffusion coefficient D, defined by (2.13). Instead, in the presence of the constant bias F the particles will preferably diffuse in the direction of the bias and in average there is a current $\langle v \rangle$, defined by (2.11), which depends on F. Notice that in the following we use the notation v instead of $\langle v \rangle$ for the current.

Let us discuss in short the overdamped and underdamped motion in a tilted periodic potential. The total potential (3.2), depicted in Fig. 3, is a corrugated plane with an average slope determined by the external force F. There exists a value of the tilting force $F = F_{\mathrm{cr}}$ such that for values $F > F_{\mathrm{cr}}$ the effective potential $U(x)$ has no minima, whereas for $F < F_{\mathrm{cr}}$ minima do occur; F_{cr} is called the critical tilting.

In the overdamped regime and in the absence of the noise $\xi(t)$, the particles in a washboard potential perform a creeping motion. If the tilting force F is large enough, so that the potential $U(x)$ has no minima, the particles move down the corrugated plane; this solution is termed running solution. If minima do exist, the particles arrive there and stop; this solution is called locked solution. In the presence of noise, the particles do not stay permanently in the locked state but will undergo noise-activated escape events. The particles thus perform in average a hopping process from one well to the next lower one [54].

In systems where inertial effects become important, in the absence of the noise a locked solution may occur if minima exist. Differently from the overdamped system, however, also a running solution can occur, even if the minima of the potential are present: namely, due to the momentum that the particles have, they may overcome the next potential barrier if the friction constant is small enough. In the presence of noise, the particles may be kicked out of the well where they are, i.e., out of the locked state. If the damping is small enough, the particles do not lose their energy very rapidly and therefore may no longer be trapped in the neighboring lower well, as they are for large friction. The particles may thus get in the running state and may stay in this state for some time. However, due to the Langevin forces, the energy of the particles fluctuates and they may again be trapped in one of the wells if their energy decreases. As a result, the particles can be again in the locked state [54].
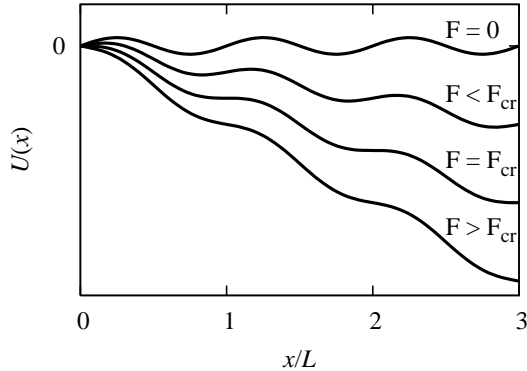
Figure 3: The tilted periodic potential $U(x) = U_0(x) - Fx$ for different values of the tilting force F; the periodic part of the potential is $U_0(x) = \sin(2\pi x/L)$.

From Eq. (3.5) one can find for the current,

$$v = \frac{\langle f(x) \rangle}{\eta}\,; \tag{3.6}$$

where the average is taken over the ensemble; $f(x)$ is given by (3.3), (3.2). Since the force $f(x)$ is nonlinear, one finds more convenient to solve the corresponding Fokker-Planck equation instead of the Langevin equation. The Fokker-Planck equation (2.38) corresponding to (3.5) is valid also for the reduced probability density and for the reduced probability current defined in the following way,

$$\hat{P}(x,t) = \sum_{n=-\infty}^{\infty} P(x + nL, t)\,, \tag{3.7}$$

$$\hat{J}(x,t) = \sum_{n=-\infty}^{\infty} J(x + nL, t)\,. \tag{3.8}$$

Furthermore,

$$\hat{P}(x + L, t) = \hat{P}(x, t)\,, \tag{3.9}$$

and the normalization condition reads,

$$\int_0^L \hat{P}(x,t)\,\mathrm{d}x = 1\,. \tag{3.10}$$

In the stationary state

$$\lim_{t\to\infty} \hat{P}(x,t) = \hat{P}_{\mathrm{st}}(x) \tag{3.11}$$

31

and from the continuity equation,

$$\lim_{t \to \infty} \hat{J}(x,t) = \hat{J}_{\text{st}} = \text{const.} \, ; \tag{3.12}$$

$$\hat{J}_{\text{st}} = \frac{f(x)}{\eta} \hat{P}_{\text{st}}(x) - D_0 \frac{\mathrm{d}}{\mathrm{d}x} \hat{P}_{\text{st}}(x) \, . \tag{3.13}$$

Equation (3.6) can be written also in the following way,

$$v = \int_{-\infty}^{\infty} \frac{f(x)}{\eta} P(x,t) \, \mathrm{d}x = \int_0^L \frac{f(x)}{\eta} \hat{P}(x,t) \, \mathrm{d}x \, . \tag{3.14}$$

In the stationary regime, making use of Eq. (3.13) and taking into account Eq. (3.9) we see that

$$v = \int_0^L \left[\hat{J}_{\text{st}} + D_0 \frac{\mathrm{d}}{\mathrm{d}x} \hat{P}_{\text{st}}(x) \right] \mathrm{d}x = \hat{J}_{\text{st}} L \, . \tag{3.15}$$

When $F = 0$ then the probability currents to the right and left are equal, $\hat{J}_{\text{st}}^+ = \hat{J}_{\text{st}}^-$, and $\hat{J}_{\text{st}} = \hat{J}_{\text{st}}^+ - \hat{J}_{\text{st}}^- = 0$ (this is nothing but detailed balance). Then, from (3.13), using also (3.3), (3.2), and the Einstein relation (2.18), we get,

$$\frac{\mathrm{d}\hat{P}_{\text{st}}(x)}{\hat{P}_{\text{st}}(x)} = -\beta \, \mathrm{d}U_0(x) \, , \tag{3.16}$$

where $\beta = (k_{\text{B}}T)^{-1}$ is the inverse temperature. Integrating Eq. (3.16) from x_0 to x and using the normalization condition (3.10) we find,

$$\hat{P}_{\text{st}}(x) = \hat{P}_{\text{st}}(x_0) \, e^{-\beta[U_0(x) - U_0(x_0)]} = N^{-1} e^{-\beta U_0(x)} \, , \tag{3.17}$$

with

$$N = \int_0^L e^{-\beta U_0(x)} \mathrm{d}x \, . \tag{3.18}$$

By that we have obtained the solution for the stationary probability density in a periodic potential.

When $F \neq 0$ then on the basis of Eqs. (3.13) and (3.15) one can write,

$$\frac{\mathrm{d}}{\mathrm{d}x} \hat{P}_{\text{st}}(x) - \beta f(x) \hat{P}_{\text{st}}(x) = -\frac{v}{LD_0} \, . \tag{3.19}$$

Multiplying the latter equation by $e^{\beta U(x)}$,

$$\frac{\mathrm{d}}{\mathrm{d}x} \left[\hat{P}_{\text{st}}(x) \, e^{\beta U(x)} \right] = -\frac{v}{LD_0} \, e^{\beta U(x)} \, . \tag{3.20}$$
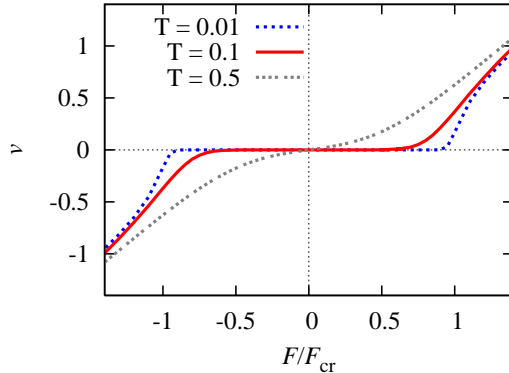
Figure 4: The stationary current v in a washboard potential with the periodic part given by $U_0(x) = \cos(2\pi x/L)$ *vs* the tilting force F. Different curves correspond to different values of temperature.

Integrating here from x to $x+L$ and using the fact that $U(x) = U_0(x) - Fx$ with $U_0(x) = U_0(x+L)$ and taking into account condition (3.9), we obtain,

$$\hat{P}_{\text{st}}(x)\, e^{\beta U(x)} \left(e^{-\beta FL} - 1 \right) = -\frac{v}{LD_0} \int_x^{x+L} e^{\beta U(x')}\mathrm{d}x' \,. \tag{3.21}$$

The latter equation can be also written as

$$\hat{P}_{\text{st}}(x) = N^{-1} e^{-\beta U(x)} \int_x^{x+L} e^{\beta U(x')}\mathrm{d}x' \,. \tag{3.22}$$

From the normalization condition (3.10) we find,

$$N = \int_0^L \mathrm{d}x\, e^{-\beta U(x)} \int_x^{x+L} e^{\beta U(x')}\mathrm{d}x' \,. \tag{3.23}$$

Herewith we have obtained the solution for the stationary probability density in a tilted periodic potential.

If instead we write Eq. (3.21) as

$$\hat{P}_{\text{st}}(x) = \frac{v}{LD_0} \left(1 - e^{-\beta FL} \right)^{-1} e^{-\beta U(x)} \int_x^{x+L} e^{\beta U(x')}\mathrm{d}x' \tag{3.24}$$

and use here the normalization condition (3.10), we find the expression for the stationary current,

$$v = \frac{LD_0 \left(1 - e^{-\beta FL} \right)}{\int_0^L \mathrm{d}x\, e^{-\beta U(x)} \int_x^{x+L} e^{\beta U(x')}\mathrm{d}x'} \,. \tag{3.25}$$
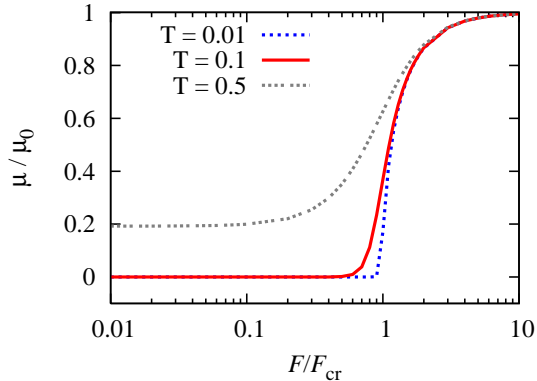
Figure 5: The mobility μ *vs* the tilting force F for the same substrate potential as used in Fig. 4; different curves correspond to different values of temperature. The linear response regime is clearly visible.

This result was first obtained by Stratonovich [92, 93] and is known as the Stratonovich formula. From here one can see that $F = 0$ implies that $v = 0$, as discussed previously. Also, taking into account that for $F \to \infty$ the potential $U(x) = U_0(x) - Fx \approx -Fx$, one obtains from the Stratonovich formula,

$$v = F\eta^{-1}, \quad \text{for} \quad F \to \infty, \tag{3.26}$$

i.e., at large values of the tilting force F the particle recovers the motion in a constant force field; the effective diffusion coefficient becomes $D = D_0$. The behavior of the stationary current v defined by Eq. (3.25) is illustrated in Fig. 4.

Instead of the current one can also study the mobility μ of the particle, defined as,

$$\mu = vF^{-1}. \tag{3.27}$$

As can be seen from Fig. 5, in the low temperature regime, $T \ll 1$, the particle mobility is close to zero for subthreshold tilting (locked state). Around the depinning threshold $F_d \simeq F_{\mathrm{cr}}$, which separates the locked and running regimes, the mobility grows sharply and in the large force limit the free particle motion described by $\mu_0 = \eta^{-1}$ is recovered (running state). If the temperature is increased, the transition from the locked to the running state is smoother. For small values of F the mobility μ is independent of the bias, as to be expected in linear response theory.

In the linear response regime the mean-square displacement in the absence of bias and the mean particle position for a vanishing bias are related
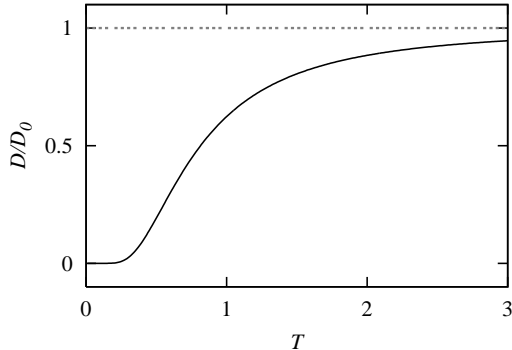
Figure 6: The effective diffusion coefficient D in the periodic potential $U_0(x) = \cos(2\pi x/L)$ *vs* the temperature T. The dashed line corresponds to the free diffusion.

in the following way,

$$\left[\langle \delta x^2(t) - \delta x^2(0)\rangle\right]_{F=0} = 2k_{\mathrm{B}}T\left[\frac{\langle x(t) - x(0)\rangle}{F}\right]_{F\to 0}, \quad t\to\infty, \quad (3.28)$$

which, using the definitions of the diffusion coefficient and the current [Eqs. (2.13), (2.11)], can be written also as,

$$D|_{F=0} = k_{\mathrm{B}}T\left(\frac{v}{F}\right)_{F\to 0} = k_{\mathrm{B}}T\mu|_{F\to 0}. \tag{3.29}$$

For a constant force $v = F\eta^{-1}$, $\mu = \eta^{-1}$ and we recover the Einstein relation (2.18). The relation (3.29), or equivalently (3.28), is thus a general form of the Einstein relation.

Equation (3.29) allows one also to find the effective diffusion coefficient in a periodic potential. Using the L'Hospital's rule we see that

$$\left(\frac{1 - e^{-\beta FL}}{F}\right)_{F\to 0} = \beta L. \tag{3.30}$$

Furthermore, for $F = 0$ the potential $U(x) = U_0(x)$ is periodic and we may perform the integration in (3.25) from 0 to L instead of from x to $x + L$ so that the double integral in the denominator of Eq. (3.25) factorizes. As a result we find for the effective diffusion coefficient in a periodic potential,

$$D = \frac{D_0}{\int\limits_0^L e^{-\beta U_0(x)}\frac{\mathrm{d}x}{L} \int\limits_0^L e^{\beta U_0(x')}\frac{\mathrm{d}x'}{L}}. \tag{3.31}$$
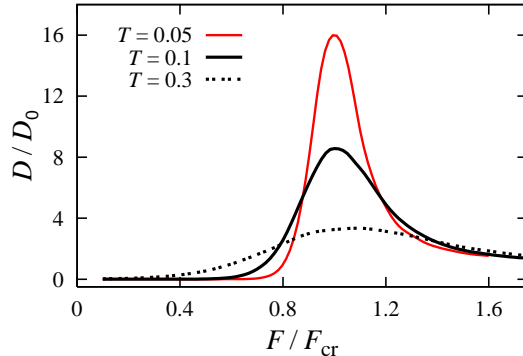
35

Figure 7: The effective diffusion coefficient D in a washboard potential with the periodic part of the potential given by $U_0(x) = \cos(2\pi x/L)$ *vs* the tilting force F. Different curves correspond to different values of temperature.

This expression was first derived by Lifson and Jackson in Ref. [89] (see also Refs. [94, 95]). By the Cauchy-Schwartz inequality [96], the denominator of (3.31) is always larger than unity: thus, the effect of any one-dimensional periodic potential is to produce a macroscopic diffusion constant which is always smaller than the free diffusion constant D_0. Of course, when the temperature is large enough, the particles do not feel much the influence of the periodic potential and free diffusion is recovered for $k_BT \gg \Delta U_0$; $\Delta U_0 = U_0(x_{\max}) - U_0(x_{\min})$ is the potential barrier between the two neighboring potential minima ($F = 0$); $x_{\min}$, $x_{\max}$ correspond to the minimum and maximum of the periodic potential. The behavior of the effective diffusion coefficient D *versus* the temperature T is depicted in Fig. 6.

A closed analytical expression for the diffusion coefficient in a periodic potential under the influence of an arbitrary tilting and temperature was derived for the overdamped regime only recently [97–99] in the renewal theory approximation [100]. The starting point in Ref. [97] was the following expression for the diffusion coefficient [97, 98, 100–102],

$$D = \frac{L^2}{2} \frac{\langle t^2(x_0 \to x_0 + L) \rangle - \langle t(x_0 \to x_0 + L) \rangle^2}{\langle t(x_0 \to x_0 + L) \rangle^3}, \qquad (3.32)$$

where x_0 is an arbitrary reference point and $\langle t^n(a \to b) \rangle$ is the n-th moment of the first passage time from a to $b > a$ for a stochastic trajectory obeying Eq. (3.5), with the assumption that $F > 0$ in order to keep those moments finite [1]. The moments of the first passage time, for the dynamics (3.5), are

---

[1]One can make this assumption with no loss of generality (see also Fig. 4), and in the following we study $F > 0$, unless indicated differently.

given by the analytical recursion relation [11]

$$\langle t^n(a \to b) \rangle = \frac{n}{D_0} \int\limits_a^b \mathrm{d}x \, e^{\beta U(x)} \int\limits_{-\infty}^x \mathrm{d}x' \, \langle t^{n-1}(x' \to b) \rangle \, e^{-\beta U(x')} \,, \quad (3.33)$$

for $n = 1, 2, \ldots$ and with $\langle t^0(x' \to b) \rangle = 1$. By introducing (3.33) into (3.32), one finds,

$$D = \frac{D_0}{N^3} \int\limits_{x_0}^{x_0+L} \frac{\mathrm{d}x}{L} \, I_+(x) \, I_-^2(x) \,, \quad (3.34)$$

where

$$N = \int\limits_{x_0}^{x_0+L} \frac{\mathrm{d}x}{L} \, I_-(x) \,, \quad (3.35)$$

$$I_\pm(x) = \frac{1}{D_0} \, e^{-\beta F L(1\pm 1)/2} \, e^{\pm\beta U(x)} \int\limits_x^{x+L} \mathrm{d}x' \, e^{\mp\beta U(x')} \,. \quad (3.36)$$

The dependence of the diffusion coefficient in a tilted periodic potential on the value of the tilting force F is plotted in Fig. 7. For small values of bias and low temperature, the diffusion coefficient is suppressed compared to the free diffusion; in linear response the diffusion coefficient is given approximately by $D(F,T) \simeq k_\mathrm{B} T \mu(F,T)$ [54]. Around the critical tilt the giant enhancement of the diffusion is observed [103]; the lower the temperature, the more prominent is the growth of the depinning diffusion peak. In the large force limit, the free diffusion regime is eventually recovered, as mentioned earlier.

The viscous friction coefficient η can be expressed also in the following way, $\eta = m\gamma$, with γ being here a damping constant and m the mass of the Brownian particle (c.f. Sec. 2.2). The condition for the underdamped regime is then, $\gamma \ll \sqrt{F_\mathrm{cr}}$. The mobility and the diffusion coefficient in the underdamped regime display a similar behavior as in the overdamped limit, with one significant difference: the depinning threshold F_d is a monotonic function of the damping constant with

$$\lim_{\gamma \to 0} F_d \simeq 3.36 \gamma \sqrt{F_\mathrm{cr}} \quad (3.37)$$

and $F_d \simeq F_\mathrm{cr}$ for $\gamma \gtrsim \sqrt{F_\mathrm{cr}}$ [54, 104].

[10]

3.4 The choice of potentials and dimensionless units

In the studies of Brownian motion in a periodic potential the easiest choice, and also the mostly exploited one, is to use a simple cosine-type potential. However, in many cases this is an oversimplification and we are closer to a real situation using more complicated potentials (see Ref. [105], and also [106]). The role of metastable and bistable potentials in the diffusive motion of particles in periodic structures was pointed out in Refs. [107,108], in the context of superionic conductors. The molecular-dynamics simulation of self-diffusion on metal surfaces [109] and experimental data for superionic conductors [110] provide the evidence that the potential barriers of different heights are important for the understanding of transport processes in corresponding systems. Potentials with barriers of different heights are also of relevance in modeling the kinetics of motor proteins [111] (see also [112]).

In this part of the work we study the dependence of the overdamped Brownian motion on periodic potentials of various shapes. This target can be achieved to a great accuracy using piecewise linear potentials (see also Ref. [78]). Piecewise linear potentials are important for at least three reasons: they can be used as a first approximation of the shape of an arbitrary potential, and they are sufficiently simple to allow an exact algebraic treatment of the relevant quantities. The third feature is that varying only some parameters it is possible to obtain a new shape of the potential, enabling to use the same analytic equations for the quantities under investigation.

The piecewise linear periodic potential with one minimum per period is characterized by the asymmetry parameter k: $0 < k < L$. The potential is symmetric if $k = L/2$ (see Fig. 8). The critical tilting force is given by $F_{cr} = A(L - k)^{-1}$, where A is the amplitude of the potential. At the critical tilting $F = F_{cr}$, the force acting on the particle in the region $[k, L]$ is zero.

For the potentials with two minima per period we assume that $0 < k_1 < k_2 < k < L$, where k_1 corresponds to the additional minimum and k_2 to the additional maximum (see Fig. 8). The potentials with one and two minima per period are considered to be comparable for the same values of the parameter k, and the corresponding right-hand potential barrier we thus name the primary barrier. In the case of the potentials with two minima per period we also assume that $0 \leq A_1 < A_2 \leq A$ and $\Delta A = A_2 - A_1 < A$, whereas we are interested in having an additional trap with a smaller potential barrier than the primary barrier (see Fig. 8). The tilting force corresponding to the disappearance of the additional minima is given by $F_{ce} = \Delta A/\Delta k$, where $\Delta k = k_2 - k_1$.

For the sake of convenience we recast the problem into a dimensionless form [2]. With no loss of generality we take the period $L = 1$ and replace the

---

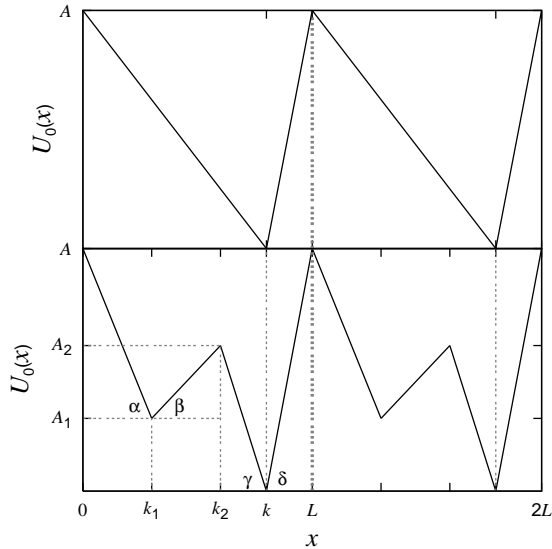[2]Note that all the quantities plotted in the figures are dimensionless.

Figure 8: The general shapes of the periodic potentials with period L: (above) simple sawtooth potential with one minimum per period; (below) piecewise linear potential with two minima per period. Concerning the double-hump potential, we call the potential barrier with the unit-height to be the main barrier, and the one with the height $\Delta A = A_2 - A_1 < 1$ the additional barrier. The parameters k_1, k_2 and k define the positions of the extrema of the potential, while the quantities α, β, γ and ΔA define the slopes (forces) for the double-hump potential.

relevant quantities with the corresponding dimensionless ones:

$$\tilde{T} = k_{\mathrm{B}} T A^{-1}, \quad \tilde{F} = F F_{\mathrm{cr}}^{-1}, \quad \tilde{D} = D \eta A^{-1}, \quad \tilde{D}_0 = D_0 \eta A^{-1}, \;\; (3.38)$$

so that

$$\tilde{D}_0 = \tilde{T}, \qquad \tilde{v} = v \eta A^{-1}. \tag{3.39}$$

We also choose $A = 1$ and for brevity, in what follows, we will omit the tilde signs above the symbols. Hence,

$$F_{\mathrm{ce}} = \frac{\Delta A \,(1 - k)}{\Delta k}, \qquad F_{\mathrm{cr}} = 1. \tag{3.40}$$

Considering the case of the double-hump potential, we refer to the critical tilt, as the value $\max(F_{\mathrm{ce}}, F_{\mathrm{cr}})$.

The dimensionless potentials that will be considered (see Fig. 8), are defined as follows ($n = 1, 2, \ldots$ is the number of the period):

(I) Simple sawtooth potential with one minimum per period:

$$\begin{aligned} U_{an}(x) &= a_{0n} - ax\,, & (n-1) &\leq x \leq k + (n-1)\,, \\ U_{bn}(x) &= -b_{0n} + bx\,, & k + (n-1) &\leq x \leq n\,, \end{aligned} \tag{3.41}$$

where

$$\begin{aligned} a_{0n} &= 1 + \tfrac{(n-1)}{k}\,, & a &= \tfrac{1-(1-F)k}{(1-k)k}\,, \\ b_{0n} &= -1 + \tfrac{n}{1-k}\,, & b &= \tfrac{1-F}{1-k}\,. \end{aligned} \tag{3.42}$$

(II) Potential with two minima per period:

$$\begin{aligned} U_{an}(x) &= a_{0n} - ax\,, & (n-1) &\leq x \leq k_1 + (n-1)\,, \\ U_{bn}(x) &= -b_{0n} + bx\,, & k_1 + (n-1) &\leq x \leq k_2 + (n-1)\,, \\ U_{cn}(x) &= c_{0n} - cx\,, & k_2 + (n-1) &\leq x \leq k + (n-1)\,, \\ U_{dn}(x) &= -d_{0n} + dx\,, & k + (n-1) &\leq x \leq n\,, \end{aligned} \tag{3.43}$$

where

$$\begin{aligned} a_{0n} &= A_1 + \tfrac{1-A_1}{k_1}\left[k_1 + (n-1)\right]\,, & a &= \tfrac{1-A_1}{k_1} + \tfrac{F}{1-k}\,, \\ b_{0n} &= -A_1 + \tfrac{\Delta A}{\Delta k}\left[k_1 + (n-1)\right]\,, & b &= \tfrac{\Delta A}{\Delta k} - \tfrac{F}{1-k}\,, \\ c_{0n} &= \tfrac{A_2}{k-k_2}\left[k + (n-1)\right]\,, & c &= \tfrac{A_2}{k-k_2} + \tfrac{F}{1-k}\,, \\ d_{0n} &= \tfrac{1}{1-k}\left[k + (n-1)\right]\,, & d &= \tfrac{1-F}{1-k}\,. \end{aligned} \tag{3.44}$$

3.5 Transport in potentials with one minimum per period

3.5.1 Analytic computations

The quantities that best characterize the stationary flow are the current v, or, equivalently, the related mobility μ, and the diffusion coefficient D, defined, correspondingly, by Eqs. (2.11), (3.27), and (2.13). Beside these quantities, the randomness parameter r is also of some case:

$$r = \lim_{t \to \infty} \frac{\langle \delta x^2(t) \rangle - \langle \delta x^2(0) \rangle}{\left[\langle x(t) \rangle - \langle x(0) \rangle\right] L} = \frac{2D}{vL}\,; \tag{3.45}$$

equivalently, one defines the Péclet factor,

$$\mathrm{Pe} = 2r^{-1} = vLD^{-1}\,. \tag{3.46}$$

In the overdamped limit the current and diffusion coefficient in a tilted periodic potential are given by Eqs. (3.25) and (3.34), respectively. Proceeding from these formulas, in the dimensionless units, the diffusion coefficient,

current, and Péclet factor in sawtooth potentials can be expressed in the following form:

$$D = TYZ^{-3} \,, \tag{3.47}$$

$$v = \varphi_0 Z^{-1} \,, \tag{3.48}$$

$$\mathrm{Pe} = \varphi_0 Z^2 (TY)^{-1} \,. \tag{3.49}$$

Here

$$\varphi_0 = 1 - \exp\left[-\frac{F}{T(1-k)}\right] \,. \tag{3.50}$$

In the case of a sawtooth potential with one minimum per period, the quantities Z and Y read,

$$Z = \int_0^k \mathrm{d}x \, H_{-a}(x) + \int_k^1 \mathrm{d}x \, H_{-b}(x) \,, \tag{3.51}$$

$$Y = \int_0^k \mathrm{d}x \, H_{+a}(x) \, H_{-a}^2(x) + \int_k^1 \mathrm{d}x \, H_{+b}(x) \, H_{-b}^2(x) \,. \tag{3.52}$$

Equations (3.51) and (3.52) contain the functions $H_{\pm a}$ and $H_{\pm b}$ where the subscripts a and b associate, correspondingly, with the limits of integration from 0 to k and from k to 1. Having defined for brevity the generalized potential $u(x) = U(x)T^{-1}$, we have,

$$
\begin{aligned}
H_{\pm a}(x) &= D_0^{-1} e^{\frac{-F(1\pm1)}{2T(1-k)}} e^{\pm u_{a1}(x)} \\
&\quad \times \left[\int_x^k \mathrm{d}x' \, e^{\mp u_{a1}(x')} + \int_k^1 \mathrm{d}x' \, e^{\mp u_{b1}(x')} + \int_1^{x+1} \mathrm{d}x' \, e^{\mp u_{a2}(x')} \right], \\
H_{\pm b}(x) &= D_0^{-1} e^{\frac{-F(1\pm1)}{2T(1-k)}} e^{\pm u_{b1}(x)} \\
&\quad \times \left[\int_x^1 \mathrm{d}x' \, e^{\mp u_{b1}(x')} + \int_1^{k+1} \mathrm{d}x' \, e^{\mp u_{a2}(x')} + \int_{k+1}^{x+1} \mathrm{d}x' \, e^{\mp u_{b2}(x')} \right].
\end{aligned}
\tag{3.53}
$$

Performing the integration in Eqs. (3.53), we finally obtain,

$$
\begin{aligned}
H_{\pm a}(x) &= \frac{\varphi_0}{a} + g\,\varphi_a \exp\left\{ \frac{a\left[\mp2x - k(1\mp1)\right]}{2T} \right\}, \\
H_{\pm b}(x) &= -\frac{\varphi_0}{b} + g\,\varphi_b \exp\left\{ \frac{b\left[\pm2(x-1) + (1-k)(1\pm1)\right]}{2T} \right\},
\end{aligned}
\tag{3.54}
$$

where the following notations are used:

$$g = \frac{1}{a} + \frac{1}{b} \,, \tag{3.55}$$

$$\varphi_a = \exp\left(\frac{1-F}{T}\right) - 1 \,, \qquad \varphi_b = 1 - \exp\left[-\frac{1-(1-F)k}{T(1-k)}\right] \,. \tag{3.56}$$

Substituting the functions $H_{\pm a, b}(x)$ given by Eqs. (3.54) into Eqs. (3.51) and (3.52), performing the integration, and introducing the notation

$$
\begin{aligned}
\tilde{\varphi}_a &= \exp\left[\tfrac{2(1-F)}{T}\right] - 1\,, \\
\tilde{\varphi}_b &= 1 - \exp\left\{-\tfrac{2[1-(1-F)k]}{T(1-k)}\right\}\,,
\end{aligned}
\tag{3.57}
$$

the quantities Z and Y can be expressed analytically as

$$
Z = \left(\frac{k}{a} - \frac{1-k}{b}\right)\varphi_0 + Tg^2\varphi_a\,\varphi_b\,,
\tag{3.58}
$$

$$
\begin{aligned}
Y ={}& \left(\frac{k}{a^3} - \frac{1-k}{b^3}\right)\varphi_0^3 + 3T\left(\frac{1}{a^3} + \frac{1}{b^3}\right)g\,\varphi_0^2\,\varphi_a\,\varphi_b \\
&+ \frac{1}{2}Tg^2\varphi_0\left(\frac{1}{a^2}\,\varphi_a^2\,\tilde{\varphi}_b - \frac{1}{b^2}\,\varphi_b^2\,\tilde{\varphi}_a\right) \\
&+ 2g^2\varphi_0\left[\frac{k}{a}\,\varphi_a^2(1 - \varphi_b) - \frac{1-k}{b}\,\varphi_b^2(1 + \varphi_a)\right] \\
&+ Tg^3\left[\frac{1}{a}\,\varphi_a^3\,\varphi_b(1 - \varphi_b) + \frac{1}{b}\,\varphi_b^3\,\varphi_a(1 + \varphi_a)\right]\,.
\end{aligned}
\tag{3.59}
$$

By that we have derived the exact algebraic expressions for the current v, the diffusion coefficient D, and the Péclet factor Pe in the sawtooth potentials with one minimum per period.

3.5.2 Asymptotic limits and particular cases

In this section we will examine the asymptotic limits and essential particular cases on the basis of the analytical formulas derived.

(I) In the absence of tilt ($F = 0$), Eqs. (3.50) and (3.56) reduce to

$$
\varphi_0 = 0\,, \qquad \varphi_a = e^{1/T} - 1\,, \qquad \varphi_b = 1 - e^{-1/T}\,,
\tag{3.60}
$$

and from Eqs. (3.47), (3.58), and (3.59) one obtains

$$
D = \frac{1}{2T\left[\cosh(T^{-1}) - 1\right]}\,.
\tag{3.61}
$$

This expression is as a special case of the general formula of the diffusion coefficient in an arbitrary unbiased periodic potential [89] [see Eq. (3.31)]. It is to be noticed that for $F = 0$ the diffusion coefficient becomes independent of the asymmetry parameter k.

(II) In the high temperature limit, one can take into account only the first order terms in the expansions of the exponents in Eqs. (3.50) and (3.56). Then

$$
\varphi_0 \approx \frac{F}{T(1-k)}, \qquad \varphi_a \approx \frac{1-F}{T}, \qquad \varphi_b \approx \frac{1-(1-F)k}{T(1-k)},
\tag{3.62}
$$

and

$$H_{\pm a,b} = T^{-1}, \qquad Z = T^{-1}, \qquad Y = T^{-3}. \tag{3.63}$$

The diffusion coefficient, current, and Péclet factor now become

$$D = T, \tag{3.64}$$

$$v = \frac{F}{1-k}, \tag{3.65}$$

$$\text{Pe} = \frac{F}{T(1-k)}. \tag{3.66}$$

(III) Under the conditions $F \gg 1$ and $FT^{-1} \gg 1$, the following approximate equations hold,

$$\varphi_0 \approx -\varphi_a \approx \varphi_b \approx 1, \qquad a \approx -b \approx \frac{F}{1-k}, \tag{3.67}$$

and

$$H_{\pm a,b} = \frac{1-k}{F}, \qquad Z = \frac{1-k}{F}, \qquad Y = \left(\frac{1-k}{F}\right)^3. \tag{3.68}$$

As a result, the expressions for D, v, and Pe coincide with Eqs. (3.64)-(3.66). Thus, at high temperatures and at large values of tilting force, the transport properties of Brownian particles are the same.

(IV) At the critical tilt ($F = 1$), one has

$$\begin{aligned}
H_{\pm a}(x) &= \frac{\varphi_0}{a} + \frac{1-k}{T} \exp\left\{ \frac{a\,[\mp 2x - k(1\mp 1)]}{2T} \right\}, \\
H_{\pm b}(x) &= \frac{\varphi_0}{a} + \frac{1-k}{T} \exp\left(-\frac{ak}{T}\right) + \frac{\varphi_0\,[\pm 2(x-1)+(1-k)(1\pm 1)]}{2T},
\end{aligned} \tag{3.69}$$

whereas in the low-temperature limit Eqs. (3.47)-(3.52) and (3.69) yield

$$D = \frac{2T}{3(1-k)^2}, \tag{3.70}$$

$$v = \frac{2T}{(1-k)^2}, \tag{3.71}$$

$$\text{Pe} = 3. \tag{3.72}$$

(V) If $F < 1$ and $(1-F)T^{-1} \gg 1$, we have the following asymptotic limits:

$$\varphi_b \approx \tilde{\varphi}_b \approx 1, \quad \varphi_a \approx e^{(1-F)/T} \gg 1, \quad \tilde{\varphi}_a \approx e^{2(1-F)/T} = \varphi_a^2. \tag{3.73}$$

Then Eqs. (3.51) and (3.52) with (3.54) yield

$$Z = Tg^2 e^{(1-F)/T}, \tag{3.74}$$

$$Y = \frac{T}{2}\,g^3\,e^{2(1-F)/T}\left\{ \left(\frac{1}{a}-\frac{1}{b}\right)\varphi_0 + 2\left[\frac{1}{a}e^{-F/(1-k)T} + \frac{1}{b}\right] \right\}, \tag{3.75}$$
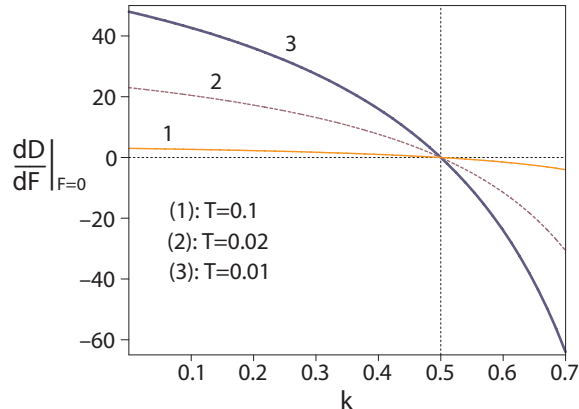
Figure 9: The plot of the derivative $\partial D / \partial F|_{F=0}$ *vs* the asymmetry parameter k for various values of temperature T.

and

$$D = \frac{2 - \varphi_0}{2Tg^2 \, e^{(1-F)/T}} \, , \tag{3.76}$$

$$v = \frac{\varphi_0}{Tg^2 \, e^{(1-F)/T}} \, , \tag{3.77}$$

$$\mathrm{Pe} = \frac{2\varphi_0}{2 - \varphi_0} = 2 \tanh\left[\frac{F}{2T(1-k)}\right] \, , \tag{3.78}$$

(cf.also Ref. [99]). If, additionally, the condition $F/T(1-k) \gg 1$ is fulfilled, then $e^{-F/T(1-k)} \approx 0$ and $\varphi_0 \approx 1$. Consequently, we have, $2D = v$ and $\mathrm{Pe} = 2$. This indicates that an extremely exact stabilization between the diffusion and current occurs in this region of parameters. The value $\mathrm{Pe} = 2$ corresponds to the Poissonian one-step hopping process.

3.5.3 Suppression of diffusion by a weak external field

As we saw, in the weak noise limit, when the conditions $(1-F)T^{-1} \gg 1$ and $F < 1$ are fulfilled, the expressions for the transport coefficients simplify substantially. In particular, one can present the diffusion coefficient and current for this case in terms of escape rates. An analysis of diffusion in a tilted smooth symmetric potential in the terms of escape statistics was carried out for various damping regimes in Ref. [113]. In the following we analyze the behaviour of diffusion in the overdamped regime under a weak
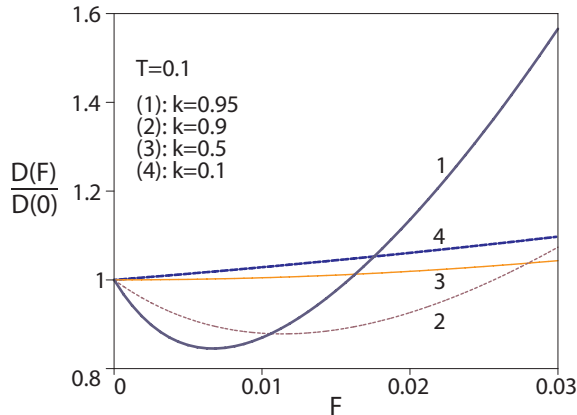
Figure 10: The plot of the diffusion coefficient *vs* the tilting force F at fixed temperature $T = 0.1$ for various values of asymmetry parameter k.

external field as well as the relationship between diffusion and current in this regime.

In the weak noise limit the transport of particles in a periodic potential subject to a small bias is influenced mainly by the heights of potential barriers. For the piecewise linear potential (3.41) the right-side and left-side barrier heights read respectively

$$
\begin{aligned}
\Delta U_+ &= 1 - F\,, \\
\Delta U_- &= 1 + \tfrac{k}{1-k}\,F\,.
\end{aligned}
\tag{3.79}
$$

The quantities $\Delta U_\pm$ [3] determine the escape rates over the corresponding barriers $(\Delta U_\pm \gg T)$

$$
w_\pm = \frac{(\Delta U_+)^2(\Delta U_-)^2}{T}\,\exp\!\left(-\frac{\Delta U_\pm}{T}\right).
\tag{3.80}
$$

Equations (3.80) can be obtained using the standard scheme for the derivation of the Kramers escape rates [63], except the expansion into Taylor series near the extrema of $U(x)$, which is not applicable in the case of a piecewise linear potential; however, in the present case this expansion is not necessary as the relevant integrals can be explicitly calculated. By means of escape rates (3.80) we can express the diffusion coefficient and current in the following form (c.f. Ref. [65]):

$$
D = \frac{1}{2}\,(w_+ + w_-)\,,
\tag{3.81}
$$

$$
v = w_+ - w_-\,.
\tag{3.82}
$$

[3]Note that the chosen scale of external force depends through the critical tilt on the asymmetry parameter k.
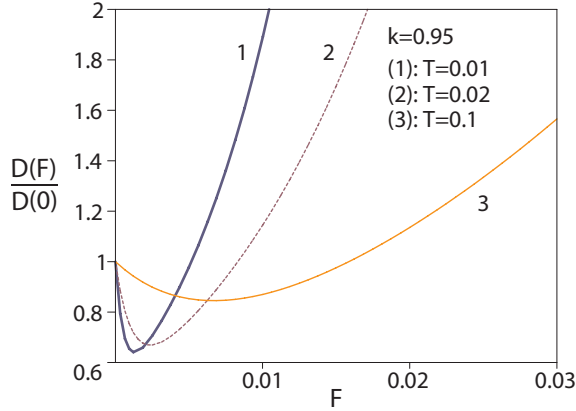
Figure 11: The plot of the diffusion coefficient *vs* the tilting force F at fixed asymmetry parameter $k = 0.95$ for various values of temperature T.

Therefore, $D(F)$ and $v(F)$ are completely determined by the rates $w_\pm$ in the relevant approximation. At $F = 0$ we have $D(0) = w$, where $w = T^{-1} e^{-1/T}$ is the escape rate in the untilted potential [c.f. Eq. (3.61)]. The expressions (3.81) and (3.82) are particular cases of the general formulas (3.34), (3.25).

The response of diffusion to the application of an infinitesimally weak tilting force is characterized by the slope of the function $D(F)$ in the limit $F \to 0$, that is by the derivative $\partial D/\partial F$ at $F = 0$. The dependence of this quantity on the asymmetry of the periodic potential is shown in Fig. 9. As one can see, the slope of $D(F)|_{F=0}$ changes its sign regardless of the temperature if the asymmetry parameter passes the value $k = 0.5$, being positive for $k < 0.5$ and negative for $k > 0.5$. Consequently, if a tiny load is applied, diffusion is reduced in the potentials with positive asymmetry (i.e., with the asymmetry in the direction of the bias). With the further increase of the tilting force the diffusion coefficient $D(F)$ passes through a minimum (see Figs. 10 and 11) followed by its rise caused by delocalization processes. In the case of the potentials with $k \leq 0.5$ the diffusion coefficient increases monotonically if an external field is turned on (see curves 3 and 4 in Fig. 10). The curves plotted in Figs. 10 and 11 demonstrate that the suppression of diffusion is favoured by larger values of k and by lower temperatures. The reduction of diffusion is maximal in the limit $k \to 1$. Let us also mention that the situation is symmetric under the following transformation: $F \to -F$ and $k \to 1 - k$.

Equation (3.81) also enables us to provide a simple interpretation of the discussed suppression of diffusion. The barrier heights $\Delta U_\pm$ *versus*
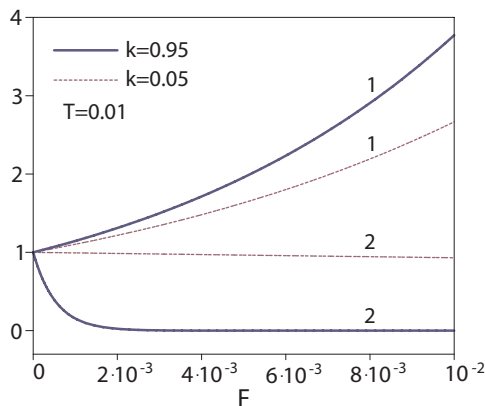
Figure 12: The plot of the normalized escape rates w_+/w (curves 1) and w_-/w (curves 2) *vs* the tilting force F at fixed temperature $T = 0.01$ for two periodic potentials with different asymmetries.

F vary at different rates in the potentials where $k \neq 0.5$ [4], resulting in the asymmetric behaviour of the escape rates $w_\pm$ under an arbitrary weak external field, as illustrated in Fig. 12. By that, as one can observe in Fig. 12, for a potential with positive asymmetry the escape rate w_- over the left-side barrier diminishes more rapidly compared with the rise of the escape rate w_+ over the right-side barrier if a very small tilting force is applied, which leads to the suppression of diffusion. Further the decrease of w_- slows down while the increase of w_+ picks up speed, i.e., the delocalization processes in the direction of bias become dominating, and the diffusion coefficient passes through a minimum. On the other hand, diffusion is promoted by a weak external field in a potential with negative asymmetry whereas the increasing contribution from w_+ prevails anyway over the decrease of w_- in this case.

From Eq. (3.81) one can evaluate approximately the tilting force $F_{\min}$, which corresponds to the minimum of the diffusion coefficient:

$$F_{\min} = T(1 - k) \ln \Xi(T, k), \tag{3.83}$$

where

$$\Xi(T, k) = \frac{k \, \Phi(T, k)[1 - k \, \Phi(T, k)] - 2T(1 - k)[2k \, \Phi(T, k) - 1]}{(1 - k)\{\Phi(T, k)[1 - k \, \Phi(T, k)] + 2T[2k \, \Phi(T, k) - 1]\}} \tag{3.84}$$

---

[4]It follows from Eq. (3.79) that in the potentials with $k > 0.5$ the increment of the left-side barrier height overcomes the decrement of the right-side barrier height as the tilting force increases. The situation is opposite for the potentials with $k < 0.5$.
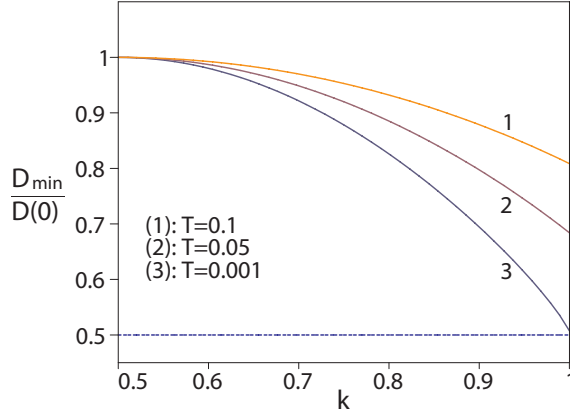
Figure 13: The plot of the ratio $D_{\min}/D(0)$ *vs* the asymmetry parameter k for various values of temperature T.

with

$$\Phi(T,k) = 1 - T(1-k)\ln\left[\frac{k - 2T(2k-1)}{1-k+2T(2k-1)}\right]. \tag{3.85}$$

Substituting $F_{\min}$ from Eq. (3.83) into Eq. (3.81), we obtain for the minimal value of the diffusion coefficient $D_{\min} \equiv D(F_{\min})$ the following expression:

$$D_{\min} = \frac{D(0)}{2\,\Xi^k(T,k)}[1 + \Xi(T,k)][1 + Tk\ln\Xi(T,k)]^2$$
$$\times\ [1 - T(1-k)\ln\Xi(T,k)]^2. \tag{3.86}$$

According to Eq. (3.86), $D_{\min}$ decreases with the increase of the asymmetry parameter k as depicted in Fig. 13. In this figure one can also observe that the minimum of the diffusion coefficient is deeper for smaller noise intensities. From Eq. (3.86) follows the limit

$$\lim_{k\to 1} D_{\min} = \frac{D(0)}{2\,\Xi_0(T)}[1 + \Xi_0(T)][1 + T\ln\Xi_0(T)]^2 \tag{3.87}$$

with

$$\Xi_0(T) = \frac{1-2T}{2T} + \ln\sqrt{\frac{1-2T}{2T}}. \tag{3.88}$$

Equation (3.87) provides the asymptotic lower bound for the maximal suppression of diffusion under a weak external field at fixed temperature T. If $T \to 0$, diffusion vanishes and the ratio $D_{\min}/D(0)$ approaches the lowest
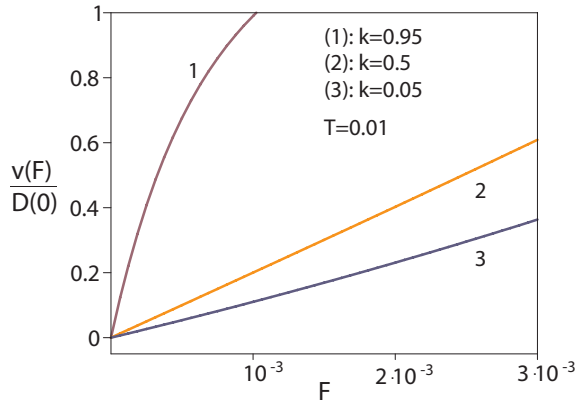
Figure 14: The plot of the current *vs* the tilting force F at fixed temperature $T = 0.01$ for various values of asymmetry parameter k.

value equal to 0.5 when $k \to 1$ (see also Fig. 13). This limiting value corresponds to the asymptotic behaviour of the escape rates at $F = F_{\min}$: if $k \to 1$ and $T \to 0$ then $w_+/w \to 1$ and $w_-/w \to 0$.

Although one can suppress the diffusion by means of an external field, the current *versus* the tilting force is always increasing due to the different roles of the backward escape processes in the diffusive and directed motion of particles. Furthermore, the growth of the current caused by a weak external force is larger just in the potentials where diffusion is reduced by a small bias (see Fig. 14). Such a behaviour becomes comprehensible from the expression of current, Eq. (3.82), according to which the rapid fall of the escape rate w_- under a very weak external field applied to a potential with positive asymmetry (see Fig. 12) acts as an additional trigger in the rise of current as bias is turned on. In Fig. 14 one should also notice that the current approaches zero with negative curvature if $k > 0.5$ and with positive curvature if $k < 0.5$ consistently with the relation [5] [103]

$$D = T(1 - k) \frac{\partial v}{\partial F} \; , \tag{3.89}$$

which becomes asymptotically exact in the limit $F \to 0$. Thus, according to Eq. (3.89), the dependence of the current on the tilting force shown in Fig. 14 reflects equivalently with Fig. 9 the peculiarities of the behaviour of diffusion in the potentials with various asymmetry subject to a weak external field.

The described interrelation between current and diffusion manifests itself also in the dependence of the Péclet number [97–99], on the tilting force.

---

[5]The pre-exponential factor $1 - k$ in Eq. (3.89) appears in connection with the definition of the dimensionless tilting force used.
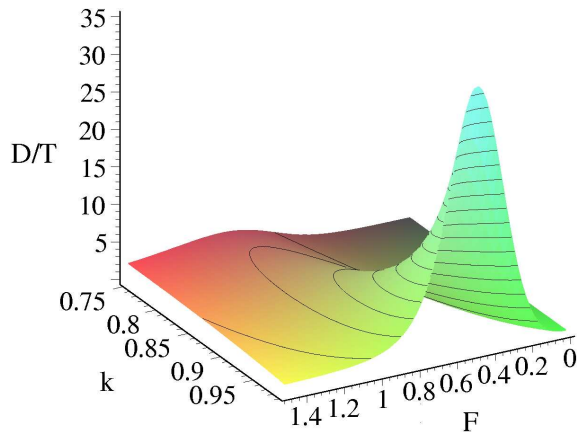
Figure 15: Diffusion coefficient *vs* tilting force F and the potential asymmetry parameter k at fixed temperature $T = 0.1$.

In the weak noise limit we obtain on the basis of Eqs. (3.81) and (3.82) that $\text{Pe} = 2(w_+ - w_-)(w_+ + w_-)^{-1}$. In the external field the Péclet number increases and approaches the value $\text{Pe} = 2$ if $w_-/w_+ \ll 1$. The system reaches the Poissonian regime earlier in the case of positive potential asymmetry due to the suppression of diffusion and the more rapid enhancement of current in the pre-Poissonian region. With the further increase of the tilting force the unidirectional one-step hopping nature of transport is preserved until the inequality $\Delta U_+ \gg T$ holds. However, if the latter condition is violated by a sufficiently strong external field [i.e., the approximate Eqs. (3.81) and (3.82) are not applicable anymore], the Péclet number starts to increase.

The broken spatial inversion symmetry of the periodic system is one of the possible conditions for the appearance of the Brownian motor effect [65, 114, 115]. As shown above, the special case of this symmetry breaking leads to the decrease of diffusion and to the increase of current of particles if a small stationary bias has been applied. Thereby the suitable asymmetry of a periodic potential favours the enhancement of the Péclet number of Brownian motion under a weak external field. This result may have a certain relationship with the conditions for the suppression of the fluctuations of current and for the increase of rectification efficiency in Brownian motor transport studied in Ref. [116].

3.5.4 Non-monotonic behavior of diffusion

In Secs. 3.5.2 and 3.5.3 we studied the behavior of the diffusion coefficient, current and Péclet factor for certain values and limits of temperature and
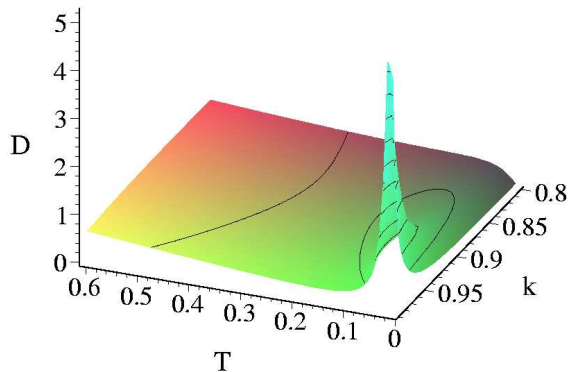
Figure 16: Diffusion coefficient *vs* the temperature T and the potential asymmetry parameter k at fixed $F = 0.95$.

tilting force. We now discuss the general dependencies of the transport characteristics on the system parameters.

The expression of the diffusion coefficient as a function of tilting force F and temperature T is given by Eq. (3.47) together with (3.58), (3.59). The diffusion coefficient as a function of F reveals a qualitatively similar behavior to that found in Refs. [97,98], exhibiting a resonant-like maximum if the temperature is sufficiently low. This effect is strongly influenced by the shape of the periodic potential, as illustrated in Fig. 15. For positive bias ($F > 0$), the increase of the value of the asymmetry parameter k favors the amplification of diffusion compared to free thermal diffusion.

The behavior of the diffusion coefficient as a function of temperature T is similar to that observed in Ref. [99] (see also Ref. [39, 117]): there exists a maximum of $D(T)$, which is followed by a minimum (see Fig. 16). The suppression of $D(T)$ is attributed to the competition between two time scales: noise driven escape time over potential barrier from the minimum along the bias, and the second time scale being the relaxation time into the next potential well from the barrier top [99]. The second time scale is weakly dependent on the noise intensity and has a small variance as opposed to the first one. When the second time scale dominates over the first one, it is expected to result in the suppression of the diffusion coefficient as a function of temperature (see Ref. [99]). The influence of the potential shape on the diffusion coefficient $D(T)$ is analogous to the one on $D(F)$: the peak of $D(T)$ becomes rapidly narrower and higher as k approaches unity.

The analytical properties of the diffusion coefficient as a function of the tilting force and temperature at the fixed value of the asymmetry coefficient are summarized by the contour-plot of the surface $D(F,T)$ in Fig. 17. The surface $D(F,T)$ exhibits two stationary points, a maximum and a saddle
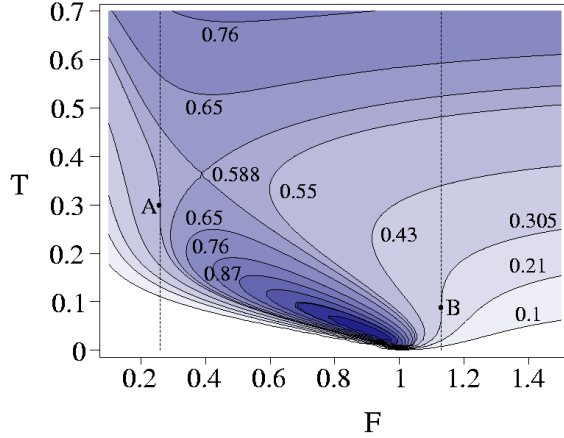
Figure 17: Contour-plot of diffusion coefficient $D = D(F,T)$ for $k = 0.95$. To the maximum and saddle points of D correspond, respectively, the values $F_M \approx 0.9144$, $T_M \approx 0.0364$, $D_M \approx 1.3086$, and $F_S \approx 0.388$, $T_S \approx 0.363$, $D_S \approx 0.588$.

point, whose coordinates are given in the figure caption. The plot reflects the characteristic features of the non-monotonic behavior of diffusion:

(I) Fig. 17 shows that the function $D(T)|_{F=\text{const}}$ has a maximum and a minimum if $F_A < F < F_B$. However, there exists a limiting value $k_E \approx 0.8285$ (see also Fig. 16). For $k < k_E$ the maximum and the saddle point of the surface $D(T,F)$ disappear, while $D(T)|_{F=\text{const}}$ is a monotonic function of temperature, the latter property being independent of bias. There also exists a limiting tilting force $F_C \approx 1.1292$: if $F > F_C$, the dependence $D(T)|_{F=\text{const}}$ is monotonic for arbitrary k. The situation is summarized in Fig. 18, where one sees that the (k,F)-space is divided into two domains where the analytical properties of the diffusion coefficient as a function of temperature are qualitatively different.

(II) Contrary to the dependence $D(T)|_{F=\text{const}}$, the function $D(F)|_{T=\text{const}}$ has a maximum for all values of the asymmetry parameter k.

As one can see in Figs. 16 and 17 the suppression of the diffusion as a function of the temperature is the larger the closer the asymmetry coefficient k and tilting force F to unity; the effect is maximal, if both conditions are fulfilled. This means that the counterintuitive phenomenon that increasing noises decreases diffusion, relies on the large ratio of relaxation to escape time. However, we remark that the nonmonotonic behavior of $D(T)$ persists in the case of a piecewise linear potential also for tilts slightly above the critical value when there is no potential minima.

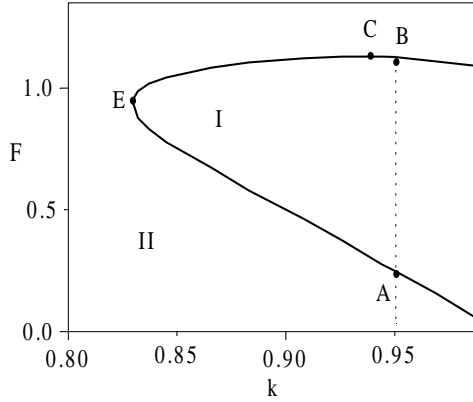One can also observe in Fig. 17 that for the potentials with $k > k_E$

Figure 18: The phase-diagram in the (k, F)-plane representing the regions corresponding to the different analytical properties of the diffusion coefficient as a function of temperature: the dependence $D(T)$ is nonmonotonic in the region I, whereas it is monotonic in the region II.

the maximal value of $D(F)$ as a function of temperature passes through a minimum, i.e., the amplification of diffusion by bias at lower noise intensity can be larger than at higher temperature.

Let us discuss the amplification of diffusion by bias in terms of probability distribution (3.22). Figure 19 represents (in terms of the dimensionless parameters) the probability distributions characteristic of various diffusion levels depending on the tilting force F. Figure 19-a illustrates the situation, where particles are mainly localized around the minima of the potential and transport is strongly suppressed. Diffusion is essentially weaker in comparison with free diffusion: $D/T \sim 10^{-6}$. The probability distribution shown in Fig. 19-b corresponds to the case where the diffusion is approximately maximal ($D/T = 3.5$) for the chosen values of temperature and asymmetry coefficient. In this case the regions with a large probability are separated by the domains where the probability is much smaller, however, large enough to allow the entrance of a sufficient number of particles into these domains. As a result, a channel of hopping-like transport is formed, leading to the enhancement of the ratio $D(F)/D_0$. The further increase of the tilting force F makes the probability distribution still more homogeneous, as seen in Fig. 19-c, and the diffusion approaches the free diffusion limit ($D/T = 1.3$ for the parameter values used in Fig. 19-c). Consequently, the amplified diffusion in the tilted periodic potential is characterized by the specific inhomogeneous probability distribution with spatially alternating domains of high and low probability. The occurrence of a maximum in the of dependence $D(T)$ can be understood in a similar way.

14
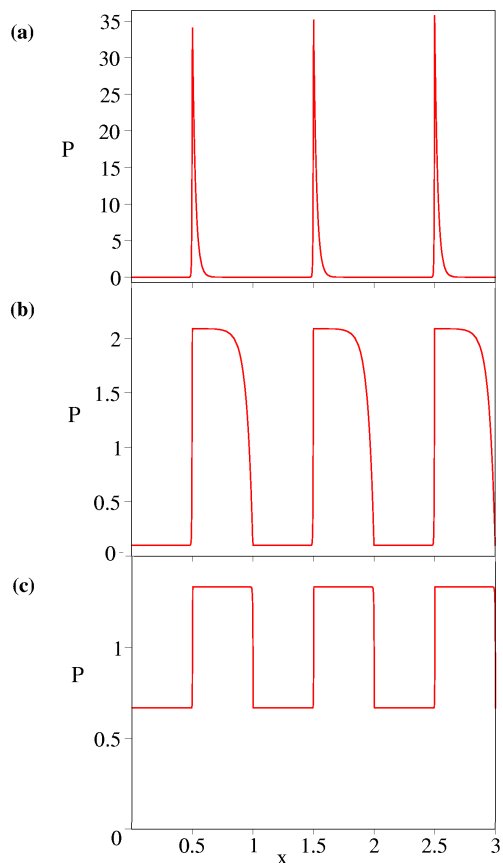
Figure 19: Probability density $P(x)$ for the temperature $T = 0.01$ and asymmetry parameter $k = 0.5$: (a) $F = 0.8$; (b) $F = 1.1$; (c) $F = 3$.

3.5.5 Relation between diffusion and directed motion

With regard to the simultaneous enhancement of diffusion and current, caused by the force F, with respect to an untilted system, the relation between D and v is of interest. One can expect that such a relationship reflects some intrinsic features of the mutual influence between diffusion and current driven by the tilt merely at lower temperatures, when the initial suppression of both components of Brownian transport by periodic potential is stronger.

The comparative plot of D and Pe *versus* F is presented in Figs. 20 and 21. One can see that the function $\text{Pe}(F)$ has a point of inflection which turns into a wide plateau at lower temperatures. For values of F, from zero
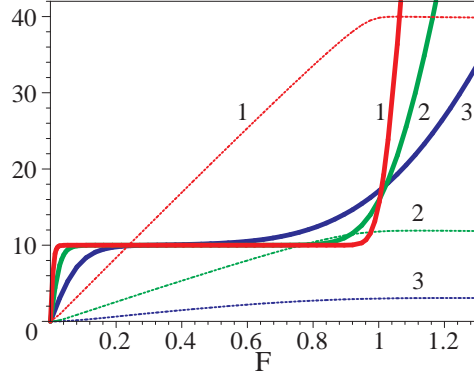
Figure 20: Comparison between the Péclet factor Pe and diffusion coefficient D as a function of tilting force F for various temperatures at fixed $k = 0.5$. Solid lines: $5 \times$ Pe, dashed lines: $\log_{10}[D(F)/D(0)]$. Curves 1: $T = 0.01$, curves 2: $T = 0.03$, curves 3: $T = 0.09$.

Figure 21: Comparison between the Péclet factor Pe and diffusion coefficient D as a function of tilting force F for $k = 0.1$ (dashed lines) and $k = 0.9$ (solid lines) at fixed $T = 0.01$. Curves 1: $\log_{10}[D(F)/D(0)]$, curves 2: $5 \times$ Pe.
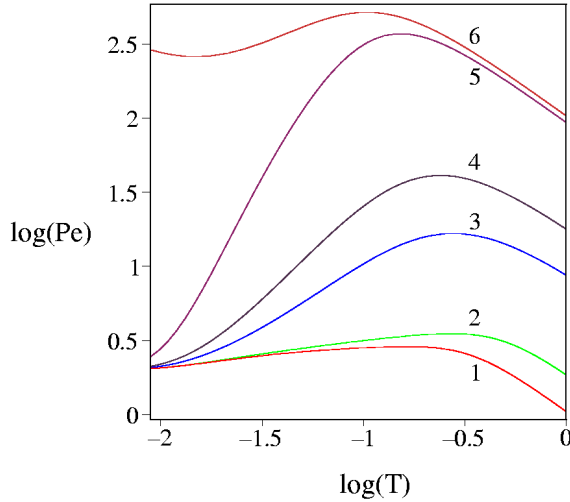
Figure 22: Péclet factor $\log_{10}(\text{Pe})$ *vs* temperature $\log_{10}(T)$ for various values of the potential asymmetry coefficient k at $F = 0.95$ (curves 1-5) and $F = 1.05$ (curve 6). (1) $k = 0.1$, (2) $k = 0.5$, (3) $k = 0.9$, (4) $k = 0.95$, curves 5, 6: $k = 0.99$.
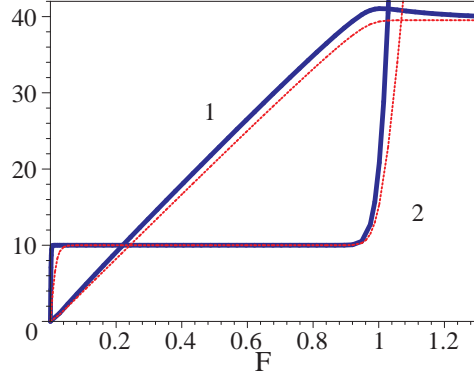
up to the end of the plateau, the behavior of $\text{Pe}(F)$ is described with great accuracy by Eq. (3.78). As the temperature grows, the plateau gradually reduces until disappears and the Péclet factor becomes monotonically increasing. We emphasize that the domain where $\text{Pe} = 2$ coincides with the domain where the increase of the diffusion coefficient as a consequence of the tilting is the most rapid. Consequently, in the region of parameters, where the substantial enhancement of diffusion (and also current) occurs, directed transport and diffusion are closely synchronized. As mentioned, the stabilization of the Péclet factor at the value $\text{Pe} = 2$ is a characteristic feature of Poissonian process [54] such as the Poisson enzymes in kinesin kinetics [118–120]. The location of the end of this region at larger values of F is quite insensitive to the shape of the periodic potential, as seen in Fig. 21, and is located approximately at critical tilt F_{cr}.

In Fig. 22 the curves of the Péclet factor *versus* temperature for various values of k and F are depicted. The function $\text{Pe}(T)$ passes through a maximum (curves 1-5) for $F < F_{\text{cr}}$, which is also present slightly above the critical tilt (curve 6). With a further increase of F, the maximum of $\text{Pe}(T)$ disappears. From Fig. 22 one can also see that the optimal level of Brownian transport, determined by the maximal value of the Péclet number, is sensitive to the shape of periodic potential: at $F < F_{\text{cr}}$ the optimal level of transport rises with an increase in k. At the same time, the larger values of k make a minimum of $D(T)$, which follows a maximum of $D(T)$
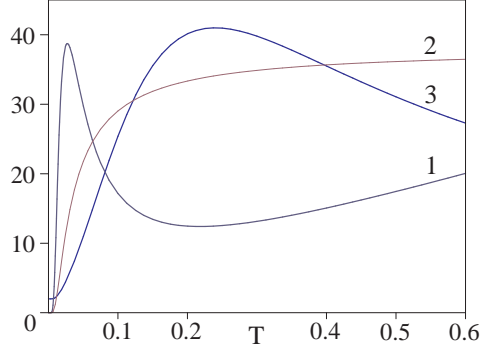
Figure 23: Diffusion coefficient, current, and Péclet factor *vs* temperature T for $k = 0.95$, $F = 0.95$: (1) $30 \times D$; (2) $2 \times v$; (3) Pe.

at a higher value of temperature, deeper (the effect can be anticipated in Fig. 16). Figure 23 shows that the enhancement of the Péclet number for a certain temperature is associated with the suppression of diffusion by the same factor (collate also Figs. 22 and 16).

3.6 Transport in potentials with two minima per period

3.6.1 Analytic computations

The analytical results for the diffusion coefficient, current and Péclet factor in a piecewise linear potential with two minima per period, defined by Eq. (3.43) with (3.44), are obtained similarly to the calculations for the simple sawtooth potential. In the case of the double-hump potential, in Eqs. (3.47)-(3.49) the quantities Z and Y now have the form (see also Fig. 8),

$$
Z = \int\limits_{0}^{k_1} dx\, H_{-a}(x) + \int\limits_{k_1}^{k_2} dx\, H_{-b}(x) + \int\limits_{k_2}^{k} dx\, H_{-c}(x) + \int\limits_{k}^{1} dx\, H_{-d}(x)\,,
$$

$$(3.90)$$

$$
Y = \int\limits_{0}^{k_1} dx\, H_{+a}(x)\, H_{-a}^2(x) + \int\limits_{k_1}^{k_2} dx\, H_{+b}(x)\, H_{-b}^2(x)
$$

$$
+ \int\limits_{k_2}^{k} dx\, H_{+c}(x)\, H_{-c}^2(x) + \int\limits_{k}^{1} dx\, H_{+d}(x)\, H_{-d}^2(x)\,. \qquad (3.91)
$$

Here

$$H_{\pm a}(x) = D_0^{-1} e^{\frac{-F(1\pm 1)}{2T(1-k)}} e^{\pm u_{a1}(x)} \left[\int\limits_x^{k_1} dy\, e^{\mp u_{a1}(y)} + \int\limits_{k_1}^{k_2} dy\, e^{\mp u_{b1}(y)} \right.$$
$$\left. + \int\limits_{k_2}^{k} dy\, e^{\mp u_{c1}(y)} + \int\limits_k^1 dy\, e^{\mp u_{d1}(y)} + \int\limits_1^{x+1} dy\, e^{\mp u_{a2}(y)} \right],$$

$$H_{\pm b}(x) = D_0^{-1} e^{\frac{-F(1\pm 1)}{2T(1-k)}} e^{\pm u_{b1}(x)} \left[\int\limits_x^{k_2} dy\, e^{\mp u_{b1}(y)} + \int\limits_{k_2}^{k} dy\, e^{\mp u_{c1}(y)} \right.$$
$$\left. + \int\limits_k^1 dy\, e^{\mp u_{d1}(y)} + \int\limits_1^{k_1+1} dy\, e^{\mp u_{a2}(y)} + \int\limits_{k_1+1}^{x+1} dy\, e^{\mp u_{b2}(y)} \right],$$

$$H_{\pm c}(x) = D_0^{-1} e^{\frac{-F(1\pm 1)}{2T(1-k)}} e^{\pm u_{c1}(x)} \left[\int\limits_x^{k} dy\, e^{\mp u_{c1}(y)} + \int\limits_k^1 dy\, e^{\mp u_{d1}(y)} \right.$$
$$\left. + \int\limits_1^{k_1+1} dy\, e^{\mp u_{a2}(y)} + \int\limits_{k_1+1}^{k_2+1} dy\, e^{\mp u_{b2}(y)} + \int\limits_{k_2+1}^{x+1} dy\, e^{\mp u_{c2}(y)} \right],$$

$$H_{\pm d}(x) = D_0^{-1} e^{\frac{-F(1\pm 1)}{2T(1-k)}} e^{\pm u_{d1}(x)} \left[\int\limits_x^1 dy\, e^{\mp u_{d1}(y)} + \int\limits_1^{k_1+1} dy\, e^{\mp u_{a2}(y)} \right.$$
$$\left. + \int\limits_{k_1+1}^{k_2+1} dy\, e^{\mp u_{b2}(y)} + \int\limits_{k_2+1}^{k+1} dy\, e^{\mp u_{c2}(y)} + \int\limits_{k+1}^{x+1} dy\, e^{\mp u_{d2}(y)} \right]. \tag{3.92}$$

The explicit algebraic expressions for Z and Y in the case of a potential with two minima per period are reported in Appendix A.

3.6.2 The case of zero bias

In the absence of bias ($F = 0$) the diffusion coefficient is given by $D = Z^{-1}$. In the case of the sawtooth potential with two minima per period we can write $Z = Z_1 + Z_2$ with

$$Z_1 = 2T \left\{ g_{\delta\alpha}\, g_{\alpha\beta} \left[\cosh\left(\frac{1-A_1}{T}\right) - 1 \right] + g_{\alpha\beta}\, g_{\beta\gamma} \left[\cosh\left(\frac{A_2-A_1}{T}\right) - 1 \right] \right.$$
$$\left. + g_{\beta\gamma}\, g_{\gamma\delta} \left[\cosh\left(\frac{A_2}{T}\right) - 1 \right] + g_{\gamma\delta}\, g_{\delta\alpha} \left[\cosh\left(\frac{1}{T}\right) - 1 \right] \right\}, \tag{3.93}$$
$$Z_2 = -2T \left\{ g_{\alpha\beta}\, g_{\gamma\delta} \left[\cosh\left(\frac{A_1}{T}\right) - 1 \right] + g_{\delta\alpha}\, g_{\beta\gamma} \left[\cosh\left(\frac{1-A_2}{T}\right) - 1 \right] \right\}.$$

The quantities $g_{\mu\nu}$, with $\mu, \nu = \alpha, \beta, \gamma, \delta$ (see Fig. 8), are defined as

$$g_{\mu\nu} = \frac{1}{\tan\mu} + \frac{1}{\tan\nu}. \tag{3.94}$$

The four terms in Z_1 correspond to the four potential barriers (in general of different height) that the particle overcomes per period due to the diffusive motion. The higher these barriers are compared to the temperature, the larger is the factor Z_1 and the more suppressed is the diffusion. The
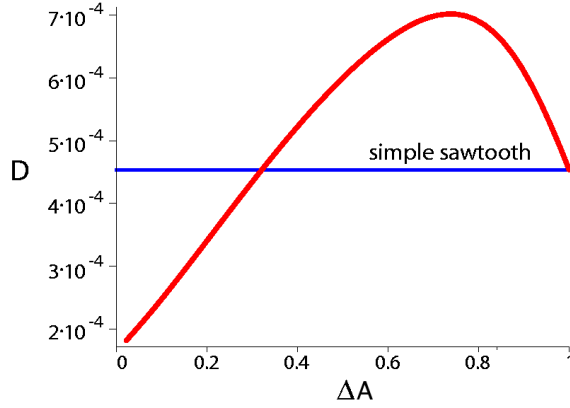
Figure 24: Diffusion coefficient D as a function of ΔA in the symmetric bi- and metastable periodic potentials in the absence of the tilting force; the temperature is $T = 0.1$.

coefficients $g_{\mu\nu}\, g_{\nu\sigma}$ take into account the shape of the minimum as well as the shape of the maximum of the potential associated with the corresponding barrier. The two terms in Z_2 take into account the differences of the extrema from the minimum value $A_1 = 0$ and from the maximum value $A_2 = 1$.

For potentials with $\Delta A = A_2 - A_1 = 1$, the factor Z_2 vanishes, i.e. $Z_2 = 0$. As correspondingly $g_{\delta\alpha}\, g_{\alpha\beta} + g_{\alpha\beta}\, g_{\beta\gamma} + g_{\beta\gamma}\, g_{\gamma\delta} + g_{\gamma\delta}\, g_{\delta\alpha} = 1$, then Z_1 does not depend anymore on the values of the asymmetry parameters $k_{1,2}$ and k (see Fig. 8), and $Z = Z_1 = 2T\,[\cosh(T^{-1}) - 1]$, like in the case of the simple sawtooth potential [c.f. Eq. (3.61)]. However, in the following we assume that $\Delta A < 1$, and then $Z_2 < 0$.

If we consider a Brownian particle moving in a bistable potential, that is, $A_1 = 0$ but $A_2 \neq 1$, then

$$
\begin{aligned}
Z_1 &= 2T\, g_{\alpha\beta\gamma\delta} \left\{ g_{\beta\gamma} \left[\cosh\!\left(\tfrac{\Delta A}{T}\right) - 1 \right] + g_{\delta\alpha} \left[\cosh\!\left(\tfrac{1}{T}\right) - 1 \right] \right\}, \\
Z_2 &= -2T\, g_{\beta\gamma}\, g_{\delta\alpha} \left[\cosh\!\left(\tfrac{1-\Delta A}{T}\right) - 1 \right].
\end{aligned}
\tag{3.95}
$$

If instead $A_2 = 1$ and $A_1 \neq 0$ then the potential is metastable and

$$
\begin{aligned}
Z_1 &= 2T\, g_{\alpha\beta\gamma\delta} \left\{ g_{\alpha\beta} \left[\cosh\!\left(\tfrac{\Delta A}{T}\right) - 1 \right] + g_{\gamma\delta} \left[\cosh\!\left(\tfrac{1}{T}\right) - 1 \right] \right\}, \\
Z_2 &= -2T\, g_{\alpha\beta}\, g_{\gamma\delta} \left[\cosh\!\left(\tfrac{1-\Delta A}{T}\right) - 1 \right].
\end{aligned}
\tag{3.96}
$$

In Eqs. (3.95) and (3.96) $g_{\alpha\beta\gamma\delta} = \sum_{\mu=\alpha,\beta,\gamma,\delta} \tan^{-1}\mu$.
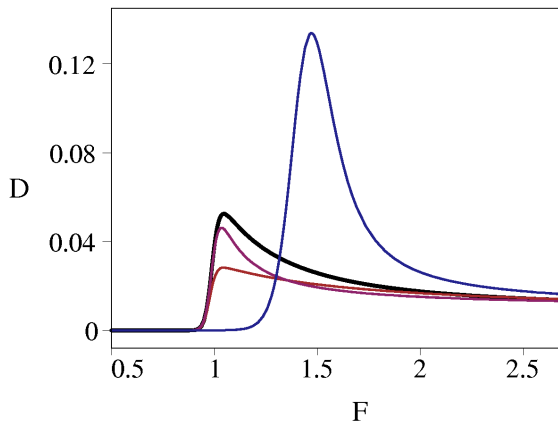
Figure 25: The enhancement and suppression of the diffusion coefficient, compared to the simple sawtooth potential, due to the additional trap. $T = 0.01$; $k = 0.6$, $\Delta A = 0.45$. In the decreasing order of the maximal values of $D(F)$: (1) $F_{ce} = 1.5$; (2) simple sawtooth potential; (3) $F_{ce} = 0.5$; (4) $F_{ce} = F_{cr} = 1$.

In the case of a symmetric metastable potential $\alpha = \beta$ and $\gamma = \delta$, for the bistable one $\alpha = \delta$ and $\beta = \gamma$, and one can see that the quantities Z_1 and Z_2, and thus the diffusion coefficient, coincide for the same values of ΔA for the two types of potentials. If the potentials are asymmetric then the behavior of the diffusion coefficients D *versus* ΔA can be different. The dependence of the diffusion coefficient in symmetric bi- and metastable potentials *versus* the additional barrier height is illustrated in Fig. 24. In this figure one can also see that it is possible to have a situation where the diffusion in a potential with two minima per period is suppressed compared to the case of a simple sawtooth potential, though from the condition $Z_2 < 0$ one could assume that an additional trap in general should promote diffusion. Namely, if the value of ΔA is sufficiently small the effective potential contains the segments where the deterministic force is approximately zero, which causes the suppression of the diffusion. Comparable results for the behaviour of $D(\Delta A)$ are found in Ref. [107] at a high friction regime. However, in Ref. [107] the motion is not completely overdamped yet and the diffusion coefficient rises at the values $\Delta A \to 0$ which obviously is an inertial effect. In the overdamped limit such a region is absent and the value of diffusion coefficient at $\Delta A = 0$ is

$$D = 2\left\{ T\left[\cosh\left(\frac{1}{T}\right) - 1 \right] + \sinh\left(\frac{1}{T}\right) + \frac{1}{2T} \right\}^{-1}. \tag{3.97}$$
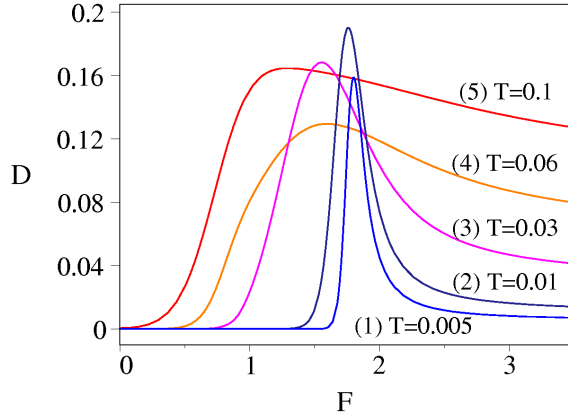
Figure 26: Diffusion coefficient $D(F)$ for different values of temperature. Potential parameters: $k_1 = 0.4$, $k_2 = 0.5$, $k = 0.6$, $A_1 = 0.55$, $A_2 = 1$; $F_{ce} = 1.8$.

3.6.3   The two-step enhancement of diffusion

Before proceeding with the discussion of the results, we first emphasize that the general character of the transport process is, compared to the corresponding simple sawtooth case, determined by the value of F_{ce}, and thus for a fixed k by the differences ΔA and Δk. The values of single parameters k_1, k_2, A_1, A_2 are of no importance, while the differences ΔA and Δk are crucial, even if the values of F_{ce}, determined by them, are the same.

A double-hump potential gives a possibility to favor or suppress the maximal value of the diffusion coefficient $D(F)$, compared to the case of the simple sawtooth potential. The situation is illustrated in Fig. 25. In the case $F_{ce} < F_{cr}$ the maximal value of $D(F)$ is decreased due to the additional potential minima. The decrease is, at fixed k and ΔA, the largest if $F_{ce} = F_{cr}$. For $F_{ce} > F_{cr}$ diffusion starts to increase. If F_{ce} is larger than the value of the tilting force, which corresponds to the maximum of $D(F)$ in the case of the simple sawtooth potential, then the maximal value of diffusion increases due to the extra trap (see also Ref. [121]).

Henceforth our main interest will be focused on the potentials with $F_{ce} > F_{cr}$, which provide new phenomena with respect to the case of the simple periodic potentials. The case $F_{ce} < F_{cr}$ does not differ much from the case of the simple sawtooth potential, if $F \to F_{cr}$. However, we remark that in biological systems the potentials, for which $F_{ce} < F_{cr}$, often play a role [111].

In Fig. 26 we have plotted the diffusion coefficient *versus* tilting force
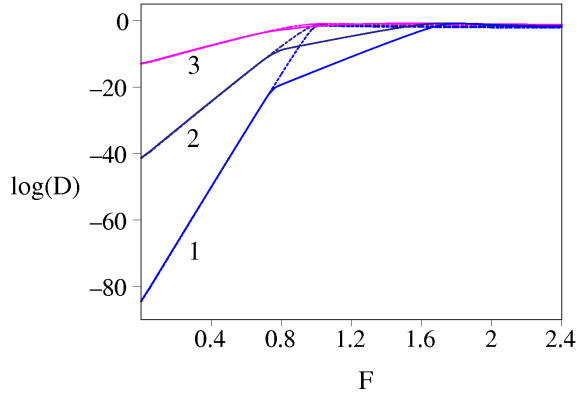
Figure 27: Diffusion coefficient $\log_{10}[D(F)]$ for different noise intensities. Solid lines: The potential parameters are the same as in Fig. 3; (1) $T = 0.005$; (2) $T = 0.01$; (3) $T = 0.03$. Dashed lines: Diffusion coefficients for the simple sawtooth potential with asymmetry parameter $k = 0.6$ at the same temperatures.

at different values of temperature, for a potential for which $F_{ce} > F_{cr}$ [6]. As can be seen, at lower noise intensities, the maximal value of the diffusion coefficient $D(F)$ can be larger than at higher noise intensities (compare curves 2, 3 and 4 with each other, or 1 with 4, or 2 with 5). At low and high values of temperature the situation is back to usual (compare curves 1 with 2, and 4 with 5). As one can see in Fig. 17 the analogous situation is observable for the simple sawtooth potential in the case $k > k_E$. However, the additional potential maximum per period with $F_{ce} > F_{cr}$ allows one to obtain the effect also for the potentials with asymmetry parameter $k < k_E$. The general behavior of the diffusion coefficient $D(T, F)$ is the same as one can see in Fig. 17, for the potential with one minimum per period.

Figure 27 represents the dependence $D(F)$ in the case of the same potential as used in Fig. 26, but in a logarithmic scale. In this plot one can distinguish two growth rates (slopes) for the diffusion coefficient (see also Fig. 29). The two rates are the more different, the lower the noise intensity, and associate with the two Poissonian processes (the latter fact will be discussed in more detail in next section). Thereby the Poissonian process in the first region coincides with the one which takes place in the corresponding simple sawtooth potential. The picture for the current is similar.

The presence of two potential barriers may lead one to think that there can be two maxima of the diffusion coefficient *versus* tilting force, but in

[6]If not marked otherwise in the figure caption, we henceforth calculate all the graphics for the same values of potential parameters: $k_1 = 0.4$, $k_2 = 0.5$, $k = 0.6$, $A_1 = 0.55$, $A_2 = 1$; $F_{ce} = 1.8$.
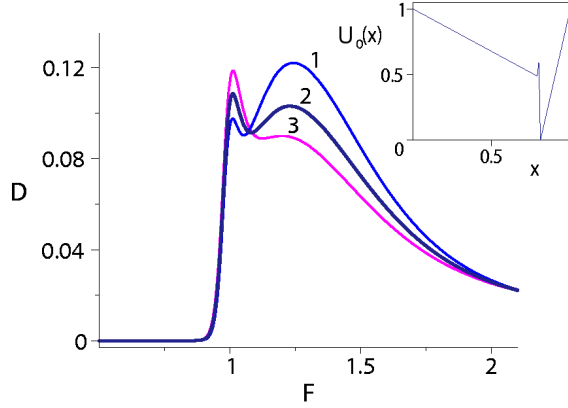
Figure 28: The existence of two maxima for diffusion coefficient *vs* tilting force F for different noise intensities: (1): $T = 0.0095$; (2): $T = 0.01$; (3): $T = 0.0105$. The potential parameters are: $k_1 = 0.79$, $k_2 = 0.8$, $k = 0.81$, $A_1 = 0.888$, $A_2 = 1$; the corresponding periodic potential is also depicted.

practice such a situation is difficult to obtain. Nevertheless, for a certain potential shape it is indeed the case (see Fig. 28).

Now, if the Brownian particle is in a simple sawtooth potential with a positive asymmetry ($k > 0.5$) and there is a very small constant force influencing the system, then the diffusion is suppressed respect to the case $F = 0$ (see Sec. 3.5.3 but also Ref. [117]). The same is valid for potentials with two minima per period if at least one of the potential minima is asymmetric to the right, this means $k_1 > k_2/2$ or/and $k > (1 - k_2)/2$. Furthermore, for a certain type of potential shape one can observe the suppression of diffusion also at the larger tilting forces giving rise to a double-maximum in the diffusion coefficient $D(F)$, as demonstrated in Fig. 28. In fact, astonishing is not the suppression of the diffusion coefficient, but its increase after the decrease. To obtain such a double-enhancement the slope of the additional potential barrier must be much bigger compared to the one of the main barrier, and the height of the barrier must be relatively small ($\Delta A = 10\,T$, $T \approx 10^{-2}$). The decrease of the diffusion coefficient *versus* tilting force takes first of all place due to the disappearance of the main potential barrier. For $F = 1$ particles can be in the region of free diffusion or trapped in the additional potential minimum. In that case for every value of F, which is very slightly larger than the previous value, we can consider the situation to be equal to the one of tilting force close to zero, whereas the actual external force is small compared to the critical force at which the potential has no minima anymore. Thus as an additional effect the diffusion is decreased similarly to the suppression which takes place at
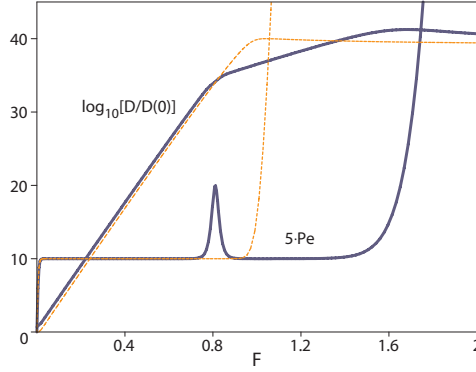
Figure 29: The comparison of the diffusion coefficient D and Péclet number Pe as the functions of tilting force F. Dashed line: simple sawtooth potential; solid line: double-hump potential with $k_1 = 0.3$, $k_2 = 0.38$, $k = 0.65$, $\Delta A = 0.4$. Temperature $T = 0.01$.

small values of the tilting, as discussed in Sec. 3.5.3. Further the diffusion coefficient increases due to the enhancement of diffusion as it takes place also in the simple potentials, and due to the delocalization process as the effective barrier height gets smaller. Since the value of the tilting is actually not zero, but is very large, and the height of the potential barrier is small compared to the temperature, then the diffusion decreases to the free diffusion level already before exceeding the critical tilting.

For most of the potentials with $\beta > \delta$, however, the diffusion coefficient $D(F)$ does not have two maxima, but the enhancement of diffusion is characterized by two regions related to the two potential minima (see Fig. 27).

3.6.4 Relation between diffusion and current

In the case of a simple sawtooth potential we showed that at low temperatures and for a subcritical tilt, i.e., for $F < F_{cr}$, the Péclet number stabilizes at the value $\text{Pe}(F) = 2$. In this parameter region, where the enhancement of diffusion is most rapid, the particles are mainly localized around the potential minima and transport can be described with great accuracy by the Poissonian hopping process.

Now, for the potentials with two minima per period for which $\beta > \delta$, there exists a threshold value of the tilting force

$$F_0 = \frac{(1 - \Delta A)(1 - k)}{1 - k - \Delta k} \tag{3.98}$$

64
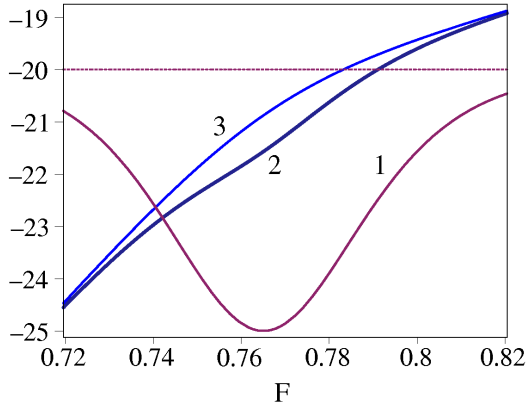
Figure 30: The appearance of the minimum in the randomness parameter $r(F)$, i.e., the maximum in the Péclet number, in the region of the crossover. The curves represent the randomness parameter, diffusion coefficient and current *vs* tilting force at $T = 0.01$: (1) $10 \times (r-3)$; (2) $\ln(2D)$; (3) $\ln(\langle \dot{x} \rangle)$; The dashed line corresponds to the randomness value $r = 1$ (Poissonian process).

at which the main potential barrier becomes smaller than the additional barrier. If $F < F_0$, particles are mainly localized near the primary traps, whereas if $F > F_0$, near the extra traps. As a result the enhancement of diffusion *versus* tilting force is realized through two different Poissonian processes. As seen in Fig. 29, the two regions of the enhancement of diffusion correspond to these different Poisson processes. Thereby the Poissonian process in the first region coincides with the one which takes place in the corresponding simple sawtooth potential.

In the region of crossover between the two regimes of the enhancement of diffusion, the Péclet number passes through a sharp maximum with the characteristic value Pe = 4. Thus, in a certain region of the tilting force a small variation of the potential has an influence on the character of transport (cf. Ref. [122]). The observed enhancement of the Péclet number appears in the region, where the growth regime of diffusion and current changes, whereas the increase of diffusion slows down compared to the increase of current (see Fig. 30). In this case the average populations of the primary traps and the extra traps are close to one another and the possibility of the localization of Brownian particles near the minima of both types is considerable, leading to the relative suppression of diffusion. The suppression is the largest if both of the potential traps are switched on with equal weights. Such a doubling of the effective number of the localization centers in the region of Poissonian process gives a qualitative explanation for the universal
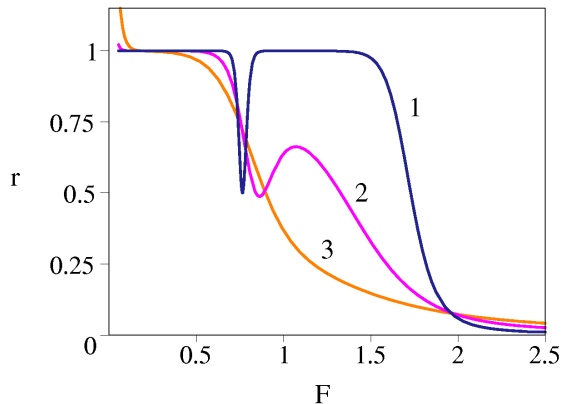
Figure 31: Randomness parameter r *vs* tilting force F for different noise intensities: (1) $T = 0.01$; (2) $T = 0.03$; (3) $T = 0.06$.

value of Péclet number $\mathrm{Pe} = 4$.

For the existence of the extremum in the Péclet number *versus* tilt, the condition $F_{\mathrm{ce}} > 1$ must be satisfied. The tilting force F_0 has a physical meaning only if the latter inequality is fulfilled, having the value in the range $0 < F_0 < 1$. This circumstance follows [7] from Eq. (3.98) together with Eq. (3.40) for F_{ce} which lead to the relation

$$(1 - F_0) = \frac{\Delta k}{1 - k - \Delta k} \left(F_{\mathrm{ce}} - 1 \right) \tag{3.99}$$

(see also Ref. [121]). If $F_{\mathrm{ce}} < 1$, the Péclet number $\mathrm{Pe}(F)$ does not have a maximum [8]. On the other hand, if $F_0 < 1$ is sufficiently close to unity, the peak of Péclet number merges into the region where the motion can no longer be described as the Poissonian process and $\mathrm{Pe}(F)$ increases monotonically. In particular, such a case is actual for the potentials for which the diffusion coefficient $D(F)$ possesses two maxima.

With the rise of temperature the peak of the Péclet number disappears. We have illustrated the situation in Fig. 31 for the randomness parameter. At higher temperature the posterior part of the plateau of randomness parameter diminishes and the minimum broadens, and finally the randomness decreases and the Péclet number increases monotonically.

In the case of the simple sawtooth potential we observed the possibility to obtain the existence of a maximum in the Péclet number *versus* tem-

---

[7]Note that for $F_{\mathrm{ce}} > 1$ the condition $\Delta k < 1 - k$ must be always fulfilled as one can see from Eq. (3.40).

[8]The inequality $F_{\mathrm{ce}} < 1$ is valid always if $\Delta k > 1 - k$ (see Eq. (3.40)) and then one can see from Eq. (3.98) that $F_0 < 0$. However, condition $F_{\mathrm{ce}} < 1$ can be satisfied also for $\Delta k < 1 - k$ which yield on the basis of Eq. (3.99) $F_0 > 1$.
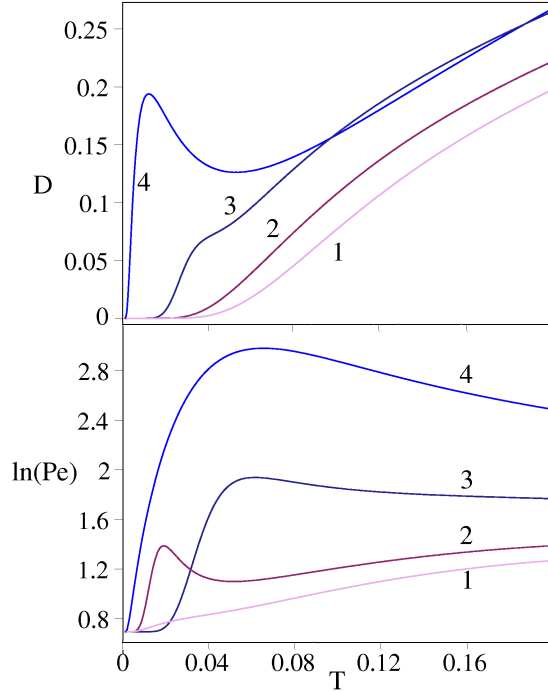
Figure 32: Diffusion coefficient D and $\ln(\text{Pe})$ *vs* temperature T for different values of tilting force F: (1) $F = 0.7$; (2) $F = 0.8$; (3) $F = 1.1$; (4) $F = 1.75$.

perature (cf. Ref. [99]), in connection with the minimum in the diffusion coefficient, for increasing noise intensity. In Ref. [117] it is pointed out that for a homogeneous system the Péclet number can show a maximum, although neither the diffusion coefficient nor the average current density shows an extremum. The present model allows us to observe for different tilts both the phenomena as one can see in Fig. 32 (the situation is actually valid also for the simple sawtooth potential, however, in Fig. 22 it is intricate to understand). Furthermore, as one can see in Fig. 33, in the region of static external force, where $\text{Pe}(F)$ exhibits a maximum (minimum in the randomness factor), the Péclet number temperature T has two maxima, and is extremely sensitive to the noise intensity.

3.7 Summary

In this chapter we carried out a comprehensive investigation of the overdamped Brownian motion in tilted periodic potentials with one and two minima per period in the presence of thermal noise. We did this for piece-
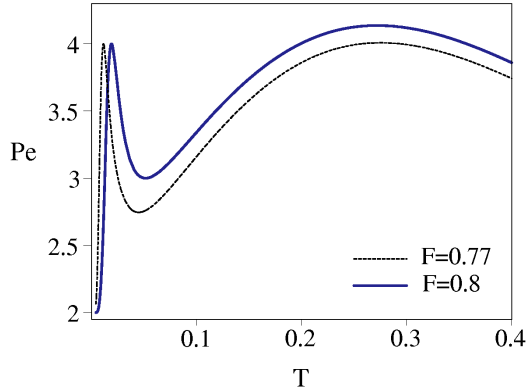
Figure 33: The existence of two maxima in the Péclet number Pe *vs* temperature T.

wise linear potentials, which can be considered as a first approximation to potentials of arbitrary shapes. We derived explicit algebraic expressions for the diffusion coefficient, particle current, and Péclet number, and analyzed their dependencies on temperature, tilting force, and the shape of the potentials.

We demonstrated that piecewise linear potentials show all effects characteristic of tilted periodic potentials. Furthermore, merely varying the potential shape allows one also to reproduce all phenomena occurring in systems with spatially periodic temperature and inhomogenous dissipation [39,117]. The transport properties of particles in the potentials with two minima per period were shown to exhibit in certain parameter regions new and qualitatively different features.

We showed that large values of the asymmetry parameter k in the direction of bias F favor the amplification of diffusion in comparison with free thermal diffusion. In the case of potentials with two minima per period the enhancement of diffusion is characterized by two regions, while for certain values of the potential parameters, the effective diffusion coefficient $D(F)$ can have two maxima. The necessary and sufficient conditions for the non-monotonic behavior of the diffusion coefficient as a function of temperature were established in the case of a simple sawtooth potential.

We showed that the potential shape has a great influence also on the Péclet number (randomness of Brownian transport) in a certain region of temperature. However, at low temperatures and subcritical tilts the Péclet number was demonstrated to have the value characteristic of a Poissonian process practically independent of the potential shape. The domain, where the Péclet factor exhibits the plateau, coincides with the domain where

the enhancement of diffusion coefficient is maximal. Consequently, in the region of parameters where substantial enhancement of diffusion occurs, current and diffusion are exactly synchronized. In the case of double-hump potentials the enhancement of diffusion is related to two different Poissonian processes, while in the region of crossover at low temperature a rise of the Péclet factor takes place. For the values of the tilting, corresponding to the enhancement of $\text{Pe}(F)$, the Péclet number *versus* noise intensity has two maxima.

In conclusion, we demonstrated that transport processes in periodic potentials are extremely sensitive to the value of noise intensity and bias, and that also the shape of the periodic potential has a significant influence in determining the character of stochastic transport.

4 Diffusion of dimers in a washboard potential

4.1 Motivation

One particular example of Brownian motion on a periodic substrate is the diffusion of atoms and molecules on crystal surfaces [19–23,123]. This mechanism is of both conceptual and technological interest [124, 125], being relevant to heterogeneous nucleation, catalysis, surface coating, thin-film growth, etc. Individual atoms diffusing on a surface can eventually meet and form dimers or trimers. For example, on a semiconductor Si(100) or Ge(100) surface, most of the deposited Si or Ge atoms form dimers. Atoms adsorbed on metal surfaces may also form closely packed islands that diffuse as a whole [126–136]. This raises the issue of the role of the internal degrees of freedom on the transport of extended objects through micro- and submicro-devices.

One of the most important problems in modern nanotechnology is how to manipulate small particles in order to perform a preassigned operation. For instance, the mobility and diffusivity of atoms adsorbed onto crystal surfaces can be controlled by applying deterministic forces [137, 138]. A direct manipulation method consists in applying a constant ("direct current" or dc) local electric field by means of a scanning tunnel microscope tip [139–141]. A selected adatom or admolecule with nonzero charge will then move in the direction of the electric force; neutral particles will be forced into a region of a stronger field due to induced polarization [142, 143]. This problem can be modeled as a Brownian motion on a tilted periodic two-dimensional substrate.

In this part of the work we study the transport of a dimer confined on a periodic substrate with a focus on the effects of the internal degrees of freedom on its mobility and diffusivity. For simplicity, we restrict our analysis to substrates in two or higher dimensions, which can be effectively reduced to one-dimensional systems. In the simple case of a dimer driven by a constant force oriented along a symmetry axis of a two-dimensional substrate, one wants to characterize the stationary transport in the force direction, whereas transverse diffusion is not affected by the bias. Of course, the results presented in this chapter apply well also to a variety of physical and biological systems, where the particle dynamics is naturally constrained to (quasi) one-dimensional substrates. Examples of current interest include colloids [144,145] or cold atoms [146,147] in optical traps, superconducting vortices in lithographed tracks [148,149], ion-channels [150], cell membranes [151], artificial and natural nanopores [152–155], molecular motors [73–75, 114,115,156–159], as well as dislocation dynamics [160–162].

4.2 Model

A monomer moving on a one-dimensional periodic substrate with potential $U_0(x) = U_0(x + L)$ under the influence of an external dc bias F and at finite temperature T can be described by the Langevin equation (3.1), where $\eta = m\gamma$ is assumed, with γ being a damping constant. For a symmetric dimer consisting of two interacting Brownian particles the corresponding Langevin equations have the form

$$
\begin{aligned}
m\ddot{x}_1 &= -\frac{\partial U(x_1,x_2)}{\partial x_1} + F - \eta\dot{x}_1 + \xi_1(t)\,, \\
m\ddot{x}_2 &= -\frac{\partial U(x_1,x_2)}{\partial x_2} + F - \eta\dot{x}_2 + \xi_2(t)\,.
\end{aligned}
\tag{4.1}
$$

Here $\xi_i(t)$, $i = 1, 2$, are two independent zero-mean stochastic processes with autocorrelation function

$$
\langle \xi_i(t)\xi_j(t') \rangle = 2\eta k_B T\, \delta_{ij}\, \delta(t - t')\,.
\tag{4.2}
$$

Note that the interparticle interaction is incorporated in the substrate potential function,

$$
U(x_1, x_2) = U_0(x_1) + U_0(x_2) + \frac{K}{2}\,(x_2 - x_1 - a_0)^2\,.
\tag{4.3}
$$

That is, we assume the interaction between the two dimer particles to be harmonic with coupling constant K and equilibrium distance a_0. The simplest choice for the periodic substrate potential is [54]

$$
U_0(x) = A_0 \cos(kx)\,,
\tag{4.4}
$$

with $k = 2\pi L^{-1}$.

The Langevin equations for a monomer and a dimer can be conveniently rescaled. By introducing suitable space, energy, and time units,

$$
\lambda = k^{-1}\,, \qquad \epsilon = A_0\,, \qquad \tau = \sqrt{\lambda^2 m/\epsilon}\,,
\tag{4.5}
$$

we define the dimensionless quantities:

$$
\begin{aligned}
\tilde{x} &= x\lambda^{-1}\,, & \tilde{L} &= L\lambda^{-1}\,, & \tilde{a}_0 &= a_0\lambda^{-1}\,, \\
\tilde{T} &= k_B T\epsilon^{-1}\,, & \tilde{F} &= \lambda F\epsilon^{-1}\,, & \tilde{K} &= \lambda^2 K\epsilon^{-1}\,, \\
\tilde{t} &= t\,\tau^{-1}\,, & \tilde{\gamma} &= \gamma\tau\,, & \tilde{\xi}(\tilde{t}) &= \lambda\,\xi(t)\epsilon^{-1}\,.
\end{aligned}
\tag{4.6}
$$

No particle can be trapped by the potential (4.4) under any circumstances for tilting larger than the critical value $\tilde{F}_{\mathrm{cr}} = 1$ (in rescaled units). In the following we drop the tilde altogether and only use dimensionless units.

After rescaling, the Langevin equation (3.1) for a monomer moving in the potential (4.4) we obtain,

$$
\ddot{x} = \sin x + F - \gamma\dot{x} + \xi(t)\,,
\tag{4.7}
$$

where the autocorrelation function of the rescaled noise is $\langle \xi(t)\,\xi(t')\rangle = 2\,\gamma T\,\delta(t - t')$. Analogously, the coupled Langevin equations (4.1) for a symmetric harmonic dimer in the same substrate potential become [see Eq. (4.3)],

$$
\begin{aligned}
\ddot{x}_1 &= \sin x_1 + F + K(x_2 - x_1 - a_0) - \gamma \dot{x}_1 + \xi_1(t)\,, \\
\ddot{x}_2 &= \sin x_2 + F - K(x_2 - x_1 - a_0) - \gamma \dot{x}_2 + \xi_2(t)\,,
\end{aligned}
\tag{4.8}
$$

with $\langle \xi_i(t)\,\xi_j(t')\rangle = 2\,\gamma T\,\delta_{ij}\delta(t - t')$.

The dimensionless Langevin equations (4.7) for a monomer and (4.8) for a dimer have been integrated numerically as explained in the next section [163]. Individual stochastic trajectories were simulated for different time lengths $t_{\max}$ and time steps Δt, so as to ensure appropriate numerical accuracy. Average quantities have been obtained as ensemble averages over 10^4 trajectories; transients effects have been estimated and subtracted.

4.3 Numerical simulation of Langevin equation with additive noise

We consider the dimensionless underdamped Langevin equation (4.7), which can be written also as

$$
\dot{x} = v\,,
\tag{4.9a}
$$
$$
\dot{v} = f(t) + \xi(t)\,,
\tag{4.9b}
$$

where $f(t) = f(x) - \gamma v$ is the sum of the periodic force $f(x) = \sin x + F$ and friction force.

We next introduce a discrete time $t_k = k\,\Delta t$, $k = 0, 1, 2, \ldots$, and integrate the Langevin equation (4.9b) from t_k to $t_{k+1} = t_k + \Delta t$; as a result we obtain,

$$
v(t_k + \Delta t) = v(t_k) + \int_{t_k}^{t_k+\Delta t} f(t)\mathrm{d}t + \int_{t_k}^{t_k+\Delta t} \xi(t)\mathrm{d}t\,.
\tag{4.10}
$$

We have to keep here in mind that even for a single realization of the white noise term, the function is highly irregular, not differentiable, and nothing but a series of delta-functions spread all over the real axis. Assuming that $f(t)$ is a continuous function, we can approximately write,

$$
\int_{t_k}^{t_k+\Delta t} f(t)\,\mathrm{d}t \approx f(t_k + \Delta t/2)\,\Delta t\,.
\tag{4.11}
$$

Denoting the second integral on the right hand side of Eq. (4.10) by $\hat{\xi}(t)$ Eq. (4.10) becomes,

$$
v(t_k + \Delta t) = v(t_k) + f(t_k + \Delta t/2)\Delta t + \hat{\xi}(t)\,.
\tag{4.12}
$$

Concerning the quantity $\hat{\xi}(t)$ we can write (see the previous section),

$$\langle \hat{\xi}(t_k) \rangle = \int_{t_k}^{t_k + \Delta t} \langle \xi(t) \rangle \, dt = 0 \,, \tag{4.13}$$

$$\langle \hat{\xi}(t_k) \hat{\xi}(t_j) \rangle = \int_{t_k}^{t_k + \Delta t} dt \int_{t_j}^{t_j + \Delta t} \langle \xi(t) \xi(t') \rangle \, dt' = 0 \quad \text{if} \quad k \neq j \,, \tag{4.14}$$

$$\langle \hat{\xi}(t_k) \hat{\xi}(t_j) \rangle = 2\gamma T \Delta t \quad \text{if} \quad k = j \,. \tag{4.15}$$

Thus,

$$\sqrt{\langle \hat{\xi}^2(t_k) \rangle} = \sqrt{2\gamma T} \sqrt{\Delta t} \,. \tag{4.16}$$

Introducing the Gaussian variable $\hat{U}(t_k)$ with zero average value and unit normalized correlation, i.e.,

$$\langle \hat{U}(t_k) \rangle = 0 \,, \tag{4.17}$$

$$\langle \hat{U}(t_k) \hat{U}(t_j) \rangle = \delta_{kj} \,, \tag{4.18}$$

we can rewrite the stochastic term $\hat{\xi}(t_k)$ in the following way,

$$\hat{\xi}(t_k) = \sqrt{2\gamma T} \sqrt{\Delta t} \, \hat{U}(t_k) \,. \tag{4.19}$$

The Langevin equation that one simulates, reads (see also Ref. [164]),

$$v(t_k + \Delta t) = v(t_k) + f(t_k + \Delta t/2) \, \Delta t + \sqrt{2\gamma T} \sqrt{\Delta t} \, \hat{U}(t_k) \,; \tag{4.20}$$

for the exctraction of the values of the random variable $\hat{U}(t_k)$, various methods are known [165].

By integrating Eq. (4.9a) between $t_k - \Delta t/2$ and $t_k + \Delta t/2$, one obtains

$$x(t_k + \Delta t/2) = x(t_k - \Delta t/2) + v(t_k) \, \Delta t \,. \tag{4.21}$$

This equation, together with Eq. (4.20), allows one to compute the time evolution of the system with error $(\Delta t)^{3/2}$. In the absence of noise and dissipation, Eqs. (4.20) and (4.21) represent the Verlet algorithm, which is precise to order $(\Delta t)^2$. In the presence of noise and dissipation the fact that the force is computed at time $t_k + \Delta t/2$ implies that both the position and velocity should be computed at time $t_k + \Delta t/2$, while only the position is known for this time – the velocity is computed at t_k. However, the error done in replacing $v(t_k + \Delta t/2)$ with $v(t_k)$ is of order $(\Delta t)^2$, which is smaller than the leading order $(\Delta t)^{3/2}$ due to the noise term [see Eq. (4.20)].

19

4.4 Results: Mobility and diffusion

When considering a pair of interacting Brownian particles, it is natural to study the motion of their center of mass

$$X = \frac{1}{2}\left(x_1 + x_2\right). \tag{4.22}$$

The average position of the center of mass is,

$$\langle X \rangle = \frac{1}{2}\left(\langle x_1 \rangle + \langle x_2 \rangle\right), \tag{4.23}$$

and the mean square displacement,

$$\begin{aligned}
\langle \delta X^2 \rangle &= \langle X^2 \rangle - \langle X \rangle^2 \\
&= \frac{1}{4}\langle \delta x_1^2 \rangle + \frac{1}{4}\langle \delta x_2^2 \rangle + \frac{1}{2}\left(\langle x_1 x_2 \rangle - \langle x_1 \rangle \langle x_2 \rangle\right).
\end{aligned} \tag{4.24}$$

For the following discussion we also introduce the relative coordinate Y,

$$Y = x_2 - x_1, \tag{4.25}$$

representing the dimer size. The quantity Y can in principle also become negative. However, this happens only when the dimer oscillations around the equilibrium position become very large. In the range of parameters that we have adopted, we have verified that Y remains positive even for small values of the elastic constant K, where one recovers the monomer limit. In fact, the distance Y can become negative if both monomers fall into the same valley. In our simulations, the dimer length (at rest) varies in the range $a_0 \in [L, 2L]$. Thus, the monomers start out in different potential valleys and are observed to stay so for all the times (i.e., configurations with $Y < 0$ do not occur).

The dimensionless Langevin equations (4.8) can be rewritten as a Langevin equation for the center of mass coordinate X and one for the dimer length Y, that is,

$$\ddot{X} = \cos\left(Y/2\right)\sin X + F - \gamma\dot{X} + Q(t)/\sqrt{2}, \tag{4.26a}$$

$$\ddot{Y} = 2\cos X \sin\left(Y/2\right) - 2K(Y - a_0) - \gamma\dot{Y} + \sqrt{2}\,q(t). \tag{4.26b}$$

Note that the two noises $Q(t) = [\xi_1(t) + \xi_2(t)]/\sqrt{2}$ and $q(t) = [\xi_2(t) - \xi_1(t)]/\sqrt{2}$ are uncorrelated and have the same statistics as $\xi_{1,2}(t)$, namely, $\langle q(t) \rangle = \langle Q(t) \rangle = 0$ and

$$\langle q(t)q(t') \rangle = \langle Q(t)Q(t') \rangle = 2\gamma T \delta(t - t'). \tag{4.27}$$

In the absence of a substrate potential the mobility of both a monomer and a dimer is $\mu_0 = \gamma^{-1}$. Correspondingly, the free diffusion coefficient for a monomer, $D_0(T) \equiv T\gamma^{-1}$, is twice as large as that for a dimer, $D_0(T/2)$.
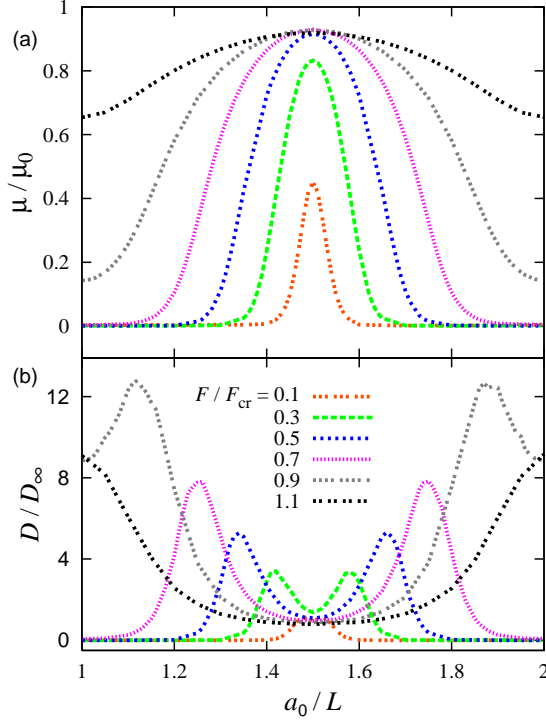
Figure 34: Mobility (a) and diffusion coefficient (b) *versus* the dimer length a_0 for different values of the tilting force F. Simulation parameters: coupling constant $K = 1.5$, temperature $T = 0.1$, and $\gamma = 1$. D_∞ is the free diffusion coefficient of the dimer, $D_\infty = D_0(T/2)$, see text.

4.4.1   The role of the dimer length

At variance with a monomer, a dimer has two degrees of freedom. This affects its diffusion dynamics [166] to the point that its diffusion coefficient D can develop a non-monotonic dependence on the dimer parameters. For instance, dimer transport strongly depends on the ratio between the period L of the substrate and the natural length a_0 of the dimer [160, 167, 168].

   In the absence of an external force, $F = 0$, at low temperature the diffusion coefficient of a rigid dimer decreases monotonically on raising the dimer length a_0 from $L/2$ to L. This can be well understood from Eq. (4.26a). In the limit $K = \infty$ the dimer length is exactly $Y = a_0$ and the force $\cos(Y/2)\sin(X)$ acting on $X(t)$, see Eq. (4.26a), corresponds to a periodic potential with amplitude $|\cos(Y/2)|$. For $a_0 = L/2 = \pi$ this quantity is zero and the dimer center of mass undergoes free diffusion. For $a_0 = L = 2\pi$ the periodic potential amplitude is maximum, $|\cos(Y/2)| = 1$; as discussed
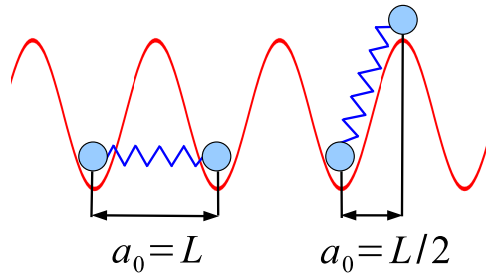
Figure 35: In the case of a rigid dimer, it is obvious that in the absence of an external bias the dimer with $a_0 = L/2$ diffuses much easier than the dimer with $a_0 = L$; in fact, the dimer with $a_0 = L/2$ undergoe free diffusion. Similarly, in the presence of an external bias ($F < F_{\rm cr}$) the dimer with $a_0 = L/2$ is much more mobil compared to the dimer with $a_0 = L$. See also Fig. 34 and text.

in Sec. 3.3, diffusion in a periodic potential is known to be suppressed compared to free diffusion [89, 94, 95]. Therefore, the maxima and minima of D *versus* a_0 coincide with the minima and the maxima of the modulating factor $|\cos(a_0/2)|$, respectively. This conclusion applies also to the case of finite elastic constants as long as $\langle Y(t) \rangle \approx a_0$, that is for rigid dimers, $K \gg 1$, at low temperatures, $T \ll 1$ (see also Fig. 35). (For the opposite limit of weak dimers, $K \ll 1$, see Sec. 4.4.2.)

In the presence of a subthreshold external force, $F < F_{\rm cr}$, the diffusion coefficient D is a nonmonotonic function of the dimer length a_0, as shown in Fig. 34(b). The numerical results in Fig. 34 have been obtained by simulating a relatively rigid, $K = 1.5$, and moderately damped, $\gamma = 1$, dimer. In the case of a strong to moderately damped monomer in a washboard potential, the curves $D(F,T)$ are known to develop a peak around $F_{\rm cr}$, where the barrier height of the tilted periodic potential vanishes [103]. Analogously, in the case of a dimer, D attains a maximum for dimer lengths such that the effective pinning force also vanishes, i.e., for a_0 equal to the distances between maxima and minima of the washboard potential, see Fig. 36. In the case of a driven rigid dimer with $F < F_{\rm cr} = 1$, this takes place for equilibrium lengths $a_0^{\pm} = (L/2)[1 \pm (2/\pi)\arcsin(F)]$. Note that $a_0^{\pm}$ are given $\mathrm{mod}(L)$ and $a_0^+ + a_0^- = L$.

Figure 34(a) demonstrates that the mobility is smallest for commensurate dimers with $a_0 = L$ and the largest for $a_0 = L/2$ (see also Fig. 35 and Ref. [160]). The smaller the applied constant force, the smaller is the a_0 range around $a_0 = L/2$, where the mobility of the dimer is significantly different from zero. For large enough tilting the dimer is considerably mobile, no matter what is the value of a_0. For $F \to \infty$ the mobility $\mu \to \mu_0$ and the
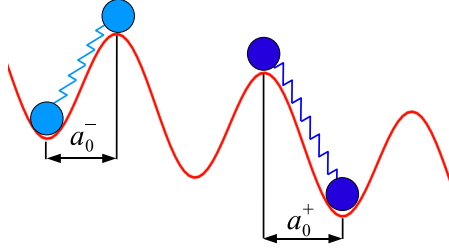
Figure 36: Dimer configurations corresponding to zero pinning force and maximum diffusion coefficient; see also Fig. 34 and text.

effective diffusion coefficient $D \to D_\infty = D_0(T/2)$. We remark that the a_0 dependences of μ and D shown in Fig. 34 are given mod(L) [160]. In fact, the system dynamics, as given by Eqs. (4.8), is invariant under the change $a_0 \to a_0 + L$ and $x_1 \to x_1 - L$ (or $x_2 \to x_2 + L$).

4.4.2 Monomer-like regimes

We now study the diffusion and mobility of a dimer *versus* the bias F. The general behavior of a dimer recalls that of a monomer, namely, both the transition of the rescaled mobility from 0 to μ_0 and the corresponding enhancement of the diffusion coefficient above its free diffusion value still occur as the tilting force is increased past the depinning threshold. The monomer dynamics is a useful benchmark to check the accuracy of our simulations for the dimer diffusion. Indeed, in the limit $K \to 0$, Eq. (4.24) boils down to $\langle \delta X^2 \rangle = \langle \delta x_1^2 \rangle / 2$, with x_1 obeying the monomer Langevin equation (4.7) with temperature T. It follows that for a weak dimer, $K \ll 1$, the ratio D/D_∞ is closely reproduced by the analytical curve $D(F, T)/D_0(T)$ obtained from Eq. (4.7) describing the monomer. This argument applies to both commensurate, Fig. 37, and incommensurate dimers, Fig. 38(b).

Rigid dimers also behave like monomers. In the limit $K \to \infty$, the solution of Eq. (4.26b) is $Y(t) \equiv Y = a_0$ and Eq. (4.26a) is then equivalent to the monomer Langevin equation (4.7) with temperature $T/2$ and substrate amplitude (critical tilt) $|\cos(a_0/2)|$. Accordingly, for commensurate dimers with a_0 equal to an integer multiple of the substrate constant L, the ratio D/D_∞ is reproduced by the curve $D(F, T/2)/D_0(T/2)$ obtained for a monomer on a tilted cosine potential with amplitude $|\cos(a_0/2)| = 1$ and temperature $T/2$ (see Fig. 37).

Note that for large values of damping the monomer curve can also be
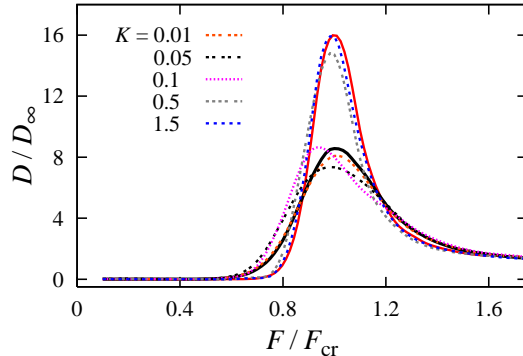
Figure 37: Diffusion coefficient D *vs* the tilting force F for a dimer length $a_0/L = 1$ and different coupling constants K; $T = 0.1$ and $\gamma = 1$. The corresponding curves for monomers of temperature T (lower solid curve) and $T/2$ (higher solid curve) are drawn for a comparison (see text).

computed analytically through the Cox formula [97–100] (see Sec. 3.3). The data in Fig. 37 confirm that for increasingly large K the depinning threshold approaches $F_{\rm cr} = 1$ from below, as the effective critical tilt $\langle |\cos(\psi/2)| \rangle$ tends to unity. Not surprisingly, for the commensurate dimer of Fig. 37, the mobility curve coincides with the monomer mobility $\mu(F, T)$ in the weak coupling limit, and with the monomer mobility at half the temperature T, $\mu(F, T/2)$, in the strong coupling limit; both limiting curves are closely approximated by the Stratonovich formula (not shown).

For $K \to \infty$ incommensurate dimers behave like monomers moving on a tilted cosine potential with amplitude $|\cos(a_0/2)| < 1$ and temperature $T/2$ (see also Fig. 39 for a finite coupling). When a_0 is equal to a half-integer multiple of the substrate constant L, the amplitude of the effective substrate acting on the dimer coordinate X vanishes, $|\cos(a_0/2)| = 0$, and the dimer diffusion becomes insensitive to the substrate, with mobility μ_0 and diffusion coefficient $D_0(T/2)$.

Figures 38 and 39 indicate that for a finite K the dimers exhibit a much more complicated behavior, which will be discussed in the forthcoming section.

4.4.3　The dependence on the coupling strength

The problem of a dimer diffusing in a washboard potential has been studied in fact in many papers, but due to the large parameter space, important effects went unnoticed. In Ref. [169] it was found that for a commensurate dimer, $D(F, T)$ had two maxima as a function of the tilting force F, whereas

Figure 38: Mobility (a) and diffusion coefficient (b) *vs* the tilting force F for an equilibrium distance $a_0/L = 1.5$ and for different values of the coupling constant K; $T = 0.1$ and $\gamma = 1$. In both panels the results are compared with the corresponding monomer curves (see text).

incommensurate dimer behaved more like a monomer, with diffusion coefficient D showing only one peak. However, as shown in Fig. 38(b), one can observe two F-maxima also in the diffusion coefficient of a noncommensurate dimer; correspondingly, the mobility curve μ *versus* F develops the nonmonotonic behavior displayed in Fig. 38(a). More remarkably, for the same temperature and damping constant of Fig. 38, commensurate dimers presented a single peaked diffusion coefficient and monotonic mobility as functions of the tilt (see Figs. 37 and 39). However, for different simulation parameters (like those in Ref. [169]) two-peaked D curves were detected for commensurate dimers, as well. Thus, a doubly peaked diffusion coefficient is no signature of the dimer-substrate commensuration: the coupling constant (Fig. 38), damping constant (Fig. 40), and the temperature also play a significant role [see Eqs. (4.29) and (4.30)].

To investigate the origin of the two competing diffusion mechanisms
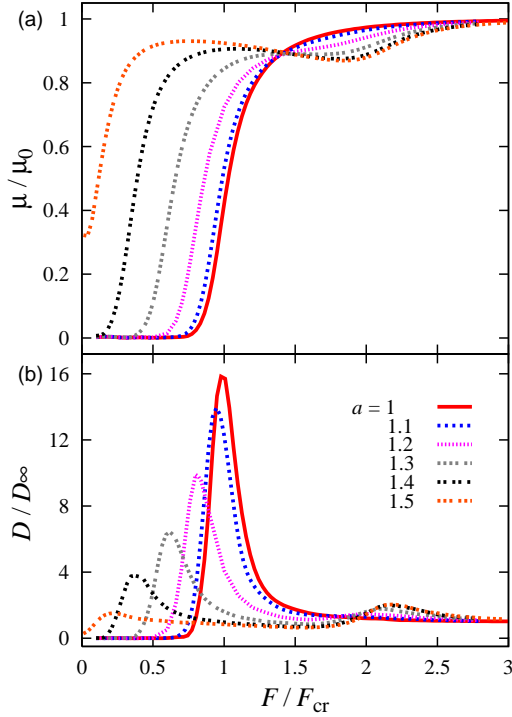
Figure 39: Mobility (a) and diffusion coefficient (b) *vs* the tilting force F for a coupling constant $K = 1.5$ and for different values of the equilibrium distance a_0. T and γ have the same values as in Figs. 38 and 37.

shown in Fig. 38, we address in detail the case of a dimer with length a_0 equal to half-integer multiple of the substrate constant L. For a finite coupling strength K, on setting $Y(t) = a_0 + \psi(t)$, the coupled Langevin equations (4.26) read,

$$\ddot{X} = -\sin(\psi/2)\sin X + F - \gamma\dot{X} + Q(t)/\sqrt{2}\,, \tag{4.28a}$$

$$\ddot{\psi} = 2\cos(\psi/2)\cos X - 2K\psi - \gamma\dot{\psi} + \sqrt{2}q(t)\,. \tag{4.28b}$$

If the dimer is sufficiently rigid and the tilting force F weak, then $\psi(t)$ is small and mostly controlled by thermal noise. From Eq. (4.28b), on neglecting the substrate force with respect to the dimer coupling, energy equipartition yields $\langle \psi^2(t) \rangle = TK^{-1}$. Moreover, the force term $\sin(\psi/2)\sin X$ in Eq. (4.28a) can be treated as resulting from a randomly flashing cosine potential with amplitude $2\langle|\sin[\psi(t)/2]|\rangle \approx |\psi|$. This can be regarded as an instance of the "parametric resonance" approach pursued by the authors of Ref. [167] in the limit $T = 0$. On assuming a Gaussian distribution for ψ,
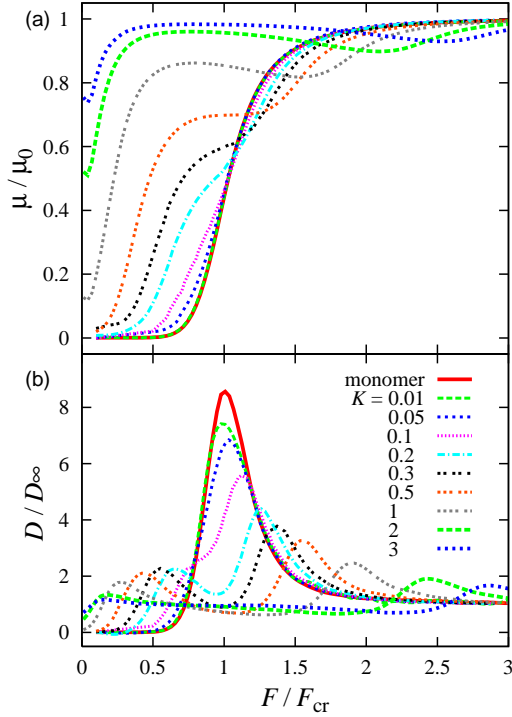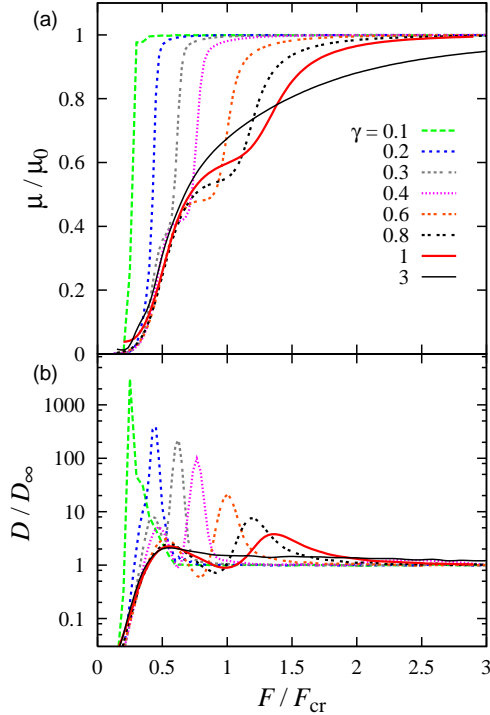
Figure 40: Mobility (a) and diffusion coefficient (b) *vs* the tilting force F for $a_0/L = 1.5$ and different values of damping constant γ; $T = 0.1$ and $K = 0.3$. Two-peaked diffusion curves are clearly distinguishable for $\gamma \leq 1$, only.

a corresponding γ-independent effective critical tilt can thus be estimated, namely,

$$F_1 \approx [(2/\pi)\langle\psi^2(t)\rangle]^{1/2} = \sqrt{2T/\pi K} \, . \qquad (4.29)$$

As pointed out in the end of Sec. 3.3, for large to intermediate values of damping, the critical tilt F_{cr} coincides with the effective dimer depinning threshold F_d. For $K \geq 0.2$, Eq. (4.29) locates rather accurately the first F-peak of the simulated diffusion coefficient reported in Fig. 38(b).

For $F > F_1$ both the dimer mobility and the diffusion coefficient tend towards their free particle values, unless an internal resonance sets in. Indeed, driven by a strong force F, the dimer center of mass acquires an almost constant speed $F\gamma^{-1}$. On inserting $X(t) \simeq Ft/\gamma$ into its right-hand side, Eq. (4.28b) becomes the Langevin equation of a Brownian oscillator subjected to a harmonic force with angular frequency $\Omega = F\gamma^{-1}$. Accordingly, the internal degree of freedom of the dimer, represented by the

coordinate Y, resonates for $F\gamma^{-1}$ approaching $\sqrt{2K - \gamma^2/2}$ (parametric resonance [167, 169–171]), thus leading to a threshold-like enhancement of the dimer diffusion [103]. Our argument can be refined further by noticing that at resonance the processes $X(t)$ and $\psi(t)$ synchronize their phases, so that the substrate force in Eq. (4.28a) does not average out any more. In the presence of synchronization, $\langle \sin(\psi/2) \sin X \rangle \simeq 1/2$, which amounts to replacing F with $F - 1/2$. In conclusion, for relatively large damping constants, namely $1 \lesssim \gamma < 2\sqrt{K}$, a resonance diffusion F peak is expected for

$$ F_2 \approx \frac{1}{2} + \gamma\sqrt{2K - \frac{\gamma^2}{2}}\,, \tag{4.30} $$

in reasonable agreement with the simulation results of Fig. 38(b) for $\gamma = 1$. Correspondingly, the mobility curves describe a two-step transition from the locked to the running state.

For weak dimers, $K < (\gamma/2)^2$, the two peaks of the diffusion coefficient tend to merge, as shown in Fig. 38(b), and in the limit $K \to 0$ a monomer dynamics is recovered (see Sec. 4.4.2). Equivalently, incommensurate dimers with $\gamma > 2\sqrt{K}$ must be regarded as overdamped as far as their internal coordinate Y is concerned; therefore, their diffusion coefficients are characterized by one maximum located around the γ-independent depinning threshold $F_{\rm d}$ in Eq. (4.29); see Fig. 40(b). When γ decreases, both diffusion peaks shift towards smaller values of F. The explanation is simple: the resonance threshold F_2 tends almost linearly to $1/2$; in the underdamped regime, the depinning threshold F_d is proportional to $\gamma = \eta m^{-1}$ as it obeys law (3.37) with $F_{\rm cr}$ given by the effective critical tilt F_1 of Eq. (4.29). This estimate for $F_{\rm d}$ in the underdamped limit is consistent with the anticipated locked-to-running transition thresholds exhibited by the mobility curves of Fig. 40(a) with $\gamma \lesssim 0.3$.

Going back to the dynamics of the damped incommensurate dimer of Fig. 38, we remark that on increasing K the resonance diffusion peaks, in addition to shifting to higher F (directly proportional to $\sqrt{K}$), flatten out on top of the plateau $D = D_0(T/2)$; as the depinning peaks move to lower F (inversely proportional to $\sqrt{K}$), for $K \to \infty$ the diffusion coefficient eventually tends to $D_0(T/2)$, as anticipated in the previous sections.

The argument presented here can be easily generalized to the case of commensurate dimers, or to any equilibrium length; the ensuing properties of commensurate *versus* noncommensurate dimers and the different monomer limits of the dimer dynamics have been anticipated, respectively, in Secs. 4.4.1 and 4.4.2.

4.5 Conclusion

In this part of the work we studied a system consisting of two harmonically interacting Brownian particles diffusing in a one-dimensional washboard potential. We found that the average current and the diffusion coefficient of such a dimer exhibit a complicated non-monotonic behavior as a function of the driving force and the ratio of the dimer length to substrate constant. In the limits of the weak ($K \to 0$) and strong ($K \to \infty$) coupling constant the expected monomer dynamics was recovered. Moreover, we studied in detail the dimer transport for different coupling strengths and damping constants. We concluded that the appearance of the second resonant peak of the diffusion coefficient *versus* the driving force is not related to the dimer length-to-substrate constant ratio, but rather to the damping-to-coupling constant ratio; the diffusion coefficient $D(F)$ possesses two peaks only for relatively low damping values.

Finally, we recall that a simple one-dimesional model is not always a viable tool to analyze transport in two or higher dimensions: such a modeling makes sense for highly symmetric substrates, only. There exist irreducible two- and three-dimensional devices where particles are driven on an asymmetric potential landscape by an ac or dc driving force perpendicularly to the symmetry axis of the potential. Such a geometry has recently attracted broad interest [172–175] in the context of separation of macromolecules, DNA, or even cells, because it is capable of inducing a transverse drift as a function of the drive and of the particle geometry: as a consequence, different objects can be separated depending on their center of mass diffusion coefficient [176]. While the motivations of the present study apply to this class of devices, too, it is clear that their characterization must take into account the dimensionality of the system at hand. Dimensional reduction is limited by the spatial symmetry of the substrate and the particles.

5 Anomalous diffusion: Basic concepts

5.1 General introduction

If the mean square displacement of the Brownian particle does not grow linearly in time, as is the case for the normal Brownian motion, but slower or faster, one then talks about anomalous diffusion. The benchmark of anomalous diffusion is thus the occurrence of a mean-square displacement of the form $\langle \delta r^2(t) \rangle \sim t^\alpha$ $(t \to \infty)$, where $\alpha \neq 1$. Depending on the anomalous diffusion exponent α, the motion can either be subdiffusive, $0 < \alpha < 1$, or superdiffusive, $\alpha > 1$.

Anomalous diffusion has been known since Richardson's treatise on turbulent diffusion in 1926 [177]. Within transport theory it has been studied since the late 1960s. In particular, its theoretical investigation was instigated by Scher and Montroll in their description of dispersive transport in amorphous semiconductors [178], a system where the traditional methods proved to fail. The predictions of their continuous time random walk approach were very distinct from its Brownian counterpart and were shown to explain a variety of physical quantities and phenomena in numerous experimental realizations.

Today, the list of systems displaying anomalous dynamical behavior is quite extensive. Examples for subdiffusive transport encompass phenomena such as charge-carrier transport in amorphous semiconductors, glasses, nuclear magnetic resonance, diffusion in percolative and porous systems, transport on fractal geometries, and dynamics of a bead in a polymeric network, as well as protein conformational dynamics, DNA unzipping [6, 179–182]. Superdiffusion or Lévy statistics are observed besides the Richardson turbulent diffusion in special domains of rotating flows, in collective slip diffusion on solid surfaces, in layered velocity fields, in bulk-surface exchange controlled dynamics in porous glasses, in the transport of micelle systems and in heterogeneous rocks, in quantum optics, single molecule spectroscopy, in the transport in turbulent plasma, bacterial motion, movement of spider monkeys (see Ref. [6, 179] and references therein). Anomalous diffusion is relevant to many other problems in physics and chemistry, in particular in electrochemistry, in geophysics and environmental physics, in biology and microbiology, in medicine, in finance and economics, in econophysics; it is characteristic to most of complex systems. The anomalous character of the transport in different systems is caused by very different mechanisms (see e.g. Ref. [5]).

Anomalous diffusion in the presence or absence of an external velocity or force field has been modeled in numerous ways, including [6]

  (1) continuous time random walk models;

(2) fractional integro-differential equations;

(3) fractal Brownian motion;

(4) generalized diffusion equations;

(5) Langevin equations;

(6) generalized Langevin equations;

(7) generalized master equations;

(8) generalized thermostatistics.

In the following sections we give a short overview of the continuous time random walk model and fractional Fokker-Planck equation.

5.2   Continuous time random walk

As discussed in Sec. 2.6, Einstein's explanation of diffusion and Pearson's random walk are both based on the same two assumptions, namely, the existence of a mean free path and of a mean time. However, these assumptions do not hold always; one such example is the transport of charge carriers in amorphous semiconductors when exposed to an electric field.

Sixty years after Pearson, in 1965, Montroll and Weiss introduced the theory of continuous time random walks [183, 184]. It was applied to transport in semiconductors in works by Scher and Lax [185], and Scher and Montroll [178]. Due to its historical importance and vivid clarity we recall here the definition of the continuous time random walk as given by Scher and Montroll [178]:

> In our model we postulate our material to be divided into a regular lattice of equivalent cells, with each cell containing many randomly distributed localized sites available for hopping carriers. Carrier transport is a succession of carrier hops from one localized site to another and finally from one cell to another. We define the hopping time to be the time interval between the moment of arrival of a carrier into one cell and the moment of arrival into the next cell into which it lands. The random distribution of sites and hence the disorder of an amorphous material is incorporated into a hopping-time distribution function $\psi(\tau)$.

The appropriate distribution $\psi(\tau)$, leading to the agreement with the experiments, was shown to possess the power-law form, $\psi(\tau) \propto \tau^{-1-\alpha}$ with $\alpha \in (0, 1)$. For this range of the fractional exponent α all the moments of the distribution $\psi(\tau)$ diverge and the corresponding process has no characteristic timescale, thus exhibiting the phenomenon of aging. As a result,

the process undergoes subdiffusion [5,6,180], i.e., the mean square displacement grows in the absence of an external force slower than linearly in time, $\langle \delta r^2(t) \rangle \sim t^\alpha$ ($0 < \alpha < 1$, $t \to \infty$).

More in general, the continuous time random walk model is based on the idea that the waiting time τ elapsing between two successive jumps as well as the length λ of a given jump are drawn from a probability distribution function $\phi(\lambda, \tau)$, which is referred to as the jump probability distribution [6]. From $\phi(\lambda, \tau)$ the jump length distribution

$$\varphi(\lambda) = \int_0^\infty \phi(\lambda, \tau) \mathrm{d}\tau \tag{5.1}$$

and the waiting time distribution

$$\psi(\tau) = \int_0^\infty \phi(\lambda, \tau) \mathrm{d}\lambda \tag{5.2}$$

can be deduced. If the jump length and waiting time are independent random variables then the jump distribution factorizes, i.e., $\phi(\lambda, \tau) = \psi(\tau)\varphi(\lambda)$. If the jump length and waiting time are coupled (Lévy walks) then $\phi(\lambda, \tau) = p(\lambda|\tau)\psi(\tau)$ or $\phi(\lambda, \tau) = p(\tau|\lambda)\varphi(\lambda)$, i.e., in a given time span the walker can only travel a maximum distance.

Different types of continuous time random walk processes can be distinguished on the basis of the characteristic waiting time

$$\mathcal{T} = \int_0^\infty \psi(\tau)\, \tau \, \mathrm{d}\tau \tag{5.3}$$

and the jump length variance

$$\Lambda^2 = \int_{-\infty}^\infty \varphi(\lambda)\, \lambda^2 \, \mathrm{d}\lambda \tag{5.4}$$

being finite or diverging [6]. Let us consider the case of the decoupled jump distribution. If both the characteristic waiting time $\mathcal{T}$ and the jump length variance Λ^2 are finite, the long time limit corresponds to normal Brownian motion. If the characteristic waiting time $\mathcal{T}$ diverges but the jump length variance Λ^2 is finite, in the long time limit the motion is subdiffusive; the process is non-Markovian. In the opposite case, i.e., the jump length variance Λ^2 diverges but the characteristic waiting time $\mathcal{T}$ is finite, then one has a Lévy flight (superdiffusion). In the case both the characteristic waiting time $\mathcal{T}$ and the jump length variance Λ^2 diverge, the competition between long rests and long jumps takes place. In general the long jumps and long waiting times introduce a "memory" in the system, i.e., the walker's behavior will be dominated by the largest jumps or longest waiting times.

As a conclusion, continuous time random walk models are a versatile framework for the description of anomalous diffusion. In the following we focus on the subdiffusive regime.

5.3   Memory produced by the long rests

Following the general picture of the continuous time random walk model we introduce, as in the case of the random walk presented in Sec. 2.6, a one-dimensional lattice $\{x_i = i\Delta x\}$ with a lattice period Δx and $i = 0, \pm 1, \pm 2, \ldots$ However, now a particle at site i hops to one of the nearest-neighbor sites $i \pm 1$ only after a random residence time τ; the probability for it is $q_i^{\pm}$; $q_i^{+} + q_i^{-} = 1$. The random time τ is extracted from a residence time distribution $\psi(\tau)$, which has the power-law form. Therefore, the jump length variance Λ^2 is finite but the characteristic waiting time $\mathcal{T}$ diverges in our problem, i.e., the system is subdiffusive, as indicated in the previous section; due to the infinite mean waiting time $\mathcal{T}$ our problem is non-Markovian, i.e., it has a memory. Such a continuous time random walk is described by a generalized master equation for the site populations $P_i(t)$, reading [184]

$$\frac{\partial}{\partial t} P_i(t) = \int_0^t \left\{ K_{i-1}^{+}(t - t') P_{i-1}(t') + K_{i+1}^{-}(t - t') P_{i+1}(t') \right.$$
$$\left. - \left[K_i^{+}(t - t') + K_i^{-}(t - t') \right] P_i(t') \right\} \, \mathrm{d}t' \,, \tag{5.5}$$

where $K_i^{\pm}(t)$ is the kernel. In the integral in Eq. (5.5), the kernel functions $K_{i\pm 1}^{\pm}(t - t')$ represent the (positive) relative contributions to the time variation $\partial P_i(t)/\partial t$ due to the particles visiting sites $i \pm 1$ at some previous times t', $0 < t' < t$, waiting there a time interval $\tau = t - t'$, and then jumping to site i at time t. Instead, the term with $K_i^{\pm}(t - t')$ represents the (negative) contribution due to the particles jumping from site i, where they arrived at some previous time t', to one of the neighboring sites $i \pm 1$ at time t. The Laplace-transform of the kernel $K_i^{\pm}(t)$ is related to the Laplace-transform of the residence time distribution $\psi_i(\tau)$ via

$$\tilde{K}_i^{\pm}(s) = q_i^{\pm} \frac{s \, \tilde{\psi}_i(s)}{1 - \tilde{\psi}_i(s)} \,. \tag{5.6}$$

Let us remind that the Laplace transform $\tilde{f}(s)$ of a function $f(t)$ is a functional transformation commonly used in the solution of differential equations and is defined as

$$\mathcal{L}[f(t)] \equiv \tilde{f}(s) = \int_0^{\infty} e^{-st} f(t) \, \mathrm{d}t \,; \tag{5.7}$$

it is said to exist if the integral (5.7) is convergent, i.e., the function $f(t)$ does not grow at a higher rate than the rate at which the exponential term e^{-st} decreases.

A possible choice for the residence time distributions is the Mittag-Leffler distribution,

$$\psi_i(\tau) = -\frac{\mathrm{d}}{\mathrm{d}\tau} E_{\alpha}[-(\nu_i \tau)^{\alpha}] \,, \tag{5.8}$$

with the survival probability E_α given by the Mittag-Leffler function,

$$E_\alpha(z) = \sum_{n=0}^{\infty} \frac{z^n}{\Gamma(n\alpha + 1)} \, ; \tag{5.9}$$

the quantity ν_i is the time-scaling parameter at site i and $\Gamma(x)$ is the Gamma function. In this case one obtains,

$$\tilde{K}_i^{\pm}(s) = q_i^{\pm} \, \nu_i^\alpha \, s^{1-\alpha} \, . \tag{5.10}$$

The corresponding generalized master equation can be recast as a fractional master equation [186], reading

$$\frac{\partial P_i(t)}{\partial t} = {}_0\hat{D}_t^{1-\alpha} \left[g_{i-1}^+ P_{i-1}(t) + g_{i+1}^- P_{i+1}(t) - (g_i^+ + g_i^-) P_i(t) \right] \tag{5.11}$$

here the quantities $g_i^{\pm} = q_i^{\pm}\nu_i^\alpha$ will be referred to as fractional forward and backward rates. Using the normalization condition for the splitting probabilities $q_i^{\pm}$ one obtains that

$$\nu_i = \left(g_i^+ + g_i^- \right)^{1/\alpha} \tag{5.12}$$

(remember that for random walk $\nu_i = g_i^+ + g_i^-$, see Sec. 2.6), and

$$q_i^{\pm} = \frac{g_i^{\pm}}{g_i^+ + g_i^-} \, , \tag{5.13}$$

in terms of the fractional rates. The symbol ${}_0\hat{D}_t^{1-\alpha}$ in Eq. (5.11) stands for the integro-differential operator of the Riemann-Liouville fractional derivative acting on a generic function of time $\chi(t)$ as [6, 180, 187]

$$_0\hat{D}_t^{1-\alpha}\chi(t) = \frac{1}{\Gamma(\alpha)} \frac{\partial}{\partial t} \int_0^t dt' \frac{\chi(t')}{(t-t')^{1-\alpha}} \, . \tag{5.14}$$

By use of the Laplace-transform method one can show that the fractional master equation (5.11) can be brought into the form [188]

$$D_*^\alpha P_i(t) = g_{i-1}^+ P_{i-1}(t) + g_{i+1}^- P_{i+1}(t) - \left(g_i^+ + g_i^- \right) P_i(t) \, , \tag{5.15}$$

where the symbol D_*^α on the left hand side denotes the Caputo fractional derivative [187],

$$D_*^\alpha \chi(t) = \frac{1}{\Gamma(1-\alpha)} \int_0^t dt' \frac{1}{(t-t')^\alpha} \frac{\partial}{\partial t'} \chi(t') \, . \tag{5.16}$$

Equation (5.15) is formally very similar to the master equation (2.22) describing the random walk, with the difference that instead of the normal time derivative $\partial/\partial t$ we have a fractional derivative (5.16).

5.4 Fractional calculus

The calculus of fractional integrals and derivatives is almost as old as calculus itself. However, about 300 years had to pass before what is now known as fractional calculus was slowly accepted as a practical instrument in physics: until about 15 years ago expressions involving fractional derivatives and integrals were pretty much restricted to the realm of mathematics, but over the past decade or two, many physicists have discovered that a number of systems, particularly those exhibiting anomalously slow diffusion, are usefully described by fractional calculus [180].

In the previous section we saw already that the fractional master equation (5.15) describing the subdiffusive system with long waiting times is not very different from the master equation (2.22) describing systems with normal diffusion. In the following we will see that a similar correspondence exists also between the diffusion equations: fractional equations generalize the equations known from the theory of normal diffusion by taking into account memory effects such as the stretching of polymers under external fields and the occupation of deep traps by charge carriers in amorphous semiconductors. Such generalized equations allow physicists to describe complex systems with anomalous behavior in much the same way as simpler systems undergoing normal diffusion.

One way to formally introduce fractional derivatives proceeds from the repeated differentiation of an integral power:

$$\frac{\mathrm{d}^n}{\mathrm{d}x^n} x^m = \frac{m!}{(m-n)!} x^{m-n} . \tag{5.17}$$

For an arbitrary power μ, repeated differentiation gives,

$$\frac{\mathrm{d}^n}{\mathrm{d}x^n} x^\mu = \frac{\Gamma(\mu+1)}{\Gamma(\mu-n+1)} x^{\mu-n} , \tag{5.18}$$

with Gamma functions replacing the factorials. The simplest interpretation of the Gamma function is that it is the generalization of the factorial for all real numbers, $\Gamma(\mu+1) = \mu\,\Gamma(\mu)$. The Gamma functions allow for a generalization to an arbitrary order of differentiation α,

$$\frac{\mathrm{d}^\alpha}{\mathrm{d}x^\alpha} x^\mu = \frac{\Gamma(\mu+1)}{\Gamma(\mu-\alpha+1)} x^{\mu-\alpha} . \tag{5.19}$$

The latter equation corresponds to the Riemann-Liouville derivative [180]; it is sufficient for handling functions that can be expanded in Taylor series.

A more general way to introduce fractional derivatives uses the fact that the n-th derivative is an operation inverse to an n-fold repeated integration:

$$\int_a^x \int_a^{y_1} \ldots \int_a^{y_{n-1}} f(y_n)\,\mathrm{d}y_n \ldots \mathrm{d}y_1 = \frac{1}{(n-1)!} \int_a^x (x-y)^{n-1} f(y)\,\mathrm{d}y . \tag{5.20}$$

Clearly, the equality is satisfied at $x = a$, and it is not difficult to see iteratively that the derivatives of both sides of the equality are equal. A generalization of the latter expression allows one to define a fractional integral of arbitrary order α via

$$_a\hat{D}_x^{-\alpha} f(x) = \frac{1}{\Gamma(\alpha)} \int_a^x (x-y)^{\alpha-1} f(y) \, \mathrm{d}y \,, \qquad x \geq a \,. \tag{5.21}$$

A fractional derivative of an arbitrary order is defined through fractional integration and successive ordinary differentiation. The α-th fractional derivative is

$$_a\hat{D}_x^{\alpha} = \frac{\mathrm{d}^n}{\mathrm{d}x^n} \, _a\hat{D}_x^{\alpha-n} \,. \tag{5.22}$$

If one deals with fractional time derivatives, one sets in general $a = 0$, in effect choosing $t = 0$ as the beginning of the system's time evolution. In particular, in generalized master and diffusion equations, a central role has the operator

$$_0\hat{D}_t^{1-\alpha} = \frac{\mathrm{d}}{\mathrm{d}t} \, _0\hat{D}_t^{-\alpha} \,. \tag{5.23}$$

The practical use of fractional calculus is underlined by the fact that, under Laplace transform, the operator $_0\hat{D}_t^{-\alpha}$ has the simple form

$$\mathcal{L}\{_0\hat{D}_t^{-\alpha} f(t)\} = s^{-\alpha} \mathcal{L}\{f(t)\} \,. \tag{5.24}$$

The most famous definitions of fractional calculus are the Riemann-Liouville definition and Grunwald-Letnikov definition that is convenient for the numerical calculations. The other definitions are for the most part variations on the themes of these two. However, it is important to keep in mind that the Caputo fractional derivative may provide genuine technical advantages.

5.5 Fractional Fokker-Planck equation

In Sec. 5.3 we saw that the continuous time random walk with a constant step size and the Mittag-Leffler distribution for the residence times can be described by the fractional master equation (5.15), or equivalently by Eq. (5.11). Using the fractional master equation (5.15) with the Caputo fractional derivative it is easy to see that in the very same way as in the case of normal Brownian motion (see Sec. 2.7) one can derive the fractional Fokker-Planck equation [6, 189, 190],

$$D_*^{\alpha} P(x,t) = \left[-\frac{\partial}{\partial x} \frac{f(x)}{\eta_\alpha} + \kappa_\alpha \frac{\partial^2}{\partial x^2} \right] P(x,t) \,; \tag{5.25}$$

the latter equation can be rewritten also as

$$\frac{\partial}{\partial t} P(x,t) = {}_0\hat{D}_t^{1-\alpha} \left[-\frac{\partial}{\partial x} \frac{f(x)}{\eta_\alpha} + \kappa_\alpha \frac{\partial^2}{\partial x^2} \right] P(x,t). \qquad (5.26)$$

Here κ_α denotes the anomalous diffusion coefficient with physical dimension $[\mathrm{m^2 s^{-\alpha}}]$. The quantity η_α denotes the generalized friction coefficient possessing the dimension $[\mathrm{kg\, s^{\alpha-2}}]$; it is related to κ_α through

$$\eta_\alpha \kappa_\alpha = k_\mathrm{B} T, \qquad (5.27)$$

thus constituting a generalized Einstein relation. The anomalous current and the anomalous diffusion coefficient are defined through fractional rates by the relations $\Delta x(g_i^+ - g_i^-) = F_i \eta_\alpha^{-1}$ and $(\Delta x)^2(g_i^+ + g_i^-)/2 = \kappa_\alpha$, having the same form as the corresponding relations for normal Brownian diffusion, determined through the corresponding escape rates (see Sec. 2.7). Equations (5.25) and (5.26) describe subdiffusive processes for $0 < \alpha < 1$ and reduce to the ordinary Fokker-Planck equation when $\alpha = 1$.

Let us mention here that taking also non-local jump statistics into account, i.e., assuming that both $\mathcal{T}$ and Λ^2 are infinite, one recovers the fractional Fokker-Planck equation in the following form,

$$\frac{\partial}{\partial t} P(x,t) = {}_0\hat{D}_t^{1-\alpha} \left[-\frac{\partial}{\partial x} \frac{f(x)}{\eta_\alpha} + \kappa_\alpha^\mu \nabla^\mu \right] P(x,t); \qquad (5.28)$$

here $\nabla^\mu \equiv \partial^\mu/\partial|x|^\mu$ is the Riesz fractional derivative and the physical dimension of the fractional diffusion coefficient κ_α^μ is $[\mathrm{m^\mu\, s^{-\alpha}}]$; $0 < \mu < 2$. The occurrence of the operator ${}_0\hat{D}_t^{1-\alpha}$ is induced by the heavy-tailed waiting times between successive jumps, whereas ∇^μ is related to the heavy-tailed distributions of the jump lengths. Equation (5.28) thus describes the competition between subdiffusion and Lévy flights. For $\mu = 2$ Eq. (5.26) is recovered.

For Markovian Lévy flights, i.e., $\alpha = 1$, Eq. (5.28) becomes,

$$\frac{\partial}{\partial t} P(x,t) = \left[-\frac{\partial}{\partial x} \frac{f(x)}{\eta} + \kappa^\mu \nabla^\mu \right] P(x,t), \qquad (5.29)$$

the physical dimension of the fractional diffusion coefficient κ^μ being $[\mathrm{m^\mu\, s^{-1}}]$. It should be noted that the Lévy noise affects only the diffusive term.

5.6 Numerical simulation of the fractional Fokker-Planck equation through the underlying continuous time random walk

5.6.1 Numerical algorithm for the continuous time random walk

The fractional Fokker-Planck equation represents the continuous limit of a continuous time random walk with the Mittag-Leffler residence time density.

Therefore, it is proper to investigate the fractional Fokker-Planck equation through the underlying continuous time random walk.

Studying the continuous time random walk in a one-dimensional potential $U(x)$, we consider an ensemble of N particles moving on a lattice $\{x_i = i\Delta x\}$, with a lattice period Δx; $i = 0, \pm 1, \pm 2, \dots$ The state of the n-th particle is defined through its current position $x^{(n)}$ and the time $t^{(n)}$ at which it will perform the next jump to a nearest-neighbor site. The n-th particle of the ensemble starts from the initial position $x^{(n)}(t_0) = x_0^{(n)}$. After a residence time τ extracted from the probability density $\psi_i(\tau)$, the particle jumps from site i to site $i+1$ or $i-1$ with probability q_i^+ or q_i^-, respectively, obeying the normalization condition $q_i^+ + q_i^- = 1$. Correspondingly, the space coordinate and the time are updated, $x^{(n)} \rightarrow x^{(n)} \pm \Delta x$ and $t^{(n)} \rightarrow t^{(n)} + \tau$. Reiterating this procedure, the full random trajectory of the random walker can be computed (see Fig. 41 and also Sec. 5.3).

In order to perform the numerical simulation, one needs to evaluate the quantities $q_i^\pm$ and ν_i and extract the waiting times τ. To extract the random numbers distributed according to the Mittag-Leffler distribution (5.8) the most convenient way is to use the following inversion formula [191] (see also Refs. [192–196]),

$$\tau = -\nu_i^{-1} \log \left\{ a \left[\frac{\sin(\alpha\pi)}{\tan(\alpha\pi b)} - \cos(\alpha\pi) \right]^{1/\alpha} \right\} ; \tag{5.30}$$

$a, b \in (0, 1)$ are independent uniform random numbers. The quantities $q_i^\pm$ and ν_i can be expressed in terms of the fractional transition rates $g_i^\pm$ as given by Eqs. (5.13) and (5.12). However, we still do not know what $g_i^\pm$ really are.

To find $g_i^\pm$ we have to discretise the fractional Fokker-Planck equation. The fractional Fokker-Planck equation (5.25) can be written in the following form,

$$D_*^\alpha P(x,t) = \kappa_\alpha \frac{\partial}{\partial x} \left\{ e^{-\beta U(x)} \frac{\partial}{\partial x} \left[e^{\beta U(x)} P(x,t) \right] \right\} . \tag{5.31}$$

Discretising the latter equation according to Eq. (2.24) we obtain,

$$\begin{aligned} D_*^\alpha \ P(x,t) = \frac{\kappa_\alpha}{(\Delta x)^2} \Big\{ & e^{-\beta[U(x-\Delta x/2)-U(x-\Delta x)]} P(x - \Delta x, t) \\ + \ & e^{-\beta[U(x+\Delta x/2)-U(x+\Delta x)]} P(x + \Delta x, t) \\ - \ & \left[e^{-\beta[U(x+\Delta x/2)-U(x)]} + e^{-\beta[U(x-\Delta x/2)-U(x)]} \right] P(x,t) \Big\} . \end{aligned} \tag{5.32}$$

Comparing the latter equation with the fractional master equation (5.15) we see that

$$g_i^\pm = [\kappa_\alpha/(\Delta x)^2] \exp[-\beta(U_{i\pm 1/2} - U_i)] ; \tag{5.33}$$

$U_i \equiv U(i\Delta x)$ and $U_{i\pm1/2} \equiv U(i\Delta x \pm \Delta x/2)$. The fractional rates (5.33) satisfy the Boltzmann relation, $g_{i-1}^+/g_i^- = \exp[\beta(U_{i-1} - U_i)]$. For $\alpha = 1$ $\kappa_\alpha \to D_0$ and we obtain the transition rates for random walk discussed in Sec. 2.6.

The fractional rates may also be chosen as

$$g_i^\pm = [\kappa_\alpha/(\Delta x)^2]\exp[-\beta(U_{i\pm1} - U_i)/2]\,. \qquad (5.34)$$

An appropriate discretisation step Δx has to satisfy the condition $|\beta(U_{i\pm1} - U_i)| \ll 1$; under this condition one can also safely replace $\beta(U_{i\pm1/2} - U_i)$ with $\beta(U_{i\pm1} - U_i)/2$ without a violation of the detailed balance condition. Furthermore, the condition $U''(x)\Delta x \ll 2U'(x)$ must be fulfilled, in order to ensure the smoothness of the potential. In the limit $\Delta x \to 0$ this so constructed, limiting continuous time random walk is described by the fractional Fokker-Planck equation (5.25), or equivalently through Eq. (5.26).

In the case of a confining potential it is sufficient to compute the splitting probabilities $q_i^\pm$ and the time scale parameters ν_i only once over a finite x-region at the beginning of the simulation. In the case of a periodic or washboard potential, the quantities $q_i^\pm$ and ν_i can be computed only for the first period. In the latter case, while the total potential $U(x)$ is not periodic, the potential differences appearing in the fractional rates can be rewritten as

$$U(x_i \pm \Delta x) - U(x_i) = U_0(x_i \pm \Delta x) - U_0(x_i) \mp F\Delta x\,, \qquad (5.35)$$

and are therefore periodic functions of x_i.

To perform the numerical measurements and compute the average $\langle Y(t)\rangle$ of a quantity $Y(t) = Y(x(t))$, one can introduce a time lattice $\{t_m^* = m\Delta t^*\}$, where $m = 0, 1, \ldots, M$, and Δt^* is a constant time interval between two consecutive measurements. For the computation of the average $\langle Y(t)\rangle$, there are at least two different strategies, which we discuss here. Both methods can be illustrated through Fig. 41.

The first possibility is as follows: each trajectory $x^{(n)}(t)$ is separately evolved with time, until the final time t_{final} is reached, $t^{(n)} \geq t_{\text{final}}$. As this n-th trajectory reaches a measurement time t_m^* (represented with dashed lines in Fig. 41), i.e., $t^{(n)} \geq t_m^*$, the quantity $Y_m^{(n)} = Y(x^{(n)}(t_m^*))$ will be computed using the coordinates corresponding to the events marked with full-circles in Fig. 41. The value $Y_m^{(n)}$ will be saved in a storage variable $Y_{\text{sum}}(t_m^*) = \sum_n Y_m^{(n)}$. After evolving all the N trajectories, the average is finally computed by normalization, $\langle Y(t_m^*)\rangle = Y_{\text{sum}}(t_m^*)/N$.

The second possibility is to evolve the whole ensemble until the times of all the trajectories $t^{(n)}$ (at which the particles will perform the next jump) exceed the fixed chosen measurement time t_m^*. We mark these events in Fig. 41 with full-circles. Then, all the corresponding positions $x^{(n)}$ and
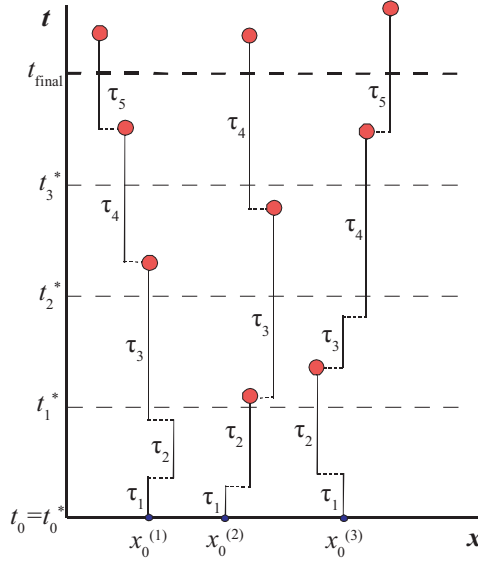
Figure 41: Sketch of the numerical algorithm: After a random waiting time τ the particle jumps from the current position $x^{(n)}$ to the position $x^{(n)} + \Delta x$ or $x^{(n)} - \Delta x$. The process is reiterated until $t^{(n)} \geq t_{\text{final}}$. The numerical measurements are performed after constant time intervals at times t_m^*. The full-circles represent the events that are used for the computation of the physical quantities.

times $t^{(n)}$ will be saved and the average $\langle Y \rangle$ at the fixed time t_m^* will be computed. The procedure is reiterated to evolve the system until the final time t_{final}.

Which of the two methods is to be preferred depends on the problem studied and the available computational resources. For example, the method in which the whole ensemble is evolved in time, allows one to save the system configuration (and therefore to stop and also restart the time evolution) and compute the average quantities after each measurement time t_m^*. Furthermore, evolving the whole system together allows one to simulate a set of N particles interacting with each other.

Let us also notice that the general scheme presented here for the continuous time random walk is valid also for $\alpha = 1$ as for this value of the fractional exponent the Mittag-Leffler distribution for the residence times becomes exponential for which normal diffusion is recovered. Also one can apply the presented procedure for the random walk discussed in Sec. 2.6. In this case, instead of assuming a residence time distribution one can also just assume that the jumps are performed at each time-step.

Finally, it is important to keep in mind that in the case of anomalously

slow diffusion the time and ensemble averages are not equal (not even for the stationary state); the phenomenon is called ergodicity breaking [197].

5.6.2 Mittag-Leffler *versus* Pareto

As pointed out in the previous section, to extract the random number distributed according to the Mittag-Leffler distribution (5.8), Eq. (5.30) can be used. However, also different methods may be used, described in this section and exploited to obtain the numerical results presented in chapters 6 and 7 [9].

According to the Tauberian theorems [184], for every $0 < \alpha < 1$ the long time behavior of the system is determined solely by the tail of the residence time distribution [198]. Therefore, any other distribution with the same asymptotic form $S_\alpha(\nu_i\tau) \sim 1/\Gamma(1-\alpha)(\nu_i\tau)^\alpha$ could be used in place of the Mittag-Leffler distribution (5.8). In fact, also the conditions $S_\alpha(0) = 1$ and $S_\alpha(x \to \infty) = 0$ must be satisfied, and the function $S_\alpha(\nu_i\tau)$ has to decrease monotonically with τ.

The Mittag-Leffler function $E_\alpha(-\xi)$, defined by Eq. (5.9), can be numerically computed at $\xi < \xi_0$ through the sum

$$E_\alpha(-\xi) \approx \sum_{h=0}^{H} \frac{(-\xi)^h}{\Gamma(1+\alpha h)}, \tag{5.36}$$

while at values of $\xi > \xi_0$ its asymptotic expansion can be used,

$$E_\alpha(-\xi) \approx -\sum_{k=1}^{K} \frac{(\xi)^{-k}}{\Gamma(1-\alpha k)}, \tag{5.37}$$

with suitable values of H, K, and ξ_0.

A suitable choice for an approximate description is a Pareto probability density, defined by

$$\psi_i(\tau) = -\frac{\mathrm{d}}{\mathrm{d}\tau} P_\alpha(\nu_i\tau), \tag{5.38}$$

with the survival probability

$$P_\alpha(\nu_i\tau) = \frac{1}{\left[1 + \Gamma(1-\alpha)^{1/\alpha}\nu_i\tau\right]^\alpha}. \tag{5.39}$$

In the simulations of the continuous time random walk we have usually employed the Pareto distribution $y = P_\alpha(\nu_i\tau)$. It is convenient numerically

---

[9]While performing the numerical simulations, we were not aware of the inversion formula (5.30).

because it can be readily inverted to provide a random residence time τ [165],

$$\tau = \nu_i^{-1} \frac{y^{-1/\alpha} - 1}{\Gamma(1-\alpha)^{1/\alpha}} \; ; \tag{5.40}$$

y is a uniform random number in $(0, 1)$.

We have numerically verified the equivalence of the Mittag-Leffler and the Pareto distribution in the computation of the asymptotic quantities. However, the difference in the behavior of the Mittag-Leffler and the Pareto residence time distribution in the limit $\alpha \to 1$ has to be noticed: namely, for $\alpha = 1$ the Mittag-Leffler distribution transforms into the exponential function, $E_1(-\nu_i\tau) \equiv \exp(-\nu_i\tau)$, while the Pareto distribution remains of a power-law type, leading to normal and anomalous diffusion, respectively. For this reason, when studying numerically fractional diffusion with $\alpha \to 1$ the Mittag-Leffler probability distribution should be used preferably.

As the Tauberian theorems ensure the equivalence of the Mittag-Leffler and the Pareto distributions only in the asymptotic limit $t \to \infty$, it is to be expected that at finite times t the two choices for the probability densities provide different results. The difference increases as the parameter α approaches the value $\alpha = 1$ (see also Ref. [199]).

5.6.3 Summary

In this section the numerical algorithm for the simulation of fractional Fokker-Planck dynamics has been detailed via the underlying continuous time random walk. Here we provide the core scheme of the time evolution algorithm used in the simulations. The core of the program is the following one:

For every measurement time $t_m = m\Delta t^*$, where $m = 1, \ldots, M$, the loop over trajectories is performed:

- For every trajectory n, where $n = 1, \ldots, N$, the following procedure is performed:

  ◇ While the next jumping time is smaller than the next measurement time, $t^{(n)} < m\Delta t^*$, the following steps are reiterated:
    – From Eq. (5.12) with (5.34) the time scale parameter ν_i at the current position i is computed. A random waiting time τ is extracted from the residence time distribution, see Sec. 5.6.2, and the next jumping time is computed, $t^{(n)} \to t^{(n)} + \tau$.
    – From Eqs. (5.13) the probabilities $q_i^{\pm}$ to perform the jump from site i to site $i \pm 1$ are computed. A uniform random

number between 0 and 1 is extracted to determine whether the particle jumps to the right or left and the new position of the particle is then computed, $x^{(n)} \to x^{(n)} \pm \Delta x$.

⋄ The coordinate $x^{(n)}$ and the next jumping time $t^{(n)}$ are stored.

- Statistical averages at time $t_m = m\Delta t^*$ are computed using the stored coordinates $\{x^{(n)}\}$.

The application of this algorithm deserves to be commented on in greater detail. First, the effect of the replacement of the Mittag-Leffler by the Pareto distribution does not affect the anomalous transport properties in the asymptotic limit. However, given the finite time available for doing simulations a difference can still be present if the parameter α assumes values close to one, i.e., close to the limit of normal diffusion. Here, the use of the Mittag-Leffler distribution, that precisely matches the fractional Fokker-Planck description, is used preferably. Otherwise, one must increase the overall time of simulations to arrive at convergent results. In order to study the fractional diffusion problem on the whole time scale, the use of the Mittag-Leffler probability density is thus unavoidable. Second, the weak ergodicity breaking [197] makes it impossible to obtain the averaged quantities with single time-averages over a single particle trajectory; this will be discussed more in detail in the forthcoming chapter.

6 Anomalously slow diffusion on periodic substrates

6.1 Motivation and general model

As detailed in Sec. 1, thermal diffusion of Brownian particles under the action of a spatially periodic force presents an active field of research, being relevant for various applications in condensed matter physics, chemical physics, nanotechnology, and molecular biology [7–11]. At the same time many biological and condensed matter systems are advantageously described as particles moving along a disordered substrate. Depending on the statistical properties of the potential, the long-time limit of the process can be quite different from that in a washboard potential [5, 35]. It has been shown that the heterogeneity of the substrate potential may lead to anomalous dynamics [5, 36, 38, 200]. In particular, over a range of forces around the stall force subdiffusion is observed [35].

Given the importance of the subdiffusion and the motion in periodic potentials in various applications [6, 156, 201], in this chapter we address the physics of the effect of the combined action of a periodic force and a random substrate.

6.2 Biased continuous time random walk

Before proceeding with the anomalous transport under the influence a spatially periodic force, let us recall the results for the biased motion. The anomalous diffusion that is biased by a constant external force F is a well established phenomenon found in many different systems. For the biased continuous time random walk the fractional rates become site-independent, $g_i^+ \equiv g^+$ and $g_i^- \equiv g^-$, as $U_{i \pm 1} - U_i = \mp F \Delta x$. Using the Laplace transform one finds the solution of the fractional master equation (5.15) for the mean particle position and for the mean square displacement [202],

$$\langle x(t) \rangle = \langle x(0) \rangle + \frac{\Delta x (g^+ - g^-)}{\Gamma(\alpha + 1)} \, t^\alpha \,, \tag{6.1}$$

$$\langle \delta x^2(t) \rangle = \langle \delta x^2(0) \rangle + \frac{(\Delta x)^2 \, (g^+ + g^-)}{\Gamma(\alpha + 1)} \, t^\alpha$$
$$+ \left[\frac{2}{\Gamma(2\alpha + 1)} - \frac{1}{\Gamma^2(\alpha + 1)} \right] (\Delta x)^2 \left(g^+ - g^- \right)^2 \, t^{2\alpha} \,. \tag{6.2}$$

The solutions of the corresponding fractional Fokker-Planck equation are in the same form of the ones for the fractional master equation; i.e.,

$$\langle x(t) \rangle = \langle x(0) \rangle + \frac{F}{\eta_\alpha} \frac{t^\alpha}{\Gamma(\alpha + 1)} \,, \tag{6.3}$$

$$\langle \delta x^2(t) \rangle = \langle \delta x^2(0) \rangle + 2\kappa_\alpha \frac{t^\alpha}{\Gamma(\alpha+1)}$$
$$+ \frac{F^2}{\eta_\alpha^2} \left[\frac{2}{\Gamma(2\alpha+1)} - \frac{1}{\Gamma^2(\alpha+1)} \right] t^{2\alpha}. \tag{6.4}$$

The fractional current is defined and numerically computed as

$$v_\alpha = \Gamma(\alpha+1) \lim_{t\to\infty} \frac{\langle x(t) \rangle - \langle x(0) \rangle}{t^\alpha}. \tag{6.5}$$

Therefore, in the case of the biased continuous time random walk $v_\alpha = F\eta_\alpha^{-1}$. With respect to the case of normal diffusion the expression for the mean square displacement contains besides a thermal contribution proportional to t^α also a ballistic-like term proportional to $t^{2\alpha}$. As a consequence, a value $\alpha < 1$ does not necessarily imply subdiffusive behavior. In fact, in the presence of bias for $0.5 < \alpha < 1$ superdiffusion takes place.

For a finite bias F, the ballistic term in Eq. (6.2) equals zero only in the case $\alpha = 1$, for which normal Brownian motion is recovered. From Eqs. (6.1), (6.2) one obtains then a generalized nonlinear Einstein relation, which is nonlinear in force and valid for a finite space step Δx,

$$\frac{\langle \delta x^2(t) \rangle - \langle \delta x^2(0) \rangle}{\langle x(t) \rangle - \langle x(0) \rangle} = \Delta x \coth(F\beta\Delta x/2). \tag{6.6}$$

In the limit $F \to 0$, Eq. (6.6) yields the well-known Einstein relation ($\alpha = 1$), $\kappa_\alpha / \mu_\alpha(0) = \beta^{-1}$, between the thermal diffusion coefficient

$$\kappa_\alpha = \Gamma(\alpha+1) \lim_{t\to\infty} \frac{[\langle \delta x^2(t) \rangle - \langle \delta x^2(0) \rangle]_{F=0}}{2t^\alpha} \tag{6.7}$$

and the linear mobility $\mu_\alpha(F=0)$,

$$\mu_\alpha(F) = \frac{v_\alpha}{F} = \Gamma(\alpha+1) \lim_{t\to\infty} \frac{\langle x(t) \rangle - \langle x(0) \rangle}{Ft^\alpha}. \tag{6.8}$$

The same Einstein relation is valid also between the submobility and the subdiffusion coefficient for any $\alpha < 1$ [203], as the ballistic term in the mean square displacement (6.2), (6.4) vanishes for $F = 0$; in the absence of bias the mean square displacement grows in time as t^α,

$$\langle \delta x^2(t) \rangle = \langle \delta x^2(0) \rangle + \frac{2\kappa_\alpha}{\Gamma(1+\alpha)} t^\alpha. \tag{6.9}$$

However, a relation analogous to the generalized nonlinear Einstein relation (6.6) ceases to be valid for $\alpha < 1$ for any finite F, as the mean square displacement becomes dominated by the ballistic contribution in the long

time limit. Instead, from Eqs. (6.1), (6.2) or (6.3), (6.4) one obtains the following asymptotic scaling relation,

$$\lim_{t\to\infty} \frac{\langle \delta x^2(t) \rangle}{\langle x(t) \rangle^2} = \frac{2\Gamma^2(\alpha+1)}{\Gamma(2\alpha+1)} - 1 \,. \tag{6.10}$$

This result no longer contains the fractional transition rates and holds true independent of the strength of the bias F and the temperature T. The relation (6.10) was first obtained in Refs. [178, 204] for a continuous time random walker exposed to a constant force.

6.3 Fractional current in washboard potentials

Considering the transport processes with anomalously slow relaxation in a tilted periodic potential (3.2) then departing from the fractional Fokker-Planck equation (5.25) one finds in the very same way as in Sec. 3.3 for the normal diffusion that the probability flux $J_\alpha(x,t)$ reaches asymptotically the stationary current value, i.e.,

$$D_\alpha^* \langle x(t) \rangle = L J_\alpha = v_\alpha \,; \tag{6.11}$$

the anomalous current v_α in a washboard potential is given in closed form by [199, 205]

$$v_\alpha = \frac{L \kappa_\alpha \left(1 - e^{-\beta F L}\right)}{\int_0^L \mathrm{d}x \, e^{-\beta U(x)} \int_x^{x+L} e^{\beta U(x')} \mathrm{d}x'} \,. \tag{6.12}$$

The latter formula represents the anomalous counterpart of the current in washboard potential known for normal diffusion and reduces to the Stratonovich formula (3.25) for $\alpha = 1$ [92,93]. As the derivation of Eq. (6.12) is analogous to the derivation of (3.25), we do not repeat it here, but refer to Sec. 3.3 and Ref. [199].

From Eq. (6.11) one sees that the mean particle position follows as

$$\langle x(t) \rangle = \langle x(0) \rangle + v_\alpha \frac{t^\alpha}{\Gamma(1+\alpha)} \,, \tag{6.13}$$

with v_α given by Eq. (6.12). Comparing Eqs. (6.13) and (6.3) we see that the expressions for the mean particle position in the constant force field and in the tilted periodic potential have the same form, with different expressions for the current.

We have tested the validity of the generalized Stratonovich formula (6.12) obtained theoretically, through the simulation of the fractional continuous time random walk in different periodic potentials:
(i) the symmetric cosine potential
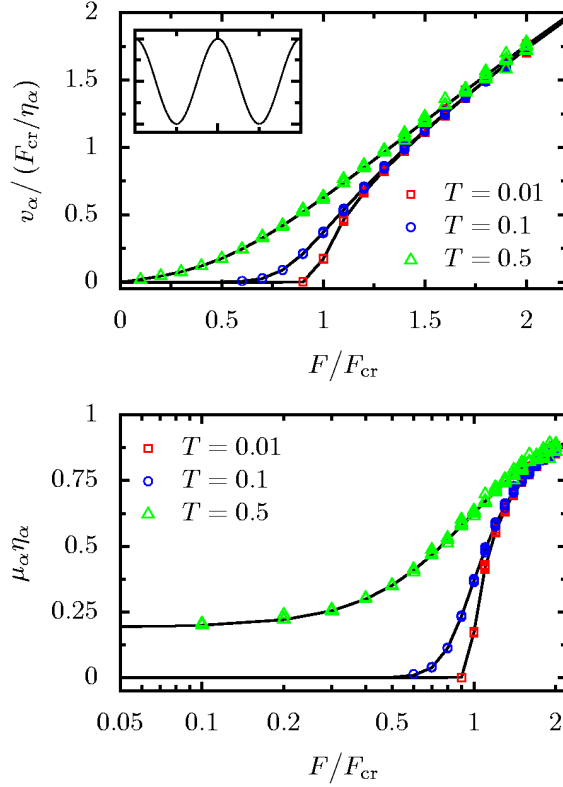
$$U_0^1(x) = \cos(2\pi x/L) \,; \tag{6.14}$$

Figure 42: Dimensionless subcurrent $v_\alpha(F)/(F_{cr}/\eta_\alpha)$ and nonlinear mobility $\mu_\alpha(F)\,\eta_\alpha$ for the case of the cosine substrate potential (6.14) (depicted in the inset) *vs* F/F_{cr}. Numerical values corresponding to different temperatures T and fractional exponents $\alpha \in [0.1, 1]$ (symbols) fit the analytic predictions from Eq. (6.12) (continuous lines).

(ii) the symmetric double-hump periodic potential

$$U_0^2(x) = [\cos(2\pi x/L) + \cos(4\pi x/L)]/2\,; \tag{6.15}$$

(iii) the asymmetric (i.e. no reflection symmetry holds), ratchet-like periodic potential

$$U_0^3(x) = [3\sin(2\pi x/L) + \sin(4\pi x/L)]/5\,. \tag{6.16}$$

The potentials (6.14), (6.15), and (6.16) are depicted in the insets of Figs. 42, 43, and 44 respectively. The potentials as well as the thermal energy k_BT, are measured in units of the potential amplitude A. For the sake of simplicity, the same symbol T is used in the following to represent the rescaled thermal energy.
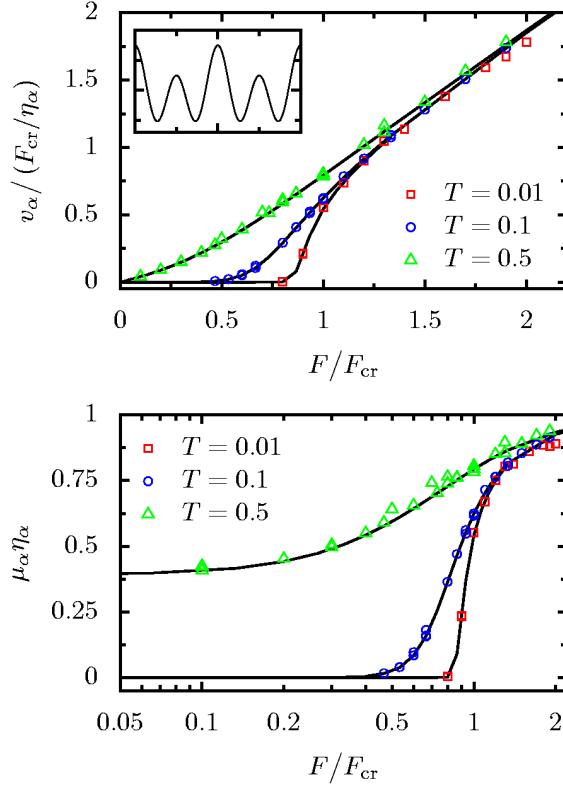
Figure 43: Same as in Fig. 42, for the double hump potential (6.15).

In the numerical simulations we have used the Pareto probability density (5.38) for $0 < \alpha \leq 0.8$ and the Mittag-Leffler density (5.8) for $0.8 < \alpha < 1$ (see the discussion in Sec. 5.6.2). For $\alpha = 1$ corresponding to a normal Brownian process we have employed the exponential residence time probability density

$$\psi_i(\tau) = -\frac{\mathrm{d}}{\mathrm{d}\tau}\exp(-\nu_i\tau). \tag{6.17}$$

As a space step we used $\Delta x = 0.001$, measured in units of the space period L. The time unit was set as $\tau_u = (\eta_\alpha L^2/A)^{1/\alpha}$. For the ensemble average 10^4 trajectories were employed, each one starting from the same initial condition $x(t_0) = x_0$. The tilting force is measured in units of the critical tilt F_{cr}. In the case of the asymmetric ratchet potential the positive critical tilt is used.

We present in Figs. 42, 43, and 44 the numerical results for the scaled fractional current $v_\alpha(F)/(F_{\mathrm{cr}}/\eta_\alpha)$ and the corresponding scaled nonlinear mobility, i.e., $\mu_\alpha(F)\eta_\alpha$, with $v_\alpha(F)$ and $\mu_\alpha(F)$ defined through Eq. (6.5)
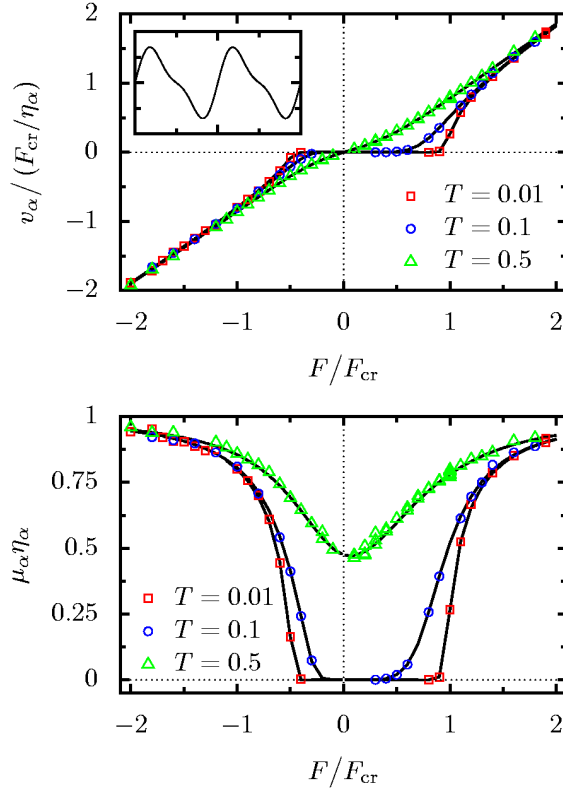
Figure 44: Same as in Fig. 42, for the ratchet potential (6.16). Here, due to the asymmetry, also negative tilting is studied.

and Eq. (6.8). The subcurrent is measured in units of $F_{\mathrm{cr}}/\eta_\alpha$, i.e., the subcurrent of a particle under the action of a constant bias $F = F_{\mathrm{cr}}$, the mobility is in units of the free mobility η_α^{-1}. Without loss of generality we have chosen $F > 0$ for the symmetric substrate potentials (6.14) and (6.15). In the case of the ratchet-like potential (6.16) also the results for negative values of the tilting force F are depicted.

We have computed the fractional current and mobility for various values of α in the interval $[0.1, 1]$. Remarkably, they do not depend on the value of the fractional exponent α [see also Eq. (6.12)]. For a given temperature T, all numerical values of $v_\alpha(F)/(F_{\mathrm{cr}}/\eta_\alpha)$ and $\mu_\alpha(F)\,\eta_\alpha$ (depicted with symbols in Figs. 42, 43, and 44), coincide with the theoretical curves resulting from Eq. (6.12) (continuous lines).

The regime of linear response at low temperatures is numerically not accessible. In this parameter regime the corresponding escape times governing the transport become far too large [11] and particles are effectively
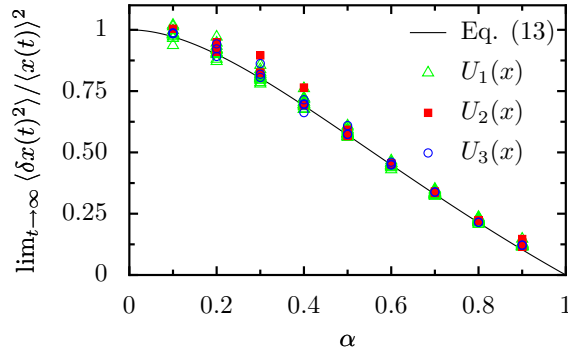
Figure 45: Universal scaling: asymptotic values of the ratio $\langle \delta x^2(t) \rangle / \langle x(t) \rangle^2$ as a function of the parameter α for anomalous diffusion. All the points corresponding to the same α but different values of tilting force F, temperature T, and shapes of substrate potential, match the function given in Eq. (6.10) (solid line) within the statistical errors. We use three different temperatures: $T = 0.01$ with the bias F ranging between $0.9 - 2.0$; correspondingly, $T = 0.1, F = 0.7 - 2.0$ and $T = 0.5, F = 0.4 - 2.0$. The open triangles correspond to the cosine potential (6.14), the filled squares to the double-hump potential (6.15) and the open circles to the asymmetric ratchet potential (6.16).

trapped in the potential minima. At values of the tilting force F close to critical at which the minima disappear, the particles become capable to escape from the potential wells and the current is enhanced. The higher the temperature, the smaller is the tilting required to allow the particles to escape (compare the curves corresponding to different temperatures T in Figs. 42, 43, and 44). At higher values of the temperature T the linear response regime is numerically observable. For tilting forces $F \gg F_{cr}$ or for $T \gg 1$ the dynamics approaches the behavior of a free continuous time random walk that is exposed to a constant bias [37, 204, 205] (see also discussion in Sec. 3.3).

6.4   Universal scaling

In Sec. 6.2 we saw that for the anomalously slow diffusion in constant force field, in the long time limit the asymptotic scaling relation (6.10) holds. We now show that the relation in (6.10) is valid also for anomalous transport in tilted periodic potentials. We prove this by mapping the dynamics onto an equivalent continuous time random walk, i.e., we consider a discrete state reduction of the continuous diffusion process $x(t)$: to this aim, we introduce a lattice with sites $\{\hat{x}_j = jL\}$, located at the minima of the

periodic part of the potential, and study the residence time distribution $\hat{\psi}_j(\tau)$ for the hopping process between sites $\{\hat{x}_j\}$. For such a system, the ratio $\hat{q}_j^+/\hat{q}_j^- = \exp(\beta F L)$ equals that of the constant force case, due to the choice $\Delta x = L$. Furthermore, the analogy between the solutions (6.1) and (6.13), both exhibiting an asymptotic power law $\propto t^\alpha$, implies the same form $\hat{\psi}_j(\tau) \propto 1/\tau^{1+\alpha}$ for $\tau \to \infty$. In fact, for $\hat{\psi}_j(\tau) \sim \alpha \hat{\nu}_j^{-\alpha}/\Gamma(1-\alpha)\tau^{1+\alpha}$, with some suitable scaling coefficients $\hat{\nu}_j$, the corresponding kernels of the generalized master equation obey $\tilde{K}_j^\pm(s) = \hat{q}_j^\pm \hat{\nu}_j^\alpha s^{1-\alpha}$ in the limit $s \to 0$. Therefore, by making use of Tauberian theorems for the Laplace-transform [184], it follows that the asymptotic solution ($t \to \infty$) is of the form (6.1), (6.2), being determined only by the asymptotic power law behavior of the residence time distribution [198], despite the fact that the values of the new fractional forward and backward rates $\hat{g}^\pm$ depend on the chosen shape for the periodic potential. Because the result in (6.10) is independent of $\hat{g}^\pm$, the scaling relation thus still holds true. It is universal in the sense that it holds independently of the detailed shape of the tilted periodic potential, the temperature T and the bias strength F.

The universal scaling in tilted periodic potentials is illustrated with Fig. 45, in which the asymptotic ratio $\langle \delta x^2(t) \rangle/\langle x(t) \rangle^2$ is plotted *versus* the fractional exponent α for the periodic potentials (6.14)-(6.16). For a given α various data are presented, corresponding to different potential shapes and values of F and T. As one can deduce, these points overlap, demonstrating that the ratio is independent of bias and temperature, as well as the specific shape of the substrate potential $U_0(x)$. At the same time, the data fit very well with the analytical expression (6.10) (continuous line).

6.5   Fractional diffusion in periodic potentials

From Eq. (6.12) we see that the anomalous current in a periodic potential (no external bias) is zero and $\langle x(t) \rangle = \langle x(0) \rangle$. As discussed in the previous section, the mean square displacement in a tilted periodic potential is of the form (6.2), or equivalently (6.4). Then, in the absence of the tilting it is of the form (6.9) with the difference that instead of the free fractional diffusion coefficient κ_α we have the effective fractional diffusion coefficient $\kappa_\alpha^{(\text{eff})}$, i.e.,

$$\langle \delta x^2(t) \rangle = \langle \delta x^2(0) \rangle + \frac{2\kappa_\alpha^{(\text{eff})}}{\Gamma(1+\alpha)}\, t^\alpha \tag{6.18}$$

(see also Ref. [206]). The latter equation defines the effective fractional diffusion coefficient $\kappa_\alpha^{(\text{eff})}$ in a periodic potential,

$$\kappa_\alpha^{(\text{eff})} = \Gamma(\alpha+1) \lim_{t \to \infty} \frac{\langle \delta x^2(t) \rangle - \langle \delta x^2(0) \rangle}{2t^\alpha}\, . \tag{6.19}$$
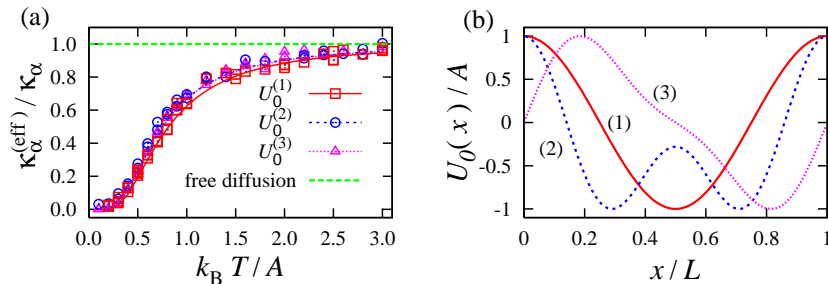
Figure 46: (a) Effective anomalous diffusion coefficient $\kappa_\alpha^{(\text{eff})}$ in a periodic potential *vs* the re-scaled temperature $k_{\text{B}}TA^{-1}$. The quantity $\kappa_\alpha^{(\text{eff})}$ is re-scaled by the corresponding free fractional diffusion coefficient κ_α. The theoretical curves obtained from equation (6.20) (lines) are compared to the numerical results (symbols). The different periodic potentials used are given by Eqs. (6.21)-(6.23). For each potential and at given temperature the numerical points are computed for some values of α within the interval $\alpha \in [0.1, 0.9]$. (b) A comparison among the different periodic potentials used for the numerics, see in (6.21)-(6.23): (1) the cosine potential $U_0^{(1)}(x)$; (2) the double hump potential $U_0^{(2)}(x) - (2a_1 - 1)$; (3) the ratchet potential $U_0^{(3)}(x)$.

The analytical expression for the effective fractional diffusion coefficient $\kappa_\alpha^{(\text{eff})}$ in a periodic potential can be derived using the fact that the Einstein relation (3.28) is valid also for the anomalous transport if $F \to 0$, as discussed in Sec. 6.2. Thus, following the same procedure as for normal diffusion (see Sec. 3.3), taking into account that the fractional current v_α is given by (6.12), one obtains the following expression for the effective fractional diffusion coefficient in a periodic potential,

$$\kappa_\alpha^{(\text{eff})} = \frac{\kappa_\alpha}{\int\limits_0^L e^{-\beta U_0(x)}\frac{\mathrm{d}x}{L} \int\limits_0^L e^{\beta U_0(x')}\frac{\mathrm{d}x'}{L}} . \tag{6.20}$$

The latter result generalizes the Lifson-Jackson formula (3.31) to the subdiffusive motion in periodic potentials; it reduces for $\alpha = 1$ to Eq. (3.31).

The behavior of equation (6.20) *versus* re-scaled temperature $k_{\text{B}}TA^{-1}$ is illustrated in Fig. 46(a) for the following periodic potentials, depicted in Fig. 46(b):

(i) a cosine potential

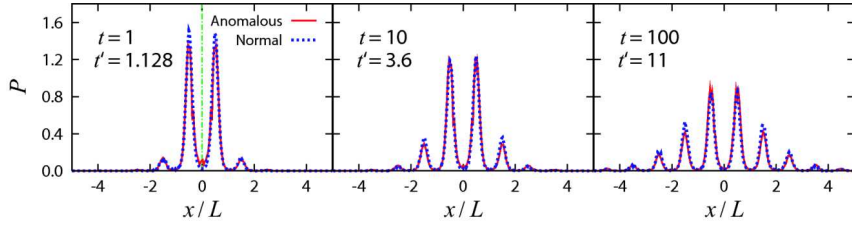$$U_0^{(1)}(x) = A\cos(2\pi x/L) , \tag{6.21}$$

Figure 47: The time evolutions of the probability densities characterizing the anomalous and normal diffusion processes in the periodic cosine potential (6.21). The dot-dashed line at $x = 0$ (left figure) represents the initial conditions at $t = 0$, $P(x,0) = \delta(x - X_0)$. The re-scaled temperature is $k_B T A^{-1} = 0.5$ and the fractional exponent is $\alpha = 0.5$. The anomalous probability density $P(x,t)$ cannot be distinguished from that of the normal case, $P(x,t')$, once the time has been re-scaled according to Eq. (6.24). Similar results are obtained for other values of $\alpha \in (0,1)$ (not depicted).

(ii) a double-hump potential

$$U_0^{(2)}(x) = Aa_1[\cos(2\pi x/L) + \cos(4\pi x/L)], \qquad (6.22)$$

with the coefficient $a_1 = 16/25$, and
(iii) a ratchet potential

$$U_0^{(3)}(x) = A[a_2 \sin(2\pi x/L) + a_3 \sin(4\pi x/L)], \qquad (6.23)$$

with $a_2 = 85/(21\sqrt{21})$, $a_3 = 25/(21\sqrt{21})$. The coefficients a_1, a_2, a_3 are chosen such that the potentials (6.21)-(6.23) have the same amplitude A. The theoretical curves are confirmed by numerical results, depicted in Fig. 46(a) with symbols. The anomalous diffusion coefficient is computed numerically as defined by Eq. (6.19). As the ratio $\kappa_\alpha^{(\text{eff})}/\kappa_\alpha < 1$, one can conclude that, analogously to the normal case, the effect of any one-dimensional non-biased periodic field is to suppress the macroscopic anomalous diffusion coefficient compared to the value in the absence of force [89] (see Sec. 3.3). Furthermore, it is to be noticed that the ratio $\kappa_\alpha^{(\text{eff})}/\kappa_\alpha$ does not depend on the fractional exponent α [see Eq. (6.20)] and moreover, the shape of the periodic potential $U_0(x)$ has only a small influence, as one can see by comparing the theoretical curves in Fig. 46(a) [c.f. Eq. (3.61) and Sec. 3.6.2].

6.6 Probability densities

In Sec. 6.5 it was demonstrated that the effective fractional diffusion coefficient in a periodic potential is of the same form as the the Lifson-Jackson
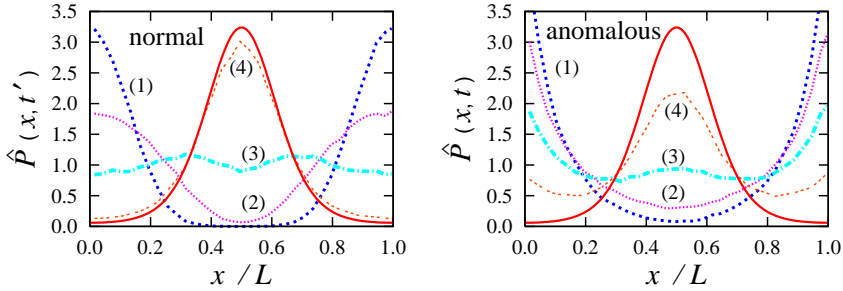
Figure 48: The different small-time evolutions of the normal (left) and anomalous (right) reduced probability densities $\hat{P}(x,t)$ and $\hat{P}(x,t')$ defined by Eq. (3.7), in the cosine potential (6.21). Curve labels (1), (2), (3) and (4) represent increasing values of re-scaled time $t' = 0.01, 0.02, 0.04, 0.11$ for the anomalous case and of time t for the normal case, related to t' through Eq. (6.24). The solid line represents the theoretical stationary solution. The re-scaled temperature is $k_{\mathrm{B}}TA^{-1} = 0.5$ and $\alpha = 0.5$ for the anomalous process, as in Fig. 47.

formula for normal diffusion. In Sec. 6.3 it was shown that the anomalous current in a washboard potential is of the same form as the Stratonvich formula describing normal stationary current. These results represent further elements of the formal analogy between fractional and normal diffusion besides the formal similarity between the Fokker-Planck and fractional Fokker-Planck equations. However, this formal analogy masks some basic physical differences. For this reason we investigate and discuss here the time-dependent probability density in configuration space as well as the density of the current variable.

We notice that in the absence of a bias, all the odd moments of the probability density are identically zero both for normal and fractional diffusion. As for the second moment, upon introducing the re-scaled time

$$t' = \frac{(t/\tau_u)^\alpha}{\Gamma(1+\alpha)}, \qquad (6.24)$$

[we remind that $\tau_u = (\eta_\alpha L^2/A)^{1/\alpha}$] it follows from Eq. (6.18) that the mean square displacement (in units of L^2) formally coincides with that of the normal diffusion case, $[\langle \delta x^2(t') \rangle - \langle \delta x^2(0) \rangle]/L^2 = 2\,T'\,t'$, independently of the fractional exponent α, wherein $T' = k_{\mathrm{B}}TA^{-1}$, with A the potential amplitude, is the re-scaled temperature. The study of the time evolution of the probability density is illustrated with the example in Fig. 47 choosing the times t for the anomalous diffusion process and the corresponding times t' for normal diffusion, so that they satisfy Eq. (6.24): the probability densities
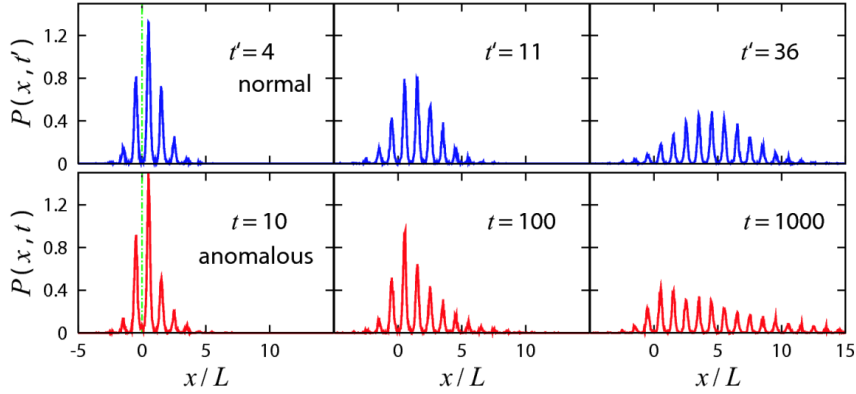
Figure 49: The time evolutions of the probability densities characterizing the normal (above) and anomalous (below) diffusion processes in a tilted cosine potential $U(x) = A\cos(2\pi x/L) - Fx$. The re-scaled temperature is $k_{\mathrm{B}}TA^{-1} = 0.5$ and the fractional exponent is $\alpha = 0.5$, as in figure 47. The tilting force is $F = 0.1 \times F_{\mathrm{cr}}$, where $F_{\mathrm{cr}} = 2\pi AL^{-1}$ is the re-scaled critical bias, corresponding to the disappearance of potential minima. Times t and t' are related through Eq. (6.24). For sufficiently small times the probability densities of the normal and anomalous processes are very similar. However, at larger times (in the long time limit) the maximum of the density for normal diffusion moves with the directed current. In contrast, the mean square displacement of an ensemble of particles undergoing fractional diffusion is dominated by the ballistic contribution and the typical stretched spreading in the direction of bias is observed, while leaving the maximum of the density near the origin.

for anomalous diffusion (continuous lines) and normal diffusion (dashed lines) processes are barely distinguishable from each other for sufficiently long evolution times.

In clear contrast, however, appreciable differences between the normal diffusion coordinate density $P(x, t')$ and the anomalous coordinate density $P(x, t)$ emerge for small times. This is best detectable by comparing the reduced probability densities (3.7), mapped onto a single spatial period, as done in Fig. 48. In the normal case (Fig. 48 left) the two initial maxima at $x = 0$ and $xL^{-1} = 1$, due to the initial conditions $\hat{P}(x, 0) = \delta(x)$, move toward the center and finally merge into the asymptotic stationary density (3.17) (solid line). On the other hand, in the anomalous case the two initial maxima gradually disappear, while a new peak grows at $xL^{-1} = 0.5$ and evolves into the stationary density $\hat{P}_{\mathrm{st}}(x)$ given by Eq. (3.17) as for the normal diffusion process: remarkably, in fractional diffusion, the probability
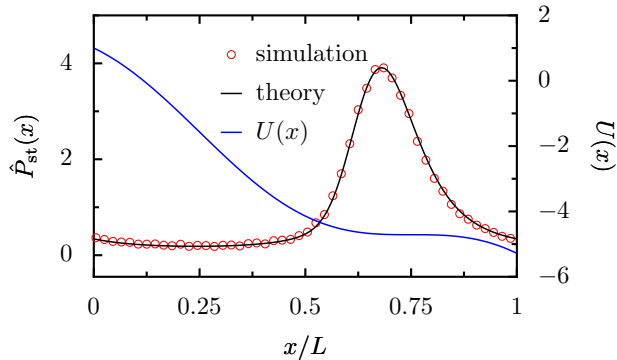
28

Figure 50: Normalized theoretical stationary, reduced probability density $\hat{P}_{st}(x)$ for $F/F_{cr} = 1$, $T = 0.1$, and $\alpha = 0.5$, computed from Eq. (3.22) (continuous line) and corresponding numerical data (circles): — left y-axis. Also the underlying potential $U(x) = \cos(x) - Fx$ is depicted: — right y-axis.

density reaches the same stationary density as in the case of normal diffusion [6].

Moreover, as soon as the process is biased by an external finite force, $F \neq 0$, a qualitative difference arises in the time evolutions of the probability densities of the anomalous and the normal processes in the long time limit as well, see also Ref. [199]. This is true even for small values of F in the linear response regime, as one can defer from Fig. 49. All this indicates a profound difference between a fractal diffusion dynamics that is based on the fractal Brownian motion introduced by Mandelbrot and van Ness [207] and the fractional diffusion based on the continuous time random walk [183]. The time evolution of the density of an ensemble of particles undergoing normal diffusion can be interpreted as a superposition of a translational motion and a spreading of the initially localized density. In this case one observes the global maximum of the probability density moving in the direction of the external bias [Fig. 49 top]. Instead, in the anomalous case, only an asymmetrical spreading of the initial density takes place, resulting in a long tail in the direction of the bias [178, 204]. The global maximum of the density remains close, however, to its initial position [Fig. 49 bottom] [199]. This intriguing behavior is related to the presence of a ballistic contribution proportional to $t^{2\alpha}$ in the mean square displacement [see Eq. (6.2) and the discussion in Sec. 6.4]. We remark that for α close to one and for small values of external bias F, at small times the term $\propto t^{\alpha}$ can prevail over the ballistic term. However, in the long-time limit the ballistic term takes over and always dominates. The latter remark may be relevant for experimental
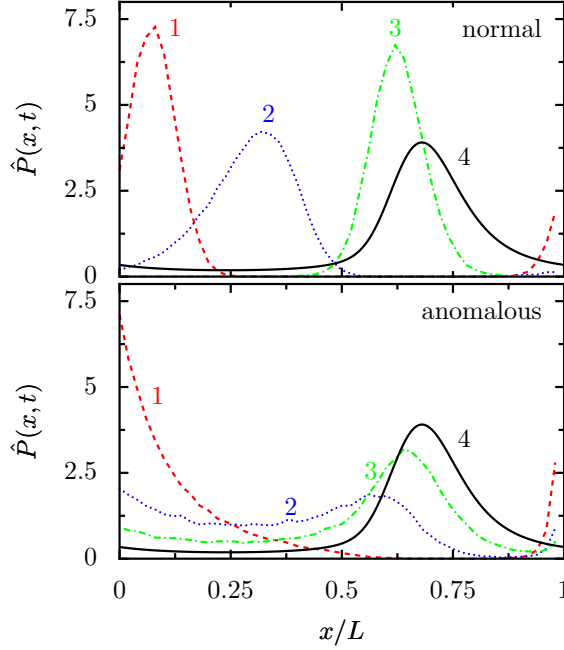
Figure 51: The time evolution for normal (above) and anomalous (below) diffusion of the reduced probability density $\hat{P}(x,t)$ within the first period $x \in [0, L)$ defined according to Eq. (3.7). In this example, the potential is $U(x) = \cos(x) - Fx$, with $F/F_{cr} = 1$, the temperature is $T = 0.1$, and the anomalous diffusion process corresponds to $\alpha = 0.5$. The curve labels 1, 2, 3, and 4, correspond to increasing values of time; the solid line (theory) represents the stationary solution $\hat{P}_{st}(x)$ defined by Eq. (3.22).

studies. In addition, it provides a crucial test that allows one to distinguish between fractal and fractional Brownian motion on a practical level.

The probability density $P(x,t)$ associated with a normal diffusion process in a washboard potential cannot relax towards a stationary, asymptotic density, due to the open-boundary nature of the system. However, the reduced asymptotic space probability density (3.7), a periodic function by definition, does relax to the asymptotic stationary density (3.22). As mentioned, in fractional diffusion, the probability density reaches the same stationary density of the normal diffusion: the corresponding proof follows along the same lines of reasoning leading to the asymptotic fractional current $v_{\alpha}(F)$ which is formally equivalent to the Stratonovich formula valid in normal diffusion (see Secs. 3.3 and 6.3 and Ref. [199]). This result is depicted in Fig. 50, for the case of diffusion taking place in a tilted cosine potential.
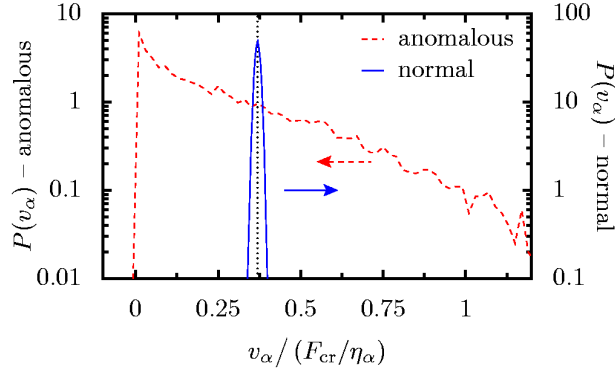
Figure 52: Anomalous (dashed line) and normal (continuous line) probability densities of the (sub)velocity, computed according to Eq. (6.25) at $t = 1000$ in rescaled time units. The potential, tilt, temperature and α value are the same as in Fig. 51. The arrows point to the corresponding y-axes. Despite the very different shapes, the two probability densities possess the same average value as given by the (fractional) Stratonovich formula (6.12), indicated with the vertical dotted line.

Even if the stationary probability density (depicted with continuous lines in Figs. 50 and 51) is the same, the relaxation to this stationary density is, however, very distinct for normal and anomalous diffusion, respectively, as shown in Fig. 51. In the case of normal diffusion, at any time instant t, the density has only one maximum, which moves from the initial position ($x = 0$) toward its asymptotic position $x = x'$. At the same time it undergoes a spreading process towards the stationary density. As more particles reach the area around $x = x'$, the peak begins to grow, eventually spreading again to relax to the stationary solution $\hat{P}_{\text{st}}(x)$ (Fig. 51 top). In clear contrast, for a case with anomalous diffusion the initial probability density undergoes a spreading in the direction of the bias. While the initial maximum of the density remains at $x = 0$, a second maximum emerges at $x \approx x'$, which continues to grow in weight as the density approaches the stationary shape $\hat{P}_{\text{st}}(x)$ (Fig. 51 bottom).

Finally, let us also investigate the probability densities of the velocities characterizing normal and anomalously slow transport in washboard potentials. For a particular trajectory realization $x^{(n)}(t)$, the corresponding (sub)velocity reads:

$$v_\alpha^{(n)} = \Gamma(\alpha + 1) \left[x^{(n)}(t) - x_0^{(n)} \right] t^{-\alpha}, \tag{6.25}$$

where $n \in 1, ..., N$ and $x_0^{(n)} = x^{(n)}(t_0)$. This (sub)velocity is a random variable and one can study the corresponding probability density. One

observes a spreading of the velocities corresponding to the broad spreading in space discussed above. The probability density for the velocity is depicted in Fig. 52 for a periodic substrate cosine potential, for $F/F_{\mathrm{cr}} = 1$, $T = 0.1$, and $\alpha = 0.5$. While the probability density for this velocity variable for normal diffusion (note the continuous line, right y-axis) possesses a Gaussian shape, in the anomalous case this probability density (see dashed line, left y-axis) assumes a very broad shape which falls off exponentially. Notably, however, the two densities have the same average, given by the Stratonovich formula, and indicated by the vertical dotted line in Fig. 52.

6.7 Conclusion

In the field of anomalous transport the main attention thus far has focused on the motion under the action of a constant or linear external force. Within the work presented in this chapter, we have investigated anomalously slow diffusion under the influence of spatially periodic forces.

The Stratonovich solution for the stationary current in a tilted periodic potential has been generalized to the case of subdiffusive transport. Moreover, we have proven that there exists a universal scaling law (6.10) — relating the mean square displacement and the mean particle position in washboard potentials — that does not involve the exact form of the periodic potential, the applied bias F, and the temperature T. This universal scaling was verified by numerical simulations.

As pointed out in Sec. 5.6.1, the weak ergodicity breaking [197] makes it impossible to obtain the averaged value of anomalous current with a single time-average over a single particle trajectory. Here occurs a profound difference with the case of normal diffusion. Such a time-averaged quantity is itself randomly distributed, as shown by the broad density in Fig. 52. In clear contrast to the situation with normal diffusion, for anomalous diffusion the current probability density is very broad and with a peak at the zero. Nevertheless, the average value of the current agrees very well with the theoretical Stratonovich value, as given by Eq. (6.12). These results in turn are close in spirit to recent work by Bel and Barkai on the weak ergodicity breaking for a spatially confined fractional diffusion [197].

Furthermore, we generalized the celebrated Lifson-Jackson result for normal diffusion in a periodic potential [89, 94, 95], to the case of anomalously slow diffusion. As a consequence, we found that, like in the case with normal diffusion, the effective anomalous diffusion becomes always suppressed over the bare value.

Our results may find ample applications in diverse areas where anomalous diffusion occurs; typical examples are superionic conductors [208] or Josephson junction dynamics [11, 209], when the role of disorder may change the normal diffusion into anomalous one.

In addition, we compared the time evolution for normal diffusion with anomalous, fractional diffusion. In doing so, we found that in a periodic potential, after a proper re-scaling of time, the corresponding asymptotic densities $P(x,t)$ for the coordinate x match each other. Distinct differences occur, however, at small evolution times. This time evolution of the densities drastically changes upon the application of a finite bias F. Now, the long time evolution between normal diffusion and anomalous diffusion becomes markedly distinct as well: while the maximum of the biased normal diffusion moves with the normal, directed current, the anomalous case is dominated by a ballistic diffusion that leaves the maximum of the density around the origin. Moreover, this characteristic difference can be put to work to discriminate between fractional and fractal Brownian diffusion.

7 Diffusion processes with anomalously slow relaxation in alternating fields

7.1 Motivation and set up of the problem

Normal Brownian motion occurring on potential landscapes that vary in time is known to exhibit a multifaceted collection of interesting phenomena, such as Brownian motors, anomalous nonlinear response behaviors, and stochastic resonance [7, 115, 156, 210, 211], to name a few. Therefore, it is tempting to ask, whether an explicit time dependent force entails a similarly versatile scenario also in the case of anomalously slow relaxation processes. This issue is in fact contained already in the first works on the motion of charge carriers in semiconductors [37], and has been the subject of some further investigations ever since, see e.g. the works [212–216], but never really has attracted proper attention on its fundamental level. Ultraslow relaxation in time dependent external potential fields thus still constitutes a challenge that is far from trivial.

A widely used approach to study subdiffusive processes is based on the fractional Fokker-Planck equation [6, 189, 190, 205]. For time independent forces the fractional Fokker-Planck equation (5.26) can be rigorously derived from continuous time random walk theory [6, 189, 190, 205].

In this chapter we show that the fractional Fokker-Planck equation in the form of (5.25), (5.26) is not correct in the case of a time dependent force $f(x,t)$. Furthermore, we argue that this fractional Fokker-Planck equation, when generalized *ad hoc* to a time dependent force, does not correspond to a physical stochastic process.

In different context, the study of a subdiffusive dynamics in the case of a purely time dependent force $f(t)$ has given rise to a fractional Fokker-Planck equation which differs from Eq. (5.26) [216]. Here, we derive an equation of similar form for the class of dichotomously alternating force fields $f(x,t) = f(x)\xi(t)$ with $\xi(t) = \pm 1$, varying in space and time. In the case of a Mittag-Leffler residence time distribution it reads,

$$\frac{\partial}{\partial t} P(x,t) = \left[-\frac{\partial}{\partial x} \frac{f(x,t)}{\eta_\alpha} + \kappa_\alpha \frac{\partial^2}{\partial x^2} \right] {}_0\hat{D}_t^{1-\alpha} P(x,t) \,. \tag{7.1}$$

Below, we prove this form in terms of continuous time random walk theory and additionally validate its correctness via the comparison of the analytical solutions of this so modified fractional Fokker-Planck equation (7.1) for a rectangular time-varying periodic force $f(x,t) \equiv f(t) = \xi(t)F$ ($F = $ const.) with the numerical simulations of the underlying continuous time random walk. Our main point is, however, that the reasoning provided in proving (7.1) forces us to scrutinize the physical validity of this so modified fractional Fokker-Planck equation (7.1) already beyond a dichotomous driving $f(t)$.

7.2 Anomalously slow processes in time dependent force fields

It is well known that neither a non-Markovian Fokker-Planck equation nor its solution with the initial condition $P(x, t) = \delta(x - x_0)$ [i.e. the two-event conditional probability $P(x, t|x_0)$] can fully define the non-Markovian stochastic process [69]. This is due to the fact that all non-Markovian processes, such as a continuous time random walk with a non-exponential waiting time distribution, lack per definition the factorization property, which would allow to express all the higher-order (multi-event) probability density functions in terms of the first two ones. Because a continuous time random walk is at the root of the fractional Fokker-Planck equation (5.26) [6, 189, 190, 205], in order to generalize the latter to the time dependent forces, one again starts from continuous time random walk theory. However, the usual scheme of merely replacing a time independent force $f(x)$ in Eq. (5.26) in an *ad hoc* manner with a time dependent force $f(t)$ is not adequate. The reason is that the underlying continuous time random walk possesses a residence time distribution with an infinite mean. Thus, any regular driving with a large but finite period is nonadiabatic. This very circumstance lies at the heart of the overall incorrectness of Eq. (5.26) for time dependent force fields.

In terms of a renewal description, a continuous time random walk is a semi-Markovian process, meaning that the sojourn times spent on the localization sites are independently distributed. Like in the previous chapter, we consider a one-dimensional continuous time random walk on a lattice $\{x_i = i\Delta x\}$ $(i = 0, \pm 1, \pm 2, \dots, \Delta x = \text{const.})$. After a time τ drawn from the residence time distribution $\psi_i(\tau)$, the particle at site i jumps with the probability $q_i^{\pm}$ to one of the nearest neighbor sites. The external force field $f(x)$ specifies both $\psi_i(\tau)$ and $q_i^{\pm}$, see Eqs. (5.34), (5.12), (5.8), and (5.13). Modulating the force $f(x)$ in time, $q_i^{\pm}$ assume obviously a time-dependence and $\psi_i^{\pm}(\tau|t) = q_i^{\pm}(t + \tau)\psi_i(t + \tau, t)$ become conditioned on the entrance time t for the site i [217]. For a Markovian continuous time random walk with time dependent rates $g_i^{\pm}(t)$ it is known that

$$\psi_i(t + \tau, t) = g_i(t + \tau) \exp\left[-\int_t^{t+\tau} g_i(t')\mathrm{d}t'\right], \tag{7.2}$$

with $g_i(t) = g_i^+(t) + g_i^-(t)$ and $q_i^{\pm}(t) = g_i^{\pm}(t)/g_i(t)$. For a driven non-Markovian continuous time random walk, however, a relation similar to Eq. (7.2) is lacking. As a result, the use of a fractional Fokker-Planck equation when generalized to the time dependent case of a time-varying force field remains moot. The usual scheme of the derivation of the generalized fractional Fokker-Planck equation from the underlying continuous time random walk can be used only if $\psi_i(\tau)$ remains unmodified by the

time dependent fields, i.e., if only the jump probabilities $q_i^{\pm}(t)$ change. We consequently find that $\psi_i^{\pm}(\tau|t) = q_i^{\pm}(t+\tau)\psi_i(\tau)$. Thus, the residence time distribution $\psi_i(\tau)$ remains unaffected only in the case of a dichotomous flashing force $f(x,t) = f(x)\xi(t)$, where $\xi(t) = \pm 1$ is a general dichotomic function of time t which can change periodically or also stochastically. Then, $q_i^{\pm}(t) = \exp[f(x_i)\xi(t)\Delta x/2]/\{\exp[f(x_i)\Delta x/2] + \exp[-f(x_i)\Delta x/2]\}$. We assume that $f(x)$ is continuous. Then, the modified fractional Fokker-Planck equation (7.1) can be derived rigorously in the continuous space limit. The derivation precisely follows the same reasoning as detailed in Sec. 2.7 (see also Ref. [205]), while taking $\psi_i(\tau)$ as the Mittag-Leffler distribution. It must be emphasized that for other driving forms $\xi(t)$, e.g., for a sinusoidal driving $F\sin(\omega t)$, this outlined derivation becomes flawed because $\psi_i(\tau)$ is affected by such time-varying fields, as unveiled already with Eq. (7.2). We remark also that due to the weak ergodicity breaking [197, 199] also the modified fractional Fokker-Planck equation (7.1) describes the dynamics of an ensemble of particles rather than the dynamics of an individual particle.

7.3 Rectangular driving force

7.3.1 Average particle position

We consider the subdiffusive dynamics in the presence of a dichotomous force, i.e., the absolute value of the force is fixed but the direction of the force flips periodically in time,

$$f(t) = \begin{cases} +F & \text{for} & n\tau_0 < t < (n+r)\tau_0 \\ -F & \text{for} & (n+r)\tau_0 < t < (n+1)\tau_0 \end{cases} . \tag{7.3}$$

Here τ_0 is the period of the time dependent force and $n = 0, 1, 2 \ldots$ The quantity $r \in (0,1)$ determines the value of the average force: $\langle f(t) \rangle_{\tau_0} = F(2r-1)$. For $r = 0.5$ the average bias is zero.

Let us begin by finding the recurrence relation for the moments $\langle x^n(t) \rangle$. Assuming in Eq. (7.1) the force of the form $f(t) = F\xi(t)$ and multiplying both sides of Eq. (7.1) by x^n and integrating over the x-coordinate one obtains,

$$\frac{\mathrm{d}\langle x^n(t) \rangle}{\mathrm{d}t} = n v_\alpha \, \xi(t) \, {}_0\hat{D}_t^{1-\alpha} \langle x^{n-1}(t) \rangle$$

$$+ \, n(n-1)\kappa_\alpha \, {}_0\hat{D}_t^{1-\alpha} \langle x^{n-2}(t) \rangle \,, \tag{7.4}$$

with $v_\alpha = F/\eta_\alpha$ $(n > 1)$. For $n = 1$ the last term on the right hand side of Eq. (7.4) is absent,

$$\frac{\mathrm{d}\langle x(t) \rangle}{\mathrm{d}t} = \frac{v_\alpha}{\Gamma(\alpha)} \, \xi(t) \, t^{\alpha-1} \,. \tag{7.5}$$
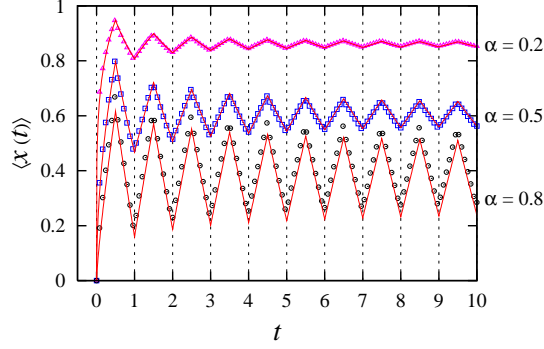
Figure 53: Average particle position $\langle x(t) \rangle$ for $r = 0.5$ and various values of the fractional exponent α: symbols represent the numerical results for the continuous time random walk obtained by averaging over 10^6 trajectories, while continuous lines represent the analytical solution (7.6) of the modified fractional Fokker-Planck equation (7.1). The time-period of the force is $\tau_0 = 1$ and $F_0/(\eta_\alpha \sqrt{\kappa_\alpha}) = 1$ is used in numerical simulations.

Upon integrating Eq. (7.5) in time, the solution for the average particle position reads:

$$\langle x(t) \rangle = \begin{cases} x_N + \frac{v_\alpha t^\alpha}{\Gamma(\alpha+1)}, & N\tau_0 \leq t < (N+r)\tau_0, \\ x'_N - \frac{v_\alpha t^\alpha}{\Gamma(\alpha+1)}, & (N+r)\tau_0 \leq t < (N+1)\tau_0, \end{cases} \tag{7.6}$$

where

$$x_N = \langle x(0) \rangle - \frac{v_\alpha(N\tau_0)^\alpha}{\Gamma(\alpha+1)} + \frac{v_\alpha\tau_0^\alpha}{\Gamma(\alpha+1)} \sum_{n=0}^{N-1} [2(n+r)^\alpha - n^\alpha - (n+1)^\alpha],$$

$$x'_N = x_N + \frac{2v_\alpha\tau_0^\alpha}{\Gamma(\alpha+1)}(N+r)^\alpha; \tag{7.7}$$

N counts the number of time periods passed.

The analytical solution (7.6) for the mean particle position $\langle x(t) \rangle$ from the modified fractional Fokker-Planck equation (7.1) is compared with the numerical solutions of the continuous time random walk in Fig. 53 for $r = 0.5$ (the average bias is zero) and different values of the fractional exponent α; in Fig. 54 the comparison is presented for $\alpha = 0.5$ and different values of r. The good agreement between our analytical and numerical results confirms that Eq. (7.1) is a correct method to describe the continuous time random walk driven by a rectangular time-dependent force. Furthermore, the results depicted in Figs. 53 and 54 exhibit the phenomenon of the "death of linear response" of the fractional kinetics to time-dependent fields in
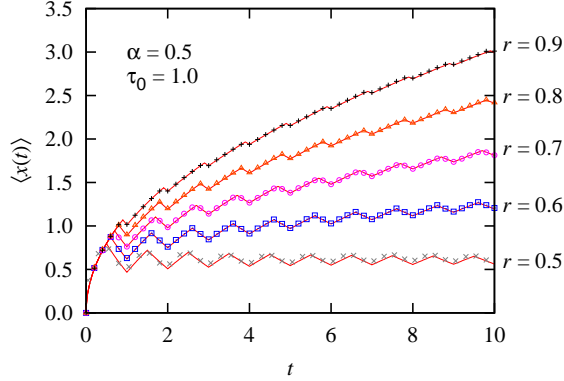
118

Figure 54: Average particle position $\langle x(t) \rangle$ for various values of the parameter r and anomalous exponent α: Symbols represent the numerical results for the continuous time random walk obtained by averaging over 10^5 trajectories (for $r = 0.5$ over 10^6 trajectories), while continuous lines represent the analytical solution (7.6) of the modified fractional Fokker-Planck equation (7.1). The time-period of the force is $\tau_0 = 1$, fractional exponent $\alpha = 0.5$, and $F_0/(\eta_\alpha \sqrt{\kappa_\alpha}) = 1$ is used in numerical simulations.

the limit $t \rightarrow \infty$, reported also in Refs. [214, 216] [10]. As a result, in the absence of an average bias, in the long-time limit the mean particle position approaches a constant value, rather than being oscillatory,

$$\langle x(\infty) \rangle = v_\alpha \tau_0^\alpha b(\alpha)/\Gamma(\alpha + 1), \tag{7.8}$$

where $b(\alpha) = \sum_{n=0}^{\infty}[2(n + 1/2)^\alpha - n^\alpha - (n + 1)^\alpha]$, with the amplitude of the oscillations decaying to zero as $1/t^{1-\alpha}$, see Eq. (7.5); for $\alpha = 1$ (normal diffusion) the particle position assumes the oscillating motion also when $t \rightarrow \infty$. The function $b(\alpha)$ describes the initial field phase effect which the system remembers forever when $\alpha < 1$. It changes monotonously from $b(0) = 1$ to $b(1) = 0$. The averaged traveled distance $\langle x(\infty) \rangle$ scales as $\tau_0^\alpha = (2\pi/\omega_0)^\alpha$, where ω_0 is the corresponding angular frequency. This "death of linear response" to time periodic fields is also in agreement with the results for a driven non-Markovian two state system [218] in the formal limit of infinite mean residence times. Notably, this feature is overcome when one introduces a cutoff of the residence times distributions at long times (yielding a finite first moment), as used already in the pioneering work [185].

---

[10]The "death of linear response" is not observed when applying the time dependent force (7.3) to the traditional fractional Fokker-Planck equation (5.26). In this case, the solution of the fractional Fokker-Planck equation and of the continuous time random walk do not agree (see also Ref. [213]).
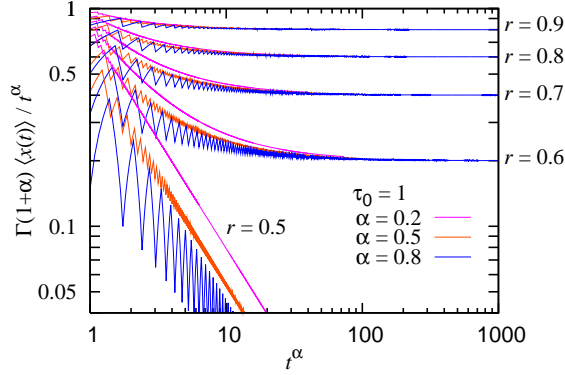
Figure 55: The analytical solution (7.6) for average particle position $\langle x(t)\rangle$ obtained from the modified fractional Fokker-Planck equation (7.1) is presented for various values of the parameter r (various values of the average bias) and anomalous exponent α. The time-period of the force is $\tau_0 = 1$, however in the long time limit the same asymptotical value is obtained for any value of τ_0.

In this case, the subdiffusive behavior emerges as a transient, crossover behavior to asymptotically normal diffusion. Then, linear response theory based on the fluctuation-dissipation theorem becomes applicable [185].

In Fig. 55 the solution (7.6) for the average particle position is presented in the long time limit for various values of α and r. The figure demonstrates that in the presence of an average bias the mean particle position grows as t^α, whereas in the absence of the bias ($r = 0.5$) $\langle x(t)\rangle/t^\alpha$ decays to zero.

7.3.2 Mean square displacement

Let us now study the mean square displacement defined by Eq. (2.12). For $n = 2$ one obtains from Eq. (7.4),

$$\frac{\mathrm{d}\langle x^2(t)\rangle}{\mathrm{d}t} = 2v_\alpha\,\xi(t)\,_0\hat{D}_t^{1-\alpha}\langle x(t)\rangle + \frac{2\kappa_\alpha}{\Gamma_\alpha}\,t^{\alpha-1}\,. \tag{7.9}$$

In order to find the analytical solution for the mean square displacement, we use the Laplace-transform method and the Fourier series expansion for $\xi(t) = \xi(t + \tau_0)$,

$$\xi(t) = \sum_{n=-\infty}^{\infty} f_n \exp(in\omega_0 t)\,, \tag{7.10}$$
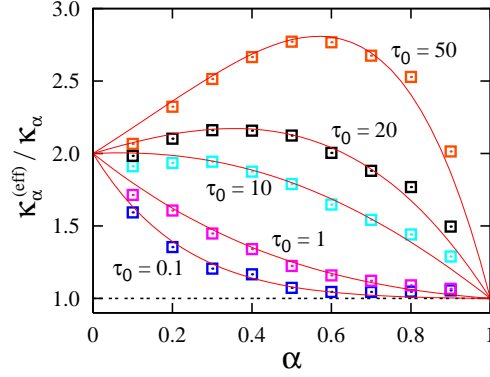
Figure 56: Scaled effective fractional diffusion coefficient $\kappa_\alpha^{(\mathrm{eff})}$ vs fractional exponent α for different driving periods τ_0. The average bias is zero ($r = 0.5$). The analytical prediction (7.14) (continuous lines) is compared with the numerical results (symbols) obtained from the continuous time random walk by averaging over 10^5 trajectories. For $\tau_0 > 2\pi \exp[-\frac{d}{d\alpha} \ln g(\alpha)|_{\alpha=0}] \approx 8.818$ the effective fractional diffusion coefficient $\kappa_\alpha^{(\mathrm{eff})}(\alpha)$ exhibits a maximum.

where

$$f_n = \frac{1}{\tau_0} \int_0^{\tau_0} \xi(t) \exp(-in\omega_0 t)\mathrm{d}t = [1 - \exp(-inr2\pi)]/(in\pi). \quad (7.11)$$

Applying them to Eq. (7.9) and assuming $\langle x(0) \rangle = 0$ and $\langle x^2(0) \rangle = 0$ we obtain (see Appendix B),

$$
\begin{aligned}
\langle x^2(t) \rangle = {} & \frac{2v_\alpha^2(2r-1)^2}{\Gamma(2\alpha+1)} t^{2\alpha} + \frac{2\kappa_\alpha}{\Gamma(\alpha+1)} t^\alpha \\
& + \frac{4v_\alpha^2(2r-1)}{\pi\omega_0^\alpha\Gamma(\alpha+1)} \left\{ \zeta(1+\alpha)\sin(\alpha\pi/2) - \sum_{n=1}^\infty \frac{\sin[(\alpha-4nr)\pi/2]}{n^{1+\alpha}} \right\} t^\alpha \\
& + \frac{8v_\alpha^2\cos(\alpha\pi/2)}{\pi^2\omega_0^\alpha\Gamma(\alpha+1)} \left[\zeta(2+\alpha) - \sum_{n=1}^\infty \frac{\cos(nr2\pi)}{n^{2+\alpha}} \right] t^\alpha. \quad (7.12)
\end{aligned}
$$

For $r = 0.5$ (average zero bias) the first and third term in the latter equation are equal to zero. Furthermore, in the long time limit the average particle position $\langle x(\infty) \rangle$ is a finite constant. The asymptotic behavior of the mean square displacement is thus proportional to t^α as in the force free case, however, characterized by an effective fractional diffusion coefficient $\kappa_\alpha^{(\mathrm{eff})}$ instead of the free fractional diffusion coefficient κ_α, i.e.,

$$\langle \delta x^2(t) \rangle = 2\kappa_\alpha^{(\mathrm{eff})} t^\alpha/\Gamma(1+\alpha) \quad \text{for} \quad t \to \infty \quad (7.13)$$
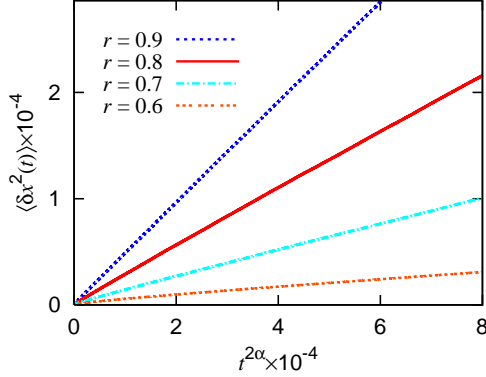
31

121

Figure 57: The mean square displacement calculated form the numerical simulation of the continuous time random walk for various values of the average bias. Fractional exponent $\alpha = 0.5$ and driving period $\tau_0 = 1$.

[c.f. Eqs. (6.9) and (6.18)]. The effective diffusion coefficient is,

$$
\begin{aligned}
\kappa_\alpha^{(\mathrm{eff})} &= \kappa_\alpha + \frac{8F^2}{\pi^2 \eta_\alpha^2 \omega_0^\alpha} \zeta(\alpha+2) \left(1 - \frac{1}{2^{\alpha+2}}\right) \cos(\alpha\pi/2) \\
&= \kappa_\alpha + g(\alpha)F^2/(\eta_\alpha^2 \omega_0^\alpha) \, ;
\end{aligned}
\tag{7.14}
$$

here

$$
g(\alpha) = (2/\pi^2)\zeta(2+\alpha)[4 - 2^{-\alpha}] \cos(\pi\alpha/2)
\tag{7.15}
$$

is a function decaying from $g(0) = 1$ towards $g(1) = 0$ and $\zeta(x)$ is the Riemann's zeta-function. The driving-induced part of the effective subdiffusion coefficient is directly proportional to the square of driving amplitude and inversely proportional to ω_0^α. For slowly oscillating force fields this leads to a profound enhancement of subdiffusion compared with the force free case: an optimal value of the fractional exponent α exists, at which the driving-induced part of the effective fractional diffusion coefficient possesses a maximum (see Fig. 56). For $\alpha = 1$ the free diffusion coefficient is recovered, this is true also in the presence of an average bias, i.e., for $r \neq 0.5$.

In the case of the anomalously slow diffusion, when $r \neq 0.5$ (finite average bias) we obtain as an approximate result for $\langle x(t)\rangle^2$ (see Appendix C),

$$
\langle x(t)\rangle^2 = \frac{v_\alpha^2 (2r-1)^2}{\Gamma^2(\alpha+1)} t^{2\alpha} + \frac{2v_\alpha^2 (2r-1)}{\Gamma(\alpha)\Gamma(\alpha+1)} \vartheta_n(t_1) t^\alpha \, ;
\tag{7.16}
$$

here $\vartheta_n(t_1)$ is a function of a parameter $t_1 \in (0, t)$ (see Appendix C).

The results (7.12) and (7.16) indicate that in the presence of a rectangular time dependent force with a finite bias the general behaviour of the

122

mean square displacement is similar to the case of a constant force, i.e., the mean square displacement consists of terms proportional to t^α and $t^{2\alpha}$ [c.f. Eq. (6.4)]. In fact, for the term proportional to $t^{2\alpha}$ in the mean square displacement $\langle \delta x^2(t) \rangle$ one obtains the coefficient [see Eqs. (7.12), (7.16)]

$$\frac{[F(2r-1)]^2}{\eta_\alpha^2} \left[\frac{2}{\Gamma(2\alpha+1)} - \frac{1}{\Gamma^2(\alpha+1)} \right] ,$$

where $F(2r-1) = \langle f(t) \rangle_{\tau_0}$ is the average force. This coefficient is exactly the same as in the case of a constant bias of the value $F(2r-1)$.

The theoretical result that the mean square displacement in the case of a rectangular force with a finite average bias behaves in the long time limit as $\langle \delta x^2(t) \rangle \propto t^{2\alpha}$ is confirmed by the numerical simulations of the continuous time random walk presented in Fig. 57. Furthermore, similarly to the case of a constant bias, or of a washboard potential, the asymptotic scaling relation (6.10) (see also Fig. 45) holds ($r \neq 0.5$, $\langle f(t) \rangle_{\tau_0} \neq 0$) between the mean square displacement and average particle position. We have validated this relation numerically.

7.4   Resumé and discussion

In this part of the work we discussed the dynamics of anomalously slow processes in time-varying potential landscapes within the continuous time random walk and fractional Fokker-Planck equation descriptions. We demonstrated that the common form of the fractional Fokker-Planck equation given by Eq. (5.26) is not valid for time dependent forces; it does not correspond to the underlying continuous time random walk modulated by an external time dependent force field. A modified form of the fractional Fokker-Planck equation, Eq. (7.1), is derived for dichotomously alternating fields. As an exactly solvable example we studied a periodic rectangular force and successfully tested the analytical results via numerical simulations of the underlying time-modulated continuous time random walk. We showed that in the absence of the average bias the average particle position reaches a constant value whereas the mean square displacement grows as t^α. We also demonstrated that a symmetric dichotomous force with average zero bias enhances the diffusion in respect to the free case, differently of the cae of normal diffusion. Furthermore, it was found that for sufficiently slow driving the effective fractional diffusion coefficient $\kappa_\alpha^{(\text{eff})}$ exhibits a maximum *versus* the fractional exponent α. In the presence of the average bias, in the long time limit the average particle position was shown to grow as t^α and the mean square displacement as $t^{2\alpha}$.

Our study, however, is not able to validate the correctness of the modified fractional Fokker-Planck equation (7.1) when extended *ad hoc* to an

arbitrary time dependent potential landscape different from the dichotomous case. A way out of the dilemma consists in relying on models of driven subdiffusion which either are based on the generalized Langevin dynamics [219,220] or on fractal Brownian motion. The challenge of modeling subdiffusion in a time-varying potential landscape thus necessitates plenty of further enlightening research.

8 Summary

In the present thesis we investigated normal and anomalously slow diffusion under the influence of forces periodic in space and diffusion with anomalously slow relaxation under the influence of forces changing in time, focusing on one-dimensional models. The motivation for such studies comes from condensed matter phyics, materials science, chemical physics, nanotechnology, and molecular biology. Furthermore, as the direct observation of cellular flows and the operation of biology inspired nanodevices are becoming experimentally more and more accessible, understanding particle diffusion in a one-dimensional system has been recognized to be a key issue in transport control.

Concerning the processes undergoing normal diffusion, the transport of Brownian particles on periodic substrates with one and two minima per period in the presence and in the absence of an external applied bias was studied. We used piecewise linear potentials which allowed us to derive the analytical expressions for the current and diffusion coefficient. It was demonstrated that transport processes in periodic substrates are very sensitive to the value of noise intensity and bias. Furthermore, it was shown that also the shape of the periodic potential has a significant influence in determining the stochastic transport. In particular, large values of the asymmetry parameter k in the direction of bias F favor the amplification of diffusion by means of tilted potential and temperature in comparison with free thermal diffusion. Moreover, in the case of a double-humped potential, the effective diffusion coefficient $D(F)$ can have two maxima.

We also investigated the diffusion of dimers consisting of two harmonically interacting Brownian monomers in a washboard potential, comparing the results with that of a single monomer. We studied the dimer transport for different coupling strengths and damping constants and found that the average current and the diffusion coefficient of such a dimer exhibit a complicated non-monotonic behavior as a function of the driving force and the ratio of the dimer length to substrate constant. We concluded that the appearance of the second resonant peak of the diffusion coefficient *versus* the driving force is not related to the dimer length-to-substrate constant ratio, but rather to the damping-to-coupling constant ratio; the diffusion coefficient $D(F)$ possesses two peaks only for relatively low damping values.

Concerning the anomalously slow diffusion in periodic substrates, the Lifson-Jackson result for the diffusion coefficient in a periodic potential and the Stratonovich solution for the stationary current in a washboard potential were generalized to the case of anomalous transport. Moreover, it was proven that the relation between the mean square displacement and the mean particle position in a tilted periodic potential is the same as in the case of a constant bias. The differences between normal and anomalously

32

slow transport processes in a periodic substrate were discussed by means of the probability distributions. Namely, in the absence of the bias, at small times the densities $P(x,t)$ for the position x were found to behave in different ways, whereas in the long time limit, after a proper re-scaling of time, the asymptotic densities $P(x,t)$ were found to match. However, in the presence of a finite bias the different behaviors of the probability densities $P(x,t)$ of normal and anomalous diffusion were found to occur also in the long time limit: while the maximum of the biased normal diffusion moves with the normal, directed current, the anomalous case is dominated by a ballistic diffusion that leaves the maximum of the density around the origin (memory effect). Furthermore, the distributions $P(v_\alpha,t)$ for the velocity v_α were found to be distinctively different for $\alpha = 1$ and $\alpha \neq 1$, corresponding respectively to normal and anomalous diffusion, even though having the same averages, given by the (generalized) Stratonovich formula. While the probability density for the normal diffusion possesses a Gaussian shape, in the anomalous case it assumes a very broad shape falling off exponentially.

Finally, the dynamics of anomalously slow processes in time-varying potential landscapes were discussed within the continuous time random walk and fractional Fokker-Planck equation descriptions. It was demonstrated that the common form of the fractional Fokker-Planck equation is not valid for time-dependent forces. A modified form of the fractional Fokker-Planck equation was derived, valid, however, for dichotomously alternating fields only. As an exactly solvable example, a periodic rectangular force was studied; the behavior of the transport was found to be very different compared to the case of normal transport processes. Namely, instead of assuming an oscillatory motion, in the absence of the average bias the mean particle position reaches a constant value; the mean square displacement grows as t^α. Differently from the normal diffusion case, the fractional diffusion coefficient becomes enhanced compared to the free fractional diffusion coefficient. In the presence of the average bias, in the long time limit the average particle position was shown to grow as t^α and the mean square displacement as $t^{2\alpha}$.

An original numerical algorithm was derived to simulate the fractional Fokker-Planck equation and the modified fractional Fokker-Planck equation through the underlying continuous time random walk dynamics. All the analytical results concerning the anomalously slow processes were tested through numerical simulations.

Summary in Estonian

Käesolevas doktoritöös on uuritud normaalset ning anomaalselt aeglast difusiooni ruumis perioodilistes jõuväljades ning anomaalselt aeglase relaksatsiooniga difusiooniprotsesse ajas muutuvates jõuväljades. Vaadeldud on ühedimensionaalseid süsteeme. Uuritud probleemid on olulised kondenseeritud aine füüsikas, materjaliteaduses, keemilises füüsikas, nanotehnoloogias ning molekulaarbioloogias.

Seoses normaalse difusiooniga on uuritud Browni osakeste transporti perioodilistel struktuuridel (ühe ning kahe miinimumiga perioodi kohta) välise rakendatud konstantse jõu olemasolul ning puudumisel. Kasutatud on tükati lineaarseid potentsiaale, mis võimaldasid tuletada täpsed analüütilised valemid voolu ning difusioonikoefitsiendi jaoks. On näidatud, et transport perioodilistel struktuuridel on väga tundlik müra intensiivsuse ning rakendatud konstantse jõu väärtuse suhtes. Samuti omab olulist rolli perioodilise potentsiaali kuju. Selle asümeetria kallutava jõu F suunas soodustab difusiooni võimendamist kallutatud perioodilistel potentsiaalidel. Perioodi kohta kahte miinimumi omavate potentsiaalide korral võib difusioonikoefitsient $D(F)$ omada kahte maksimumi.

Doktoritöös on uuritud ka kahest harmooniliselt interakteeruvast Browni osakesest koosnevate dimeeride difusiooni kallutatud perioodilistel potentsiaalidel, võrreldes tulemusi monomeeri jaoks saadutega. Dimeeride transporti on uuritud erinevate interaktsioonikonstandi väärtuste korral ning on leitud, et seda iseloomustavad keskmine vool ning difusioonikoefitsient kui kallutava jõu ning dimeeri pikkuse ja substraadi konstandi suhte funktsioonid omavad keerukat mittemonotoonset iseloomu. Kokkuvõttes võib öelda, et teise resonantse difusioonikoefitsiendi maksimumi ilmnemine *versus* kallutav jõud ei ole seotud dimeeri pikkuse ja substraadi konstandi suhtega, nagu leitud eelnevalt artiklis [169], vaid pigem sumbuvuse ja interaktsiooni tugevuse suhtega; difusioonikoefitsient $D(F)$ omab kahte maksimumi üksnes suhteliselt väikeste sumbuvusteguri väärtuste korral.

Uurides anomaalselt aeglast difusiooni perioodilistel substraatidel on leitud, et Lifson-Jacksoni tulemus difusioonikoefitsiendi jaoks perioodilistel potentsiaalidel ning Stratonovichi tulemus statsionaarse voolu jaoks kallutatud perioodilistel potentsiaalidel on üldistatavad ka anomaalse transpordi juhule. Lisaks sellele on tõestatud, et dispersiooni ja osakese keskmise koordinaadi vahel kehtib kallutatud perioodilistel potentsiaalidel sama seos nagu konstantse jõuvälja korral. Uurides tõenäosusjaotusi on kirjeldatud erinevusi normaalse ning anomaalselt aeglase transpordi vahel. Kallutuse puudumisel käituvad jaotused $P(x,t)$ koordinaadi x jaoks lühemas ajaskaalas erinevalt, pikemas ajaskaalas aga, pärast sobivat aja skaleeringut, nad ühtivad. Kallutuse olemasolul leiti normaalset ning anomaalset difusiooni kirjeldavad tõenäosusjaotused $P(x,t)$ käituvat erinevalt ka pikemas ajaskaalas:

normaalse difusiooni korral konstantses jõuväljas liigub tõenäosusjaotuse maksimum jõuvektori suunas, kuna aga anomaalse transpordi puhul on domineerivaks ballistiline difusioon ning tõenäosusjaotuse maksimum on määratud algtingimusega (süsteemil on mälu). Jaotused $P(v_\alpha, t)$ kiiruse v_α jaoks leiti olevat oluliselt erinevad $\alpha = 1$ (normaalne difusioon) ning $\alpha \neq 1$ (subdifusioon) korral, vaatamata sellele, et nendel juhtudel langevad kiiruse keskväärtused kokku, olles määratud (üldistatud) Stratonovichi valemiga. Normaalse difusiooni korral on tõnäosustihedus $P(v_\alpha, t)$ antud Gaussi jaotusega; anomaalse difusiooni korral on $P(v_\alpha, t)$ kuju oluliselt laiem, kahanedes kiiruse kasvades eksponentsiaalselt.

Viimasena on uuritud anomaalselt aeglast difusiooni ajas muutvates jõuväljades ajas pideva uitliikumise ning fraktsionaalse Fokker-Plancki võrrandi formalismis. On näidatud, et fraktsionaalse Fokker-Plancki võrrandi tavapärane kuju ei ole sobiv kirjeldamaks subdifusiooni ajast sõltuvatel potentsiaalidel. Tuletatud on modifitseeritud fraktsionaalne Fokker-Plancki võrrand, mis on kehtiv siiski vaid dihotoomselt muutuvate väljade korral. Täpselt lahenduva näitena on uuritud ajas tükati konstantset perioodilist jõudu. Leiti, et transport osutub siin olevat vägagi erinev võrreldes normaalse difusiooniga: keskmise jõu puudumisel ei ole liikumine ostsilleeruv, nagu normaalsel juhul, vaid osakese keskmine koordinaat omandab asümptootiliselt konstantse väärtuse; dispersioon kasvab ajas nagu t^α. Erinevalt normaalse difusiooni juhust, saab fraktsionaalne difusioon võimendatud võrreldes vaba fraktsionaalse difusiooniga. Keskmise jõu olemasolul kasvab osakese keskmine koordinaat nagu t^α ning dispersioon nagu $t^{2\alpha}$.

Tuletatud on ka algupärane numbriline algorütm simuleerimaks fraktsionaalset Fokker-Plancki võrrandit ning modifitseeritud Fokker-Plancki võrrandit ajas pideva uitliikumise dünaamika kaudu. Kõik analüütilised tulemused anomaalselt aeglase difusiooni jaoks on kontrollitud numbriliste simulatsioonide abil.

Acknowledgments

As the work presented in this thesis is done in collaboration, I want to thank all the co-authors for their contributions. Special thanks go to Teet Örd who was the first person to introduce me the fascinating topic of stochastic processes and Igor Goychuk who introduced me the field of anomalous diffusion and fractional dynamics. I am grateful to Peter Hänggi and Fabio Marchesoni for their support and their hospitality during my stays at the universities of Augsburg and Camerino, and I cannot forget the hospitality of prof. Ulrich Eckern and Luca Gammaitoni. My sincere gratitude goes to Fabio Marchesoni, Marco Patriarca and Igor Goychuk for their efforts to read the manuscript and for their comments. I also appreciate the support and understanding of Raivo Stern and Martti Raidal during the last year of my studies.

Appendixes

A Analytical results for piecewise linear potentials with two maxima per period

The analytical results for the diffusion coefficient, current and Péclet factor are given by Eqs. (3.47)-(3.49). Performing the integrations in Eqs. (3.92) one obtains after cumbersome calculations the algebraic expressions for the quantities Z and Y, given by Eqs. (3.90) and (3.91), in the case of the sawtooth potential with two maxima per period:

$$
\begin{aligned}
Z = {} & \varphi_0 \left(k_1\, g_{ab} - k_2\, g_{bc} + k\, g_{cd} - \frac{1}{d} \right) + \frac{T}{a}\, S_1 (1 - \lambda_1) \\
& + \frac{T}{b}\, S_2 (1 - \lambda_2) - \frac{T}{c}\, S_3 (1 - \lambda_3) + \frac{T}{d}\, S_4 (1 - \lambda_4) \,,
\end{aligned}
\tag{A.1}
$$

$$
\begin{aligned}
Y = {} & \varphi_0^3 \left[k_1 \left(\frac{1}{a^3} + \frac{1}{b^3} \right) - k_2 \left(\frac{1}{b^3} + \frac{1}{c^3} \right) + k \left(\frac{1}{c^3} + \frac{1}{d^3} \right) - \frac{1}{d^3} \right] \\
& + T\varphi_0^2 \left[\frac{(1-\lambda_1)}{a^3} \left(2S_1 + S_1' \right) + \frac{(1-\lambda_2)}{b^3} \left(2S_2 + \lambda_2^{-1} S_2' \right) \right. \\
& \left. - \frac{(1-\lambda_3)}{c^3} \left(2S_3 + S_3' \right) + \frac{(1-\lambda_4)}{d^3} \left(2S_4 + \lambda_4^{-1} S_4' \right) \right] \\
& + T \left\{ \frac{(1-\lambda_1)}{a}\, S_1^2 \left[\lambda_1 S_1' + \frac{\varphi_0}{2a} (1+\lambda_1) \right] + \frac{1-\lambda_2}{b}\, S_2^2 \left[S_2' - \frac{\varphi_0}{2b} (1+\lambda_2) \right] \right. \\
& \left. - \frac{(1-\lambda_3)}{c}\, S_3^2 \left[\lambda_3 S_3' + \frac{\varphi_0}{2c} (1+\lambda_3) \right] + \frac{(1-\lambda_4)}{d}\, S_4^2 \left[S_4' - \frac{\varphi_0}{2d} (1+\lambda_4) \right] \right\} \\
& + 2\varphi_0 \left[\frac{k_1}{a}\, \lambda_1 S_1 S_1' - \frac{\Delta k}{b}\, S_2 S_2' + \frac{k-k_1}{c}\, \lambda_3 S_3 S_3' - \frac{1-k}{d}\, S_4 S_4' \right] .
\end{aligned}
\tag{A.2}
$$

Here

$$
g_{ab} = \frac{1}{a} + \frac{1}{b}, \quad g_{bc} = \frac{1}{b} + \frac{1}{c}, \quad g_{cd} = \frac{1}{c} + \frac{1}{d}, \quad g_{ad} = \frac{1}{a} + \frac{1}{d};
\tag{A.3}
$$

$$
\begin{aligned}
& \lambda_1 = \exp\left[-\frac{Fk_1}{T(1-k)} - \frac{1-A_1}{T} \right], && \lambda_2 = \exp\left[\frac{F\Delta k}{T(1-k)} - \frac{\Delta A}{T} \right], \\
& \lambda_3 = \exp\left[\frac{F(k-k_2)}{T(1-k)} + \frac{A_2}{T} \right], && \lambda_4 = \exp\left(-\frac{1-F}{T} \right), \\
& \lambda_5 = \exp\left[\frac{F(k-k_1)}{T(1-k)} + \frac{A_1}{T} \right], && \lambda_6 = \exp\left[\frac{F(1-k_1)}{T(1-k)} - \frac{1-A_1}{T} \right], \\
& \lambda_7 = \exp\left[\frac{F(1-k_2)}{T(1-k)} - \frac{1-A_2}{T} \right];
\end{aligned}
\tag{A.4}
$$

$$
\begin{aligned}
S_1 &= -g_{ab} + g_{bc}\lambda_2^{-1} - g_{cd}\lambda_5^{-1} + g_{ad}\lambda_6^{-1}\,, \\
S_1' &= g_{ab}\lambda_6^{-1} - g_{bc}\lambda_7^{-1} + g_{cd}\lambda_4^{-1} - g_{ad}\,, \\
S_2 &= -g_{ab}\left(1 - \varphi_0\right) + g_{bc}\lambda_2^{-1} - g_{cd}\lambda_5^{-1} + g_{ad}\lambda_6^{-1}\,, \\
S_2' &= g_{ab} - g_{bc}\,\lambda_2\left(1 - \varphi_0\right) + g_{cd}\,\lambda_5\left(1 - \varphi_0\right) - g_{ad}\,\lambda_6\left(1 - \varphi_0\right)\,, \\
S_3 &= -g_{ab}\lambda_2(1 - \varphi_0) + g_{bc}(1 - \varphi_0) - g_{cd}\lambda_3^{-1} + g_{ad}\lambda_7^{-1}\,, \\
S_3' &= g_{ab}\lambda_5^{-1} - g_{bc}\lambda_3^{-1} + g_{cd}\left(1 - \varphi_0\right) - g_{ad}\,\lambda_4\left(1 - \varphi_0\right)\,, \\
S_4 &= -g_{ab}\,\lambda_5\left(1 - \varphi_0\right) + g_{bc}\,\lambda_3\left(1 - \varphi_0\right) - g_{cd}\left(1 - \varphi_0\right) + g_{ad}\lambda_4^{-1}\,, \\
S_4' &= g_{ab}\lambda_5^{-1} - g_{bc}\lambda_3^{-1} + g_{cd} - g_{ad}\,\lambda_4\left(1 - \varphi_0\right)\,.
\end{aligned} \tag{A.5}
$$

B   Calculation of $\langle x^2(t)\rangle$ for the anomalously slow transport under the influence of a rectangular driving force

Using the property $\mathcal{L}\{\mathrm{d}f(t)/\mathrm{d}t\} = s\mathcal{L}\{f(t)\} - f(0)$ and assuming the initial conditions $\langle x(t)\rangle = 0$ and $\langle x^2(t)\rangle = 0$ we obtain from Eq. (7.9),

$$
\mathcal{L}\{\langle x^2t\rangle\} = \frac{2\kappa_\alpha}{s^{\alpha+1}} + \frac{2v_\alpha}{s}\,\mathcal{L}\{\xi(t)\,_0\hat{D}_t^{1-\alpha}\langle x(t)\rangle\}\,. \tag{B.1}
$$

Considering that

$$
\mathcal{L}\{\,_0\hat{D}_t^{1-\alpha}\langle x(t)\rangle\} = s^{1-\alpha}\mathcal{L}\{\langle x(t)\rangle\} = s^{-\alpha}\mathcal{L}\{\mathrm{d}\langle x(t)\rangle/\mathrm{d}t\}\,,
$$

one obtains,

$$
\mathcal{L}\{\xi(t)\,_0\hat{D}_t^{1-\alpha}\langle x(t)\rangle\} = \sum_{n=-\infty}^{\infty} \frac{f_n}{(s - in\omega_0)^\alpha}\,\mathcal{L}_{s-in\omega_0}\left\{\frac{\mathrm{d}\langle x(t)\rangle}{\mathrm{d}t}\right\}\,. \tag{B.2}
$$

Using Eq. (7.5), it follows,

$$
\mathcal{L}_{s-in\omega_0}\left\{\frac{\mathrm{d}\langle x(t)\rangle}{\mathrm{d}t}\right\} = v_\alpha \sum_{m=-\infty}^{\infty} \frac{f_m}{[s - i\omega_0(n+m)]^\alpha}\,. \tag{B.3}
$$

Inserting (B.2) and (B.3) into Eq. (B.1) we obtain,

$$
\mathcal{L}\{\langle x^2t\rangle\} = \frac{2\kappa_\alpha}{s^{\alpha+1}} + \frac{2v_\alpha^2}{s} \sum_{n=-\infty}^{\infty} \frac{f_n}{(s - in\omega_0)^\alpha} \sum_{m=-\infty}^{\infty} \frac{f_m}{[s - i\omega_0(n+m)]^\alpha}\,. \tag{B.4}
$$

Let us separate in Eq. (B.4) the terms $m = 0$ and $n = 0$,

$$
\begin{aligned}
\mathcal{L}\{\langle x^2(t)\rangle\} &= \frac{2\kappa_\alpha}{s^{\alpha+1}} + \frac{2v_\alpha^2 f_0^2}{s^{2\alpha+1}} + \frac{2v_\alpha^2 f_0}{s^{\alpha+1}} \sum_{\substack{m=-\infty \\ m\neq 0}}^{\infty} \frac{f_m}{(s - im\omega_0)^\alpha} \\
&\quad + \frac{2v_\alpha^2}{s} \sum_{\substack{n=-\infty \\ n\neq 0}}^{\infty} \frac{f_n}{(s - in\omega_0)^\alpha} \sum_{m=-\infty}^{\infty} \frac{f_m}{[s - i\omega_0(n+m)]^\alpha}\,.
\end{aligned} \tag{B.5}
$$

In the long time limit, i.e., in the limit $s \to 0$, in the double sum only terms with $m = -n$ contribute, giving thus,

$$\mathcal{L}\{\langle x^2(t)\rangle\} = \frac{2\kappa_\alpha}{s^{\alpha+1}} + \frac{2v_\alpha^2 f_0^2}{s^{2\alpha+1}} + \frac{2v_\alpha^2 f_0}{\omega_0^\alpha s^{\alpha+1}} \sum_{\substack{m=-\infty \\ m\neq 0}}^{\infty} \frac{f_m}{(-im)^\alpha}$$

$$+ \frac{2v_\alpha^2}{\omega_0^\alpha s^{\alpha+1}} \sum_{\substack{n=-\infty \\ n\neq 0}}^{\infty} \frac{|f_n|^2}{(-in)^\alpha} . \tag{B.6}$$

Let us compute the sums. Considering that

$$\sum_{\substack{m=-\infty \\ m\neq 0}}^{\infty} \frac{f_m}{(-im)^\alpha} = \sum_{m=1}^{\infty} \left[\frac{f_m}{(-im)^\alpha} + \frac{f_{-m}}{(im)^\alpha} \right] ,$$

and replacing here f_m from (7.11), one obtains,

$$\sum_{\substack{m=-\infty \\ m\neq 0}}^{\infty} \frac{f_m}{(-im)^\alpha} = \frac{2}{\pi} \left\{ \zeta(1+\alpha)\sin(\alpha\pi/2) - \sum_{m=1}^{\infty} \frac{\sin[(\alpha-4mr)\pi/2]}{m^{1+\alpha}} \right\} . \tag{B.7}$$

Analogously,

$$\sum_{\substack{n=-\infty \\ n\neq 0}}^{\infty} \frac{|f_n|^2}{(-in)^\alpha} = \frac{4}{\pi^2}\cos(\alpha\pi/2) \left[\zeta(2+\alpha) - \sum_{n=1}^{\infty} \frac{\cos(nr2\pi)}{n^{2+\alpha}} \right] . \tag{B.8}$$

Replacing these sums into Eq. (B.6) and considering that $f_0 = 2r - 1$, we get,

$$\mathcal{L}\{\langle x^2(t)\rangle\} = \frac{2v_\alpha^2(2r-1)^2}{s^{2\alpha+1}} + \frac{2\kappa_\alpha}{s^{\alpha+1}}$$

$$+ \frac{4v_\alpha^2(2r-1)}{\pi\omega_0^\alpha s^{\alpha+1}} \left\{ \zeta(1+\alpha)\sin(\alpha\pi/2) - \sum_{m=1}^{\infty} \frac{\sin[(\alpha-4mr)\pi/2]}{m^{1+\alpha}} \right\}$$

$$+ \frac{8v_\alpha^2}{\pi^2\omega_0^\alpha s^{\alpha+1}} \cos(\alpha\pi/2) \left[\zeta(2+\alpha) - \sum_{n=1}^{\infty} \frac{\cos(nr2\pi)}{n^{2+\alpha}} \right] . \tag{B.9}$$

Taking here the inverse Laplace transform one obtains the expression for $\langle x^2(t)\rangle$ [Eq.(7.12)].

C   Calculation of $\langle x(t)\rangle^2$ for the anomalously slow transport under the influence of a rectangular driving force

Using Eq. (7.5), the quantity $\langle x(t)\rangle^2$ can be written in the following way,

$$\langle x(t)\rangle^2 = \frac{2v_\alpha^2}{\Gamma^2(\alpha)} \int_0^t dt' \int_0^{t'} \xi(t')\, t'^{\alpha-1}\, \xi(t'')\, t''^{\alpha-1}\, dt''. \tag{C.1}$$

Exploiting the property $\mathcal{L}\{\int_0^t f(t')\, dt'\} = s^{-1}\mathcal{L}\{f(t')\}$ and denoting $t' = t$, $t'' = t'$, we can write,

$$\mathcal{L}\ \{\langle x(t)\rangle^2\} = \frac{2v_\alpha^2}{\Gamma^2(\alpha)s}\, \mathcal{L}\left\{ \xi(t)\, t^{\alpha-1} \int_0^t \xi(t')\, t'^{\alpha-1}\, dt' \right\} \tag{C.2}$$

$$= \frac{2v_\alpha^2}{\Gamma^2(\alpha)s} \sum_{n=-\infty}^{\infty} f_n \sum_{m=-\infty}^{\infty} f_m\, \mathcal{L}_{s-in\omega_0}\left\{ t^{\alpha-1} \int_0^t \exp(im\omega_0 t')t'^{\alpha-1}dt' \right\}.$$

For $\alpha = 1$ the latter equation gives,

$$\mathcal{L}\{\langle x(t)\rangle^2\} = \frac{2v_\alpha^2}{s} \sum_{n=-\infty}^{\infty} \frac{f_n}{s - in\omega_0} \sum_{m=-\infty}^{\infty} \frac{f_m}{s - i\omega_0(n+m)}. \tag{C.3}$$

Comparing this result with Eq. (B.4) we see that $\mathcal{L}\{\langle \delta x^2(t)\rangle\} = 2\kappa_\alpha s^{-2}$, and thus $\langle \delta x^2(t)\rangle = 2\kappa_\alpha t$, as it should be for normal Brownian motion.

For $0 < \alpha < 1$ the integral $\int_0^t \exp(im\omega_0 t')\, t'^{\alpha-1}\, dt'$ in Eq. (C.2) diverges at $t = 0$. Let us divide this integral into two parts. Then

$$\int_0^t \exp(im\omega_0 t')\, t'^{\alpha-1}\, dt' = \int_0^{t_1} \exp(im\omega_0 t')\, t'^{\alpha-1}\, dt'$$

$$+ \int_{t_1}^t \exp(im\omega_0 t')\, t'^{\alpha-1}\, dt' = \chi_m(\tau) + \frac{\exp(im\omega_0 t)\, t^{\alpha-1}}{im\omega_0}$$

$$-\frac{\alpha-1}{im\omega_0} \int_{t_1}^t \exp(im\omega_0 t')\, t'^{\alpha-2}\, dt' \tag{C.4}$$

$(0 < t_1 < t)$, where

$$\chi_m(t_1) = t_1^\alpha \exp(im\omega_0 t_1)\left(\frac{1}{\alpha} - \frac{1}{im\omega_0 t_1} \right) - im\omega_0 \int_0^{t_1} \exp(im\omega_0 t')t'^\alpha dt'. \tag{C.5}$$

The integral $\int_0^{t_1} \exp(im\omega_0 t')\, t'^\alpha\, dt'$ does not diverge.

Let us separate in Eq. (C.2) the terms $m = 0$ and $n = 0$. In the long time limit, the contribution from $\int_{t_1}^{t} \exp(im\omega_0 t') t'^{\alpha-2} dt'$ is negligible and we can write,

$$\mathcal{L}\left\{\langle x(t)\rangle^2\right\} = \frac{v_\alpha^2 f_0^2}{s^{2\alpha+1}} \frac{\Gamma(2\alpha+1)}{\Gamma^2(\alpha+1)} + \frac{v_\alpha^2 f_0}{s} \frac{\Gamma(2\alpha+1)}{\Gamma^2(\alpha+1)} \sum_{\substack{n=-\infty \\ n\neq 0}}^{\infty} \frac{f_n}{(s-in\omega_0)^{2\alpha}}$$

$$+ \frac{2v_\alpha^2 f_0}{\Gamma(\alpha) s^{\alpha+1}} \sum_{\substack{m=-\infty \\ m\neq 0}}^{\infty} f_m \chi_m(t_1)$$

$$+ \frac{2v_\alpha^2 f_0}{s\omega_0} \frac{\Gamma(2\alpha-1)}{\Gamma^2(\alpha)} \sum_{\substack{m=-\infty \\ m\neq 0}}^{\infty} \frac{f_m}{im(s-im\omega_0)^{2\alpha-1}}$$

$$+ \frac{2v_\alpha^2}{\Gamma(\alpha)s} \sum_{\substack{n=-\infty \\ n\neq 0}}^{\infty} \frac{f_n}{(s-in\omega_0)^\alpha} \sum_{\substack{m=-\infty \\ m\neq 0}}^{\infty} f_m \chi_m(t_1)$$

$$+ \frac{2v_\alpha^2}{\omega_0 s} \frac{\Gamma(2\alpha-1)}{\Gamma^2(\alpha)} \sum_{\substack{n=-\infty \\ n\neq 0}}^{\infty} f_n \sum_{\substack{m=-\infty \\ m\neq 0}}^{\infty} \frac{f_m}{im[s-i\omega_0(n+m)]^{2\alpha-1}} . \qquad \text{(C.6)}$$

In the long time limit, i.e., in the limit $s \to 0$, in the double sum only terms with $m = -n$ contribute. The contribution from the last term in the latter equation is proportional to $1/s^{2\alpha}$, which for $\alpha < 1$ is always smaller than the one arising from $1/s^{\alpha+1}$. Thus, in the long time limit we can neglect all the other terms except the first and third in the last equation, and we obtain,

$$\mathcal{L}\{\langle x(t)\rangle^2\} = \frac{v_\alpha^2 (2r-1)^2}{s^{2\alpha+1}} \frac{\Gamma(2\alpha+1)}{\Gamma^2(\alpha+1)} + \frac{2v_\alpha^2(2r-1)}{\Gamma(\alpha)s^{\alpha+1}} \sum_{\substack{m=-\infty \\ m\neq 0}}^{\infty} f_m \chi_m(t_1) . \quad \text{(C.7)}$$

Taking here the inverse Laplace transform one obtains the expression for $\langle x(t)\rangle^2$ [Eq.(7.16)].

References

[1] A. Fick, Phil. Mag. 10 (1855) 30.

[2] A. Fick, Über Diffusion, Ann. Phys. 94 (1855) 59.

[3] A. Einstein, Über die von der molekularkinetischen Theorie der Wärme gefordete Bewegung von in ruhenden Flüssigkeiten suspendierten Teilchen, Ann. Phys. 17 (1905) 549.

[4] A. Einstein, Zur Theorie der Brownschen Bewegung, Ann. Phys. 19 (1906) 371.

[5] J. P. Bouchaud, A. Georges, Anomalous diffusion in disordered media: Statistical mechanisms, models and physical applications, Phys. Rep. 195 (1990) 127.

[6] R. Metzler, J. Klafter, The random walk's guide to anomalous diffusion: A fractional dynamics approach, Phys. Rep. 339 (2000) 1.

[7] P. Hänggi, F. Marchesoni, 100 years of Brownian motion, Chaos 15 (2005) 026101.

[8] P. Hänggi, A. Alvarez-Chillida, M. Morillo, New Horizons in Stochastic Complexity, Physica A 351.

[9] P. Hänggi, F. Marchesoni, Stochastic systems: from randomness to complexity, Physica A 325.

[10] J. A. Freund, L. Schimansky-Geier, Diffusion in discrete ratchets, Phys. Rev. E 60 (1999) 1304.

[11] P. Hänggi, P. Talkner, M. Borkovec, Reaction Rate Theory: Fifty Years After Kramers, Rev. Mod. Phys. 62 (1990) 251.

[12] P. Fulde, L. Pietronero, W. R. Schneider, S. Strassler, Problem of Brownian Motion in a Periodic Potential, Phys. Rev. Lett. 35 (1975) 1776.

[13] W. Dietrich, P. Fulde, I. Peschel, Adv. Phys. 29 (1980) 527.

[14] M. Mazroui, Y. Boughaleb, Interacting Brownian particles in a two dimensional periodic potential, Physica A 227 (1996) 93.

[15] B. Shapiro, I. Dynan, M. Gitterman, G. H. Weiss, Shapiro steps in the fluxon motion in superconductors, Phys. Rev. B 46 (1992) 8416.

[16] V. Ambegaokar, B. I. Halperin, Voltage Due to Thermal Noise in the dc Josephson Effect, Phys. Rev. Lett. 22 (1969) 1364.

[17] A. Barone, G. Paterno, Physics and Applications of the Josephson Effect, Wiley, New York, 1982.

[18] M. J. Rice, A. R. Bishop, J. A. Krumhansl, S. E. Trullinger, Weakly Pinned Fröhlich Charge-Density-Wave Condensates: A New, Nonlinear, Current-Carrying Elementary Excitation, Phys. Rev. Lett. 36 (1976) 432.

[19] J. W. M. Frenken, J. F. van der Veen, Observation of Surface Melting, Phys. Rev. Lett. 54 (1985) 134.

[20] B. Pluis, A. W. D. van der Gon, J. W. M. Frenken, J. F. van der Veen, Crystal-Face Dependence of Surface Melting, Phys. Rev. Lett. 59 (1987) 2678.

[21] D. C. Senft, G. Ehrlich, Long Jumps in Surface Diffusion: One-Dimensional Migration of Isolated Adatoms, Phys. Rev. Lett. 74 (1995) 294.

[22] T. R. Linderoth, S. Horch, E. Laegsgaard, I. Stensgaard, F. Besenbacher, Surface Diffusion of Pt on Pt(110): Arrhenius Behavior of Long Jumps, Phys. Rev. Lett. 78 (1997) 4978.

[23] P. Talkner, E. Hershkovitz, E. Pollak, P. Hänggi, Controlling activated surface diffusion by external fields, Surf. Sci. 437 (1999) 198.

[24] G. I. Nixon, G. W. Slater, Entropic trapping and electrophoretic drift of a polyelectrolyte down a channel with a periodically oscillating width, Phys. Rev. E 53 (1996) 4969.

[25] D. Reguera, J. M. Rubi, A. Pérez-Madrid, Controlling anomalous stresses in soft field-responsive systems, Phys. Rev. E 62 (2000) 5313.

[26] A. I. Burshtein, Y. Georgievskii, Energy activation of adiabatic and nonadiabatic electron transfer, J. Chem. Phys. 100 (1994) 7319.

[27] W. Schleich, C. S. Cha, J. D. Cresser, Quantum noise in a dithered-ring-laser gyroscope, Phys. Rev. A 29 (1984) 230.

[28] T. Katsouleas, J. M. Dawson, Unlimited Electron Acceleration in Laser-Driven Plasma Waves, Phys. Rev. Lett. 51 (1983) 392.

[29] K. Wiesenfeld, D. Pierson, E. Pantazelou, C. Dames, F. Moss, Stochastic resonance on a circle, Phys. Rev. Lett. 72 (1994) 2125.

[30] C. Kurrer, K. Schulten, Noise-induced synchronous neuronal oscillations, Phys. Rev. E 51 (1995) 6213.

[31] A. Taloni, F. Marchesoni, Single-file diffusion on a periodic substrate, Phys. Rev. Lett. 96 (2006) 020601.

[32] G. Coupier, M. S. Jean, C. Guthmann, Single file diffusion in macroscopic Wigner rings, Phys. Rev. E 73 (2006) 031112.

[33] F. Marchesoni, A. Taloni, Subdiffusion and Long-Time Anticorrelations in a Stochastic Single File, Phys. Rev. Lett. 97 (2006) 106101.

[34] S. Herrera-Velarde, R. C. neda Priego, Structure and dynamics of interacting Brownian particles in one-dimensional periodic substrates, J. Phys.: Condens. Matter 19 (2007) 226215.

[35] Y. Kafri, D. K. Lubensky, D. R. Nelson, Biophys. J. 86 (2004) 3373.

[36] J. P. Bouchaud, A. Comtet, A. Georges, P. L. Doussal, Classical diffusion of a particle in a one-dimensional random force field, Ann. Phys. (N.Y.) 201 (1990) 285.

[37] H. Scher, E. W. Montroll, Anomalous transit-time dispersion in amorphous solids, Phys. Rev. B 12 (1975) 2455.

[38] J. W. Haus, K. W. Kehr, Diffusion in regular and disordered lattices, Phys. Rep. 150 (1987) 263.

[39] B. Lindner, L. Schimansky-Geier, Noise-Induced Transport with Low Randomness, Phys. Rev. Lett. 89 (2002) 230602.

[40] R. Brown, A brief account of microscopical observations made in the months of June, July and August, 1827, on the particles contained in the pollen of plants; and on the general existence of active molecules in organic and inorganic bodies, Edinburgh new Philosophical Journal July-September (1828) 358–371.

[41] B. J. Ford, Brownian movement in clarkia pollen: A reprise of the first observations, The Microscope 40 (4) (1992) 235.

[42] J. M. Nye, Molecular Reality, Macdonald, London, 1972.

[43] G. Gouy, J. Physique 7 (1888) 561.

[44] G. Gouy, Rev. Gén. Sci. 6 (1895) 1.

[45] G. Gouy, C. R. Acad. Sci., Paris 109 (1889) 102.

[46] M. D. Haw, Colloidal suspensions, Brownian motion, molecular reality: a short history, J. Phys.: Condens. Matter 14 (2002) 7769.

35

[47] L. Bachelier, Théorie de la spéculation, Annales Scientifiques de l'École Normale Supérieure 3 (17) (1900) 21.

[48] P. H. C. (Ed.), MIT Press, Cambridge, 1964.

[49] L. Bachelier, M. Davis, A. Etheridge, Louis Bachelier's Theory of Speculation: The Origins of Modern Finance, Princeton University Press, Princeton, 2006.

[50] K. Pearson, The problem of the random walk, Nature 72 (1905) 294.

[51] L. Rayleigh, Nature 72 (1905) 318.

[52] K. Pearson, Nature 72 (1905) 342.

[53] A. Einstein, Investigations on the Theory of the Brownian Movement, Dover, New York, 1956.

[54] H. Risken, The Fokker-Planck Equation, Springer-Verlag, Berlin, 1996.

[55] H. A. Kramers, Brownian motion in a field of force and the diffusion model of chemical reactions, Physica 7 (1940) 284.

[56] J. E. Moyal, J. Roy. Stat. Soc. (London) B 11 (1949) 150.

[57] M. Smoluchowski, Zur kinetischen Theorie der Brownschen Molekularbewegung und der Suspensionen, Annalen der Physik 21 (1906) 756.

[58] P. Langevin, Comptes Rendus 146 (1908) 530.

[59] D. S. Lemons, A. Gythiel, Am. J. Phys. 65 (1997) 1079.

[60] W. T. Coffey, Y. P. Kalmykov, J. T. Waldron, The Langevin Equation, World Scientific, New Jersey, 2004.

[61] D. T. Gillespie, Fluctuation and dissipation in Brownian motion, Am. J. Phys. 61 (1993) 1077.

[62] B. G. de Grooth, A simple model for Brownian motion leading to the Langevin equation, Am. J. Phys. 67 (1999) 1248.

[63] C. W. Gardiner, Handbook of Stochastic Methods, Springer-Verlag, Berlin, 2002.

[64] N. G. van Kampen, Stochastic processes in physics and chemistry, North-Holland, Amsterdam, 1992.

[65] P. Reimann, Brownian motors: noisy transport far from equilibrium, Phys. Rep. 361 (2002) 57.

[66] J. B. Johnson, Thermal Agitation of Electricity in Conductors, Phys. Rev. 32 (1928) 97.

[67] I. Nyquist, Thermal Agitation of Electric Charge in Conductors, Phys. Rev. 32 (1928) 110.

[68] H. B. Callen, T. A. Welton, Irreversibility and Generalized Noise, Phys. Rev. 83 (1951) 34.

[69] P. Hänggi, H. Thomas, Stochastic Processes: Time-Evolution, Symmetries and Linear Response, Phys. Rep. 88 (1982) 207.

[70] J. Kula, M. Kostur, J. Łuczka, Brownian transport controlled by dichotomic and thermal fluctuations, Chem. Phys. 235 (1998) 27.

[71] R. Graham, A. Schenzle, Stabilization by multiplicative noise, Phys. Rev. A 26 (1982) 1676.

[72] R. F. Fox, M. H. Choi, Rectified Brownian motion and kinesin motion along microtubules, Phys. Rev. E 63 (2001) 051901.

[73] F. Jülicher, A. Ajdari, J. Prost, Modeling molecular motors, Rev. Mod. Phys. 69 (1997) 1269.

[74] N. Thomas, R. A. Thornhill, The physics of biological molecular motors, J. Phys. D 31 (1998) 253.

[75] S. Leibler, D. A. Huse, J. Cell Biol. 121 (1993) 1357.

[76] K. Svoboda, C. F. Schmidt, B. J. Schnapp, S. M. Block, Nature 365 (1993) 721.

[77] J. Łuczka, Ratchets, molecular motors, and noise-induced transport, Cell. Mol. Biol. Lett. 1 (1996) 311.

[78] R. D. Astumian, Thermodynamics and Kinetics of a Brownian Motor, Science 276 (1997) 917.

[79] N. G. van Kampen, Adv. Chem. Phys. 34 (1976) 245.

[80] A. D. Fokker, Ann. Physik 43 (1914) 810.

[81] M. Planck, Sitzber. Preuss. Akad. Wiss., 1917, p. 324.

[82] M. v. Smoluchowski, Ann. Physik 48 (1915) 1103.

[83] O. Klein, Arkiv for Mathematik, Astronomi, och Fysik 16 (1921) No 5.

[84] M. v. Smoluchowski, Physic. Zeitschr. 13 (1912) 1069.

[85] R. P. Feynman, R. B. Leighton, M. Sands, The Feynman Lectures on Physics, Addison Wesley, Reading, MA, 1963.

[86] J. M. R. Parrondo, P. Espanol, Criticism of Feynman's analysis of the ratchet as an engine, Am. J. Phys. 64 (1996) 1125.

[87] T. R. Kelly, I. Tellitu, J. P. Sestelo, Angew. Chem. Int. Ed. Engl. 36 (1997) 1866.

[88] T. R. Kelly, J. P. Sestelo, I. Tellitu, New Molecular Devices: In Search of a Molecular Ratchet, J. Org. Chem. 63 (1998) 3655.

[89] S. Lifson, J. L. Jackson, On the Self-Diffusion of Ions in a Polyelectrolyte Solution, J. Chem. Phys. 36 (1962) 2410.

[90] R. Ferrando, R. Spadacini, G. E. Tommei, Correlation functions in surface diffusion: the multiple-jump regime, Surf. Sci. 311 (1994) 411.

[91] R. Ferrando, R. Spadacini, G. E. Tommei, Diffusion in a periodic potential in the strong collision limit, Chem. Phys. Lett. 202 (1993) 248.

[92] R. L. Stratonovich, Radiotekh. Electron. (Moscow) 3 (1958) 497.

[93] P. I. Kuznetsov, R. L. Stratonovich, V. I. T. (Eds.), Pergamon, Oxford, 1965.

[94] R. Festa, E. G. d'Agliano, Diffusion coefficient for a Brownian particle in a periodic field of force : I. Large friction limit, Physica A 90 (1978) 229.

[95] D. L. Weaver, Effective diffusion coefficient of a Brownian particle in a periodic potential, Physica 98A (1979) 359.

[96] G. Arfken, Mathematical Methods for Physicsts, Academic Press, San Diego, 1985.

[97] P. Reimann, C. van den Broeck, H. Linke, P. Hänggi, J. M. Rubi, A. Pérez-Madrid, Giant Acceleration of Free Diffusion by Use of Tilted Periodic Potentials, Phys. Rev. Lett. 87 (2001) 010602.

[98] P. Reimann, C. van den Broeck, H. Linke, P. Hänggi, J. M. Rubi, A. Pérez-Madrid, Diffusion in tilted periodic potentials: Enhancement, universality, and scaling, Phys. Rev. E 65 (2002) 031104.

[99] B. Lindner, M. Kostur, L. Schimansky-Geier, Fluct. Nois Lett. 1 (2001) R25.

[100] D. R. Cox, Renewal Theory, Methuen & Co., London, 1962.

[101] M. Khantha, V. Balakrishnan, First passage time distributions for finite one-dimensional random walks, Pramana 21 (1983) 111.

[102] P. Reimann, C. V. den Broeck, Intermittent diffusion in the presence of noise, Physica D 75 (1994) 509.

[103] G. Costantini, F. Marchesoni, Threshold diffusion in a tilted washboard potential, Europhys. Lett. 48 (1999) 491.

[104] M. Borromeo, G. Costantini, F. Marchesoni, Critical Hysteresis in a Tilted Washboard Potential, Phys. Rev. Lett. 82 (1999) 2820.

[105] I. Kosztin, K. Schulten, Fluctuation-Driven Molecular Transport Through an Asymmetric Membrane Channel, Phys. Rev. Lett. 93 (2004) 238102.

[106] M. Kostur, J. Łuczka, Multiple current reversal in brownian ratchets, Phys. Rev. E 63 (2001) 021101.

[107] A. Asaklil, Y. Boughaleb, M. Mazroui, M. Chhib, L. E. Arroum, Diffusion of Brownian particles: dependence on the structure of the periodic potentials, Solid State Ionics 159 (2003) 331.

[108] A. Asaklil, M. Mazroui, Y. Boughaleb, Fokker-Planck dynamics in a bistable periodic potential, Eur. Phys. J. B 10 (1999) 91.

[109] F. Montalenti, R. Ferrando, Jumps and concerted moves in Cu, Ag, and Au(110) adatom self-diffusion, Phys. Rev. B 59 (1998) 5881.

[110] H. P. Weber, H. Schulz, J. Chem. Phys. 85 (1986) 475.

[111] G. Lattanzi, A. Maritan, Force dependent transition rates in chemical kinetics models for motor proteins, J. Chem. Phys. 117 (2002) 10339.

[112] M. Nishiyama, E. Muto, Y. Inoue, T. Yanagida, H. Higuchi, Nat. Cell Biol. 3 (2001) 425.

[113] M. Borromeo, F. Marchesoni, Backward-to-Forward Jump Rates on a Tilted Periodic Substrate, Phys. Rev. Lett. 84 (2000) 203.

[114] P. Hänggi, F. Marchesoni, F. Nori, Brownian motors, Ann. Phys. (Leipzig) 14 (2005) 51.

36

[115] R. D. Astumian, P. Hänggi, Brownian Motors, Phys. Today 55 (11) (2002) 33.

[116] L. Machura, M. Kostur, P. Talkner, J. Łuczka, F. Marchesoni, P. Hänggi, Brownian motors: Current fluctuations and rectification efficiency, Phys. Rev. E 70 (2004) 061105.

[117] D. Dan, A. M. Jayannavar, Giant diffusion and coherent transport in tilted periodic inhomogeneous systems, Phys. Rev. E 66 (2002) 041106.

[118] K. Svoboda, P. P. Mitra, S. M. Block, Proc. Natl. Acad. Sci. USA 91 (1994) 11782.

[119] M. J. Schnitzer, S. M. Block, Nature 388 (1997) 386.

[120] K. Visscher, M. J. Schnitzer, S. M. Block, Nature 400 (1999) 184.

[121] E. Heinsalu, T. Örd, R. Tammelo, Peculiarities of Brownian motion depending on the structure of the periodic potentials, Acta Physica Polonica B 36 (2005) 1613.

[122] M. Kostur, G. Knapczyk, J. Łuczka, Optimal transport and phase transition in dichotomic ratchets, Physica A 325 (2003) 69.

[123] M. Borromeo, F. Marchesoni, A.c.-driven jump distributions on a periodic substrate, Surf. Sci. 465 (2000) L771.

[124] A. G. Naumovets, Y. S. Vedula, Surface diffusion of adsorbates, Surf. Sci. Rep. 4 (1985) 365.

[125] R. Gomer, Diffusion of adsorbates on metal surfaces, Rep. Prog. Phys. 53 (1990) 917.

[126] M. Porto, M. Urbakh, J. Klafter, Atomic Scale Engines: Cars and Wheels, Phys. Rev. Lett. 84 (2000) 6058.

[127] S. C. Wang, G. Ehrlich, Structure, stability, and surface diffusion of clusters: Ir_x on Ir(111), Surf. Sci. 239 (1990) 301.

[128] G. Kellogg, Diffusion behavior of Pt adatoms and clusters on the Rh(100) surface, Appl. Surf. Sci. 67 (1993) 134.

[129] S. C. Wang, G. Ehrlich, Diffusion of Large Surface Clusters: Direct Observations on Ir(111), Phys. Rev. Lett. 79 (1997) 4234.

[130] S. C. Wang, U. Kürpick, G. Ehrlich, Surface Diffusion of Compact and Other Clusters: Ir_x on Ir(111), Phys. Rev. Lett. 81 (1998) 4923.

[131] A. F. Voter, Classically exact overlayer dynamics: Diffusion of rhodium clusters on Rh(100), Phys. Rev. B 34 (1986) 6819.

[132] C.-L. Liu, J. B. Adams, Structure and diffusion of clusters on Ni surfaces, Surf. Sci. 268 (1992) 73.

[133] C. Massobrio, P. Blandin, Structure and dynamics of Ag clusters on Pt(111), Phys. Rev. B 47 (1993) 13687.

[134] J. C. Hamilton, M. S. Daw, S. M. Foiles, Dislocation Mechanism for Island Diffusion on fcc (111) Surfaces, Phys. Rev. Lett. 74 (1995) 2760.

[135] S. V. Khare, N. C. Bartelt, T. L. Einstein, Diffusion of Monolayer Adatom and Vacancy Clusters: Langevin Analysis and Monte Carlo Simulations of their Brownian Motion, Phys. Rev. Lett. 75 (1995) 2148.

[136] D. S. Sholl, R. T. Skodje, Diffusion of Clusters of Atoms and Vacancies on Surfaces and the Dynamics of Diffusion-Driven Coarsening, Phys. Rev. Lett. 75 (1995) 3158.

[137] A. G. Naumovets, Z. Zhang, Fidgety particles on surfaces: how do they jump, walk, group, and settle in virgin areas?, Surf. Sci. 500 (2002) 414.

[138] T. Ala-Nissila, R. Ferrando, S. C. Ying, Adv. Phys. 51 (2002) 949.

[139] B. S. Swartzentruber, Direct Measurement of Surface Diffusion Using Atom-Tracking Scanning Tunneling Microscopy, Phys. Rev. Lett. 76 (1996) 459.

[140] W. Wulfhekel, B. J. Hattink, H. J. W. Zandvliet, G. Rosenfeld, B. Poelsema, Dynamics and Energetics of Si Ad-dimers and Ad-dimer Clusters on Ge(100), Phys. Rev. Lett. 79 (1997) 2494.

[141] H. J. W. Zandvliet, T. M. Galea, E. Zoethout, B. Poelsema, Diffusion Driven Concerted Motion of Surface Atoms: Ge on Ge(001), Phys. Rev. Lett. 84 (2000) 1523.

[142] S. Savel'ev, F. Marchesoni, F. Nori, Controlling Transport in Mixtures of Interacting Particles using Brownian Motors, Phys. Rev. Lett. 91 (2003) 010601.

[143] S. Savel'ev, F. Marchesoni, F. Nori, Manipulating Small Particles in Mixtures far from Equilibrium, Phys. Rev. Lett. 92 (2004) 160602.

[144] Q. H. Wei, C. Bechinger, P. Leiderer, Single-File Diffusion of Colloids in One-Dimensional Channels, Science 287 (2000) 625.

[145] C. Lutz, M. Kollmann, C. Bechinger, Single-File Diffusion of Colloids in One-Dimensional Channels, Phys. Rev. Lett. 93 (2004) 026001.

[146] R. Gommers, S. Bergamini, F. Renzoni, Dissipation-Induced Symmetry Breaking in a Driven Optical Lattice, Phys. Rev. Lett. 95 (2005) 073003.

[147] R. Gommers, S. Denisov, F. Renzoni, Quasiperiodically Driven Ratchets for Cold Atoms, Phys. Rev. Lett. 96 (2006) 240604.

[148] J. F. Wambaugh, C. Reichhardt, C. J. Olson, F. Marchesoni, F. Nori, Superconducting Fluxon Pumps and Lenses, Phys. Rev. Lett. 83 (1999) 5106.

[149] A. Tonomura, Applications of electron holography, Rev. Mod. Phys. 59 (1987) 639.

[150] D. A. Doyle, J. M. Cabral, R. A. Pfuetzner, A. Kuo, J. M. Gulbis, S. L. Cohen, B. T. Chait, R. MacKinnon, The Structure of the Potassium Channel: Molecular Basis of K^+ Conduction and Selectivity, Science 280 (1998) 69.

[151] B. A. *et al.*, Molecular Biology of the Cell, Garland, New York, 1994.

[152] J. Kärger, D. M. Ruthven, Diffusion in Zeolites and Other Microporous Solids, Wiley, New York, 1992.

[153] S. Matthias, F. Muller, Nature 424 (2003) 53.

[154] Z. Siwy, A. Fulinski, Fabrication of a Synthetic Nanopore Ion Pump, Phys. Rev. Lett. 89 (2002) 198103.

[155] C. Kettner, P. Reimann, P. Hänggi, F. Müller, Drift ratchet, Phys. Rev. E 61 (2000) 312.

[156] P. Reimann, P. Hänggi, Introduction to the Physics of Brownian Motors, Appl. Phys. A 75 (2002) 169.

[157] J. L. Mateos, Current reversals in deterministic ratchets: points and dimers, Physica D 168-169 (2002) 205.

[158] J. L. Mateos, Walking on ratchets with two Brownian motors, Fluct. Noise Lett. 4 (2004) L161.

[159] J. L. Mateos, A random walker on a ratchet, Physica A 351 (2005) 79.

[160] M. Patriarca, P. Szelestey, E. Heinsalu, Brownian model of dissociated dislocations, Acta Phys. Pol. B 36 (2005) 1745.

[161] G. Schoeck, W. Püschl, Mat. Sci. Eng. A 189 (1994) 61.

[162] G. Schoeck, Scripta Metal. Mat. 30 (1994) 611.

[163] P. E. Kloeden, E. Platen, Numerical Solution of Stochastic Differential Equations, Springer, Berlin, 1999.

[164] M. S. Miguel, R. Toral, Stochastic effects in physical systems, in: E. Titapegui, W. Zelle (Eds.), Instabilities and nonequilibrium structures VI, Kluewer, 1997.

[165] W. H. Press, B. P. Flannery, S. A. Teulolsky, W. Vetterling, Numerical Recipes in C: The Art of Scientific Computing, Cambridge University Press, Cambridge, 2 edition, 1992.

[166] O. M. Braun, Role of entropy barriers for diffusion in the periodic potential, Phys. Rev. E 63 (2000) 011102.

[167] C. Fusco, A. Fasolino, Microscopic mechanisms of thermal and driven diffusion of non rigid molecules on surfaces, Thin Solid Films 428 (2003) 34.

[168] O. M. Braun, Adiabatic motion of an atomic chain in periodic potential, Surf. Sci. 230 (1990) 262.

[169] O. M. Braun, R. Ferrando, G. E. Tommei, Stimulated diffusion of an adsorbed dimer, Phys. Rev. E 68 (2003) 051101.

[170] T. Strunz, F.-J. Elmer, Driven Frenkel-Kontorova model. I. Uniform sliding states and dynamical domains of different particle densities, Phys. Rev. E 58 (1998) 1601.

[171] C. Cattuto, F. Marchesoni, Unlocking of an Elastic String from a Periodic Substrate, Phys. Rev. Lett. 79 (1997) 5070.

[172] D. Ertas, Lateral Separation of Macromolecules and Polyelectrolytes in Microlithographic Arrays, Phys. Rev. Lett. 80 (1998) 1548.

[173] A. Oudenaarden, S. G. Boxer, Brownian Ratchets: Molecular Separations in Lipid Bilayers Supported on Patterned Arrays, Science 285 (1999) 1046.

[174] L. R. Huang, P. Silberzan, J. O. Tegenfeldt, E. C. Cox, J. C. Sturm, R. H. Austin, H. Craighead, Role of Molecular Size in Ratchet Fractionation, Phys. Rev. Lett. 89 (2002) 178301.

[175] M. Berger, J. Castelino, R. Huang, M. Shah, R. H. Austin, Design of a microfabricated magnetic cell separator, Electrophoresis 22 (2001) 3883.

[176] S. Savelev, V. Misko, F. Marchesoni, F. Nori, Separating particles according to their physical properties: Transverse drift of underdamped and overdamped interacting particles diffusing through two-dimensional ratchets, Phys. Rev. B 71 (2005) 214303.

[177] L. F. Richardson, Proc. Roy. Soc. 110 (1926) 709.

[178] H. Scher, E. W. Montroll, Anomalous transit-time dispersion in amorphous solids, Phys. Rev. B 12 (1975) 2455.

[179] R. Metzler, J. Klafter, The restaurant at the end of the random walk: recent developments in the description of anomalous transport by fractional dynamics, J. Phys. A: Math. Gen 37 (2004) R161.

[180] I. M. Sokolov, J. Klafter, A. Blumen, Fractional kinetics, Phys. Today 55 (11) (2002) 48.

[181] H. Yang, G. Luo, P. Karnchanaphanurach, T.-M. Louie, I. Rech, S. Cova, L. Xun, X. S. Xie, Protein Conformational Dynamics Probed by Single-Molecule Electron Transfer, Science 302 (2003) 262.

[182] S. C. Kou, X. S. Xie, Generalized Langevin Equation with Fractional Gaussian Noise: Subdiffusion within a Single Protein Molecule, Phys. Rev. Lett. 93 (2004) 180603.

[183] E. W. Montroll, G. H. Weiss, Random walks on lattices. II, J. Math. Phys. 6 (1965) 167.

[184] G. H. Weiss, Aspects and Applications of the Random Walk, North-Holland, Amsterdam, 1994.

[185] H. Scher, M. Lax, Stochastic transport in a disordered solid. I. Theory, Phys. Rev. B 7 (1973) 4491.

[186] I. M. Sokolov, R. Metzler, Towards deterministic equations for Lévy walks: The fractional material derivative, Phys. Rev. E 67 (2003) 010101.

[187] R. Gorenflo, F. Mainardi, in: A. Carpinteri, F. Mainardi (Eds.), Fractals and Fractional Calculus in Continuum Mechanics, Springer, Wien, 1997, pp. 223–276.

[188] R. Hilfer, L. Anton, Fractional master equations and fractal time random walks, Phys. Rev. E 51 (1995) R848.

[189] R. Metzler, E. Barkai, J. Klafter, Anomalous Diffusion and Relaxation Close to Thermal Equilibrium: A Fractional Fokker-Planck Equation Approach, Phys. Rev. Lett. 82 (1999) 3563.

[190] E. Barkai, Fractional Fokker-Planck equation, solution, and application, Phys. Rev. E 63 (2001) 046118.

[191] T. J. Kozubowski, S. T. Rachev, Univariate Geometric Stable Laws, J. Comput. Anal. Appl. 1 (1999) 177.

[192] A. G. Pakes, Mixture representations for symmetric generalized Linnik laws, Statist. Probab. Lett. 37 (1998) 213.

[193] T. J. Kozubowski, Mixture representation of Linnik distribution revisited, Statist. Probab. Lett. 38 (1998) 157.

[194] T. J. Kozubowski, J. Comput. Appl. Math. 116 (2000) 221.

[195] T. J. Kozubowski, Fractional moment estimation of linnik and mittag-leffler parameters, Math. Comput. Model. 34 (2001) 1023.

[196] K. Jayakumar, Mittag-leffler process, Math. Comput. Model. 37 (2003) 1427.

[197] G. Bel, E. Barkai, Weak Ergodicity Breaking in the Continuous-Time Random Walk, Phys. Rev. Lett. 94 (2005) 240602.

[198] F. Mainardi, A. Vivoli, R. Gorenflo, Fluct. Noise Lett. 5 (2005) L291.

[199] E. Heinsalu, M. Patriarca, I. Goychuk, G. Schmid, P. Hänggi, Fractional Fokker-Planck dynamics: Numerical algorithm and simulations, Phys. Rev. E 73 (2006) 046133.

[200] B. Derrida, Velocity and diffusion constant of a periodic one-dimensional hopping model, J. Stat. Phys. 31 (1983) 433.

[201] I. M. Sokolov, J. Klafter, From diffusion to anomalous diffusion: A century after Einstein's Brownian motion, Chaos 15 (2005) 026103.

[202] R. Metzler, J. Klafter, I. M. Sokolov, Anomalous transport in external fields: Continuous time random walks and fractional diffusion equations extended, Phys. Rev. E 58 (1998) 1621.

[203] E. Barkai, V. N. Fleurov, Generalized Einstein relation: A stochastic modeling approach, Phys. Rev. E 58 (1998) 1296.

[204] M. Shlesinger, Asymptotic solutions of continuous-time random walks, J. Stat. Phys. 10 (1974) 421.

[205] I. Goychuk, E. Heinsalu, M. Patriarca, G. Schmid, P. Hänggi, Current and universal scaling in anomalous transport, Phys. Rev. E. 73 (2006) 020101(R).

[206] E. Heinsalu, M. Patriarca, I. Goychuk, P. Hänggi, Fractional diffusion in periodic potentials, J. Phys.: Condens. Matter 19 (2007) 065114.

[207] B. B. Mandelbrot, J. W. V. Ness, SIAM Rev. 10 (1968) 422.

[208] W. Dieterich, P. Fulde, I. Peschel, Theoretical models for superionic conductors, Adv. Physics 29 (1980) 527.

[209] R. L. Kautz, Noise, chaos and the Josephson voltage standard, Rep. Progr. Phys. 59 (1996) 935.

[210] M. Borromeo, F. Marchesoni, Noise-assisted transport on symmetric periodic substrates, Chaos 15 (2005) 026110.

[211] L. Gammaitoni, P. Hänggi, P. Jung, F. Marchesoni, Stochastic resonance, Rev. Mod. Phys. 70 (1998) 223.

[212] I. M. Sokolov, A. Blumen, J. Klafter, Dynamics of annealed systems under external fields: CTRW and the fractional Fokker-Planck equations, Europhys. Lett. 56 (2001) 175.

[213] I. M. Sokolov, A. Blumen, J. Klafter, Linear response in complex systems: CTRW and the fractional Fokker-Planck equations, Physica A 302 (2001) 268.

[214] F. Barbi, M. Bologna, P. Grigolini, Linear Response to Perturbation of Nonexponential Renewal Processes, Phys. Rev. Lett. 95 (2005) 220601.

[215] I. M. Sokolov, Linear response to perturbation of nonexponential renewal process: A generalized master equation approach, Phys. Rev. E 73 (2006) 067102.

[216] I. M. Sokolov, J. Klafter, Field-Induced Dispersion in Subdiffusion, Phys. Rev. Lett. 97 (2006) 140602.

[217] I. Goychuk, P. Hänggi, Theory of non-Markovian stochastic resonance, Phys. Rev. E 69 (2004) 021104.

[218] I. Goychuk, P. Hänggi, Non-Markovian Stochastic Resonance, Phys. Rev. Lett. 91 (2003) 070601.

[219] H. Mori, Progr. Theor. Phys. 33 (1965) 423.

[220] R. Kubo, Rep. Progr. Phys. 29 (1966) 255.

Attached original publications

E. Heinsalu, R. Tammelo, T. Örd,
Diffusion and current of Brownian particles in tilted piecewise linear potentials:
Amplification and coherence, Phys. Rev. E **69**, 021111 (2004).

II

E. Heinsalu, R. Tammelo, T. Örd,
Correlation between diffusion and coherence in the Brownian motion on tilted periodic potential, Physica A **340**, 292 (2004).

III

E. Heinsalu, T. Örd, R. Tammelo,
Diffusion and coherence in tilted piecewise linear double-periodic potentials,
Phys. Rev. E **70**, 041104 (2004).

IV

E. Heinsalu, T. Örd, R. Tammelo,
*Peculiarities of Brownian motion depending on the structure of the
periodic potentials*, Acta Physica Polonica B **36**, 1613 (2005).

V

M. Patriarca, P. Szelestey, E. Heinsalu,
Brownian model of dissociated dislocations,
Acta Physica Polonica B **36**, 1745 (2005).

VI

VII

I. Goychuk, E. Heinsalu, M. Patriarca, G. Schmid, P. Hänggi,
Current and universal scaling in anomalous transport,
Phys. Rev. E **73**, 020101(R) (2006).

VIII

E. Heinsalu, M. Patriarca, I. Goychuk, G. Schmid, P. Hänggi,
Fractional Fokker-Planck dynamics: Numerical algorithm and simulations,
Phys. Rev. E **73**, 046133 (2006).

X

E. Heinsalu, M. Patriarca, I. Goychuk, P. Hänggi,
Use and Abuse of a Fractional Fokker-Planck Dynamics for Time-Dependent Driving, Phys. Rev. Lett. **99**, 120602 (2007).

XI

CURRICULUM VITAE

Name:	Els Heinsalu
Date and place of birth:	13.04.1980, Rakvere
Nationality:	Estonian
Contact-address:	National Institute of Chemical Physics and Biophysics, Rävala 10, 12618 Tallinn, Estonia
Phone:	+372 5159037
E-mail:	els@kbfi.ee

Education:

- 2004 University of Tartu, M. Sc. in theoretical physics

- 2002 University of Tartu, B. Sc. in physics

- 1998 Gymnasium Rakvere

Present occupation:

- National Institute of Chemical Physics and Biophysics, researcher

- Tartu University, Doctoral school of material science and material technology, extraordinary researcher

Professional employment:

- National Institute of Chemical Physics and Biophysics, researcher, since September 2007

- University of Tartu, Doctoral school of material science and material technology, extraordinary researcher, October 2005 - June 2008

- University of Tartu, Institute of (Theoretical) Physics, PhD student, September 2004 - June 2008

- University of Tartu, Institute of Theoretical Physics, extraordiary researcher, September 2004 - August 2007

261

- Philipps-University Marburg, Department of Chemistry, Computer Simulation Group, PhD student, scientific coworker, September 2004 - April 2005

Visited institutions:

- University of Perugia, Department of Physics, March-April 2008

- University of Camerino, Department of Physics, January-July 2007

- UNAM, Centro de Investigacion en Energia, Temixco, January 2007

- University of Augsburg, Institute of Theoretical Physics, June 2005 - June 2006

- University of Augsburg, Institute of Theoretical Physics, January-March 2005

- Polytechnic of Turin, Department of Mathematics, November 2004

- CERN, Compact Muon Solenoid experiment, June-August 2004

- Helsinki University of Technology, Laboratory of Computational Engineering, February, June 2004

Research interests:

- diffusion processes

- statistical physics and its applications to complex systems

Teaching experience:

- Diffusion processes: Models and applications (FKTF.00.007), 2 AP (3 ECTS), University of Tartu, 2007/2008 fall

Current grants and projects:

- "Modern methods of statistical physics: applications to diffusion processes in complex systems", Estonian Science Foundation grant No 7466 (2008-2011)

- "Noise-induced phenomena in non-homogeneous and anisotropic media", Estonian Science Foundation grant No 6789 (2006-2009)

- "Stochastic processes in nonequilibrium physical systems", Target Financed Project No 0182647s04 (2004-2008) of the Ministry of Education and Research of Estonia

Past grant funding:

- Archimedes Foundation, Kristjan Jaak Scholarships, grant to visit the group of Prof F. Marchesoni at the University of Camerino (2006)

- European Science Foundation, StochDyn Project, Exchange Grant to visit the group of Prof F. Marchesoni at the University of Camerino (2006)

- Archimedes Foundation, Kristjan Jaak Scholarships, grant to visit the group of Prof P. Hänggi at the University of Augsburg (2005)

- "Dynamics of generalized Brownian particles in quasiperiodic nonlinear media", Estonian Science Foundation Grant No 5662 (2003-2005)

- European Science Foundation, StochDyn Project, Exchange Grant to visit the group of Prof P. Hänggi at the University of Augsburg (2004)

Honours and awards:

- The Estonian national contest for student research papers, 1-st award in doctoral level, Natural sciences and engineering (2006)

- Prize of the University of Mynster (2005)

- The student prize of Estonian Physical Society (2004)

- The 2-nd award of the Estonian Academy of Science for student research papers (2004)

- Margot M. and Herbert R. Linna scholarship, Estonian World Council (2003)

- The 2-nd award of the Estonian Academy of Science for student research papers (2002)

- Prize of the University of Mynster (2002)

- Scholarship of Fund Rotalia (2001)

- Scholarship of Gymnasium Rakvere (1998)

ELULUGU

Nimi:	Els Heinsalu
Sünni aeg ja koht:	13.04.1980, Rakvere
Kodakondsus:	eesti
Kontaktaadress:	Keemilise ja Biloogilise Füüsika Instituut, Rävala 10, 12618 Tallinn
Telefon:	+372 51 59037
E-mail:	els@kbfi.ee

Haridus:

- 2004 Tartu Ülikool, M. Sc. teoreetilises füüsikas
- 2002 Tartu Ülikool, B. Sc. füüsikas
- 1998 Rakvere Gümnaasium

Praegune töökoht:

- Keemilise ja Biloogilise Füüsika Instituut, teadur
- Tartu Ülikool, Materjaliteaduse ja materjalide tehnoloogia doktorikool, erakorraline teadur

Teenistuskäik:

- Keemilise ja Biloogilise Füüsika Instituut, alates september 2007, teadur
- Tartu Ülikool, Materjaliteaduse ja materjalide tehnoloogia doktorikool, oktoober 2005 - juuni 2008, erakorraline teadur
- Tartu Ülikool, (teoreetilise) füüsika instituut, september 2004 - juuni 2008, doktorant
- Tartu Ülikool, teoreetilise füüsika instituut, september 2004 - august 2007, erakorraline teadur
- Philipps-Ülikool Marburg, füüsikalise keemia instituut, arvutisimulatsioonide töögrupp, september 2004 - aprill 2005, doktorant, teaduslik kaastööline

Külastatud teadusasutused:

- Perugia Ülikool, füüsika teaduskond, märts-aprill 2008

- Camerino Ülikool, füüsika teaduskond, jaanuar-juuli 2007

- UNAM, Centro de Investigacion en Energia, Temixco, jaanuar 2007

- Augsburgi Ülikool, teoreetilise füüsika instituut, juuni 2005 - juuni 2006

- Augsburgi Ülikool, teoreetilise füüsika instituut, jaanuar-märts 2005

- Torino Polütehnikum, matemaatika teaduskond, november 2004

- CERN, Compact Muon Solenoid eksperiment, juuni-august 2004

- Helsingi Tehnikaülikool, numbrilise modelleerimise laboratoorium, veebruar, juuni 2004

Teadustöö põhisuunad:

- difusiooni protsessid

- statistiline füüsika ning selle rakendused koplekssüsteemidele

Õppetöö kogemus:

- Difusiooni protsessid: mudelid ja rakendused (FKTF.00.007), 2 AP (3 ECTS), Tartu Ülikool, 2007/2008 sügissemester

Jooksvad projektid:

- "Statistilise füüsika kaasasegsed meetodid: rakendused difusiooni protsessidele komplekssüsteemides", Eesti Teadusfondi grant nr 7466 (2008-2011)

- "Müra poolt indutseeritud nähtused mittehomogeensetes ja anisotroopsetes keskkondades", Eesti Teadusfondi grant nr 6789 (2006-2009)

- "Stohhastilised protsessid mittetasakaalulistes füüsikalistes süsteemides", Eesti Haridus- ja Teadusministeeriumi sihtfinatseeritav teema nr 0182647s04 (2004-2008)

Lõppenud projektid:

- Euroopa Teadusfond, StochDyn Project, Exchange Grant külastamaks prof F. Marchesoni töögruppi Camerino Ülikoolis (2006)

- Sihtasutus Archimedes, Kristjan Jaak Stipendiumid, stipendium õppening teadustööks Camerino Ülikoolis, prof F. Marchesoni uurimisgrupis (2006)

- Sihtasutus Archimedes, Kristjan Jaak Stipendiumid, stipendium õppening teadustööks Augsburgi Ülikoolis, prof P. Hänggi uurimisgrupis (2005)

- "Üldistatud Browni osakeste dünaamika kvaasiperioodilises mittelineaarses keskkonnas", Eesti Teadusfondi grant nr 5662 (2003-2005)

- Euroopa Teadusfond, StochDyn Project, Exchange Grant külastamaks prof P. Hänggi töögruppi Augsburgi Ülikoolis (2004)

Auhinnad ja stipendiumid:

- I preemia doktoriõppe üliõpilaste astmes, loodusteaduste ja teh-nika valdkond, Eesti üliõpilaste teadustööde riiklik konkurss 2006

- Münsteri Ülikooli uurimisstipendium 2005

- Eesti Füüsika Seltsi üliõpilaspreemia 2004

- II auhind, Eesti Teaduste Akadeemia üliõpilastööde konkurss 2004

- Margot M. ja Herbert R. Linna stipendium, Ülemaailmne Eesti Kesknõukogu, 2003

- II auhind, Eesti Teaduste Akadeemia üliõpilastööde konkurss 2002

- Münsteri Ülikooli auhind 2002

- Rotalia Fondi stipendium 2001

- Rakvere Gümnaasiumi stipendium 1998

DISSERTATIONES PHYSICAE
UNIVERSITATIS TARTUENSIS

1. **Andrus Ausmees.** XUV-induced electron emission and electron-phonon interaction in alkali halides. Tartu, 1991.
2. **Heiki Sõnajalg.** Shaping and recalling of light pulses by optical elements based on spectral hole burning. Tartu, 1991.
3. **Sergei Savihhin.** Ultrafast dynamics of F-centers and bound excitons from picosecond spectroscopy data. Tartu, 1991.
4. **Ergo Nõmmiste.** Leelishalogeniidide röntgenelektronemissioon kiiritamisel footonitega energiaga 70–140 eV. Tartu, 1991.
5. **Margus Rätsep.** Spectral gratings and their relaxation in some low-temperature impurity-doped glasses and chrystals. Tartu, 1991.
6. **Tõnu Pullerits.** Primary energy transfer in photosynthesis. Model calculations. Tartu, 1991.
7. **Olev Saks.** Attoampri diapasoonis voolude mõõtmise füüsikalised alused. Tartu, 1991.
8. **Andres Virro.** AlGaAsSb/GaSb heterostructure injection lasers. Tartu, 1991.
9. **Hans Korge.** Investigation of negative point discharge in pure nitrogen at atmospheric pressure. Tartu, 1992.
10. **Jüri Maksimov.** Nonlinear generation of laser VUV radiation for high-resolution spectroscopy. Tartu, 1992.
11. **Mark Aizengendler.** Photostimulated transformation of aggregate defects and spectral hole burning in a neutron-irradiated sapphire. Tartu, 1992.
12. **Hele Siimon.** Atomic layer molecular beam epitaxy of A^2B^6 compounds described on the basis of kinetic equations model. Tartu, 1992.
13. **Tõnu Reinot.** The kinetics of polariton luminescence, energy transfer and relaxation in anthracene. Tartu, 1992.
14. **Toomas Rõõm.** Paramagnetic H^{2-} and F^+ centers in CaO crystals: spectra, relaxation and recombination luminescence. Tallinn, 1993.
15. **Erko Jalviste.** Laser spectroscopy of some jet-cooled organic molecules. Tartu, 1993.
16. **Alvo Aabloo.** Studies of crystalline celluloses using potential energy calculations. Tartu, 1994.
17. **Peeter Paris.** Initiation of corona pulses. Tartu, 1994.
18. **Павел Рубин.** Локальные дефектные состояния в CuO_2 плоскостях высокотемпературных сверхпроводников. Тарту, 1994.
19. **Olavi Ollikainen.** Applications of persistent spectral hole burning in ultra-fast optical neural networks, time-resolved spectroscopy and holographic interferometry. Tartu, 1996.
20. **Ülo Mets.** Methodological aspects of fluorescence correlation spectroscopy. Tartu, 1996.

21. **Mikhail Danilkin.** Interaction of intrinsic and impurity defects in CaS:Eu luminophors. Tartu, 1997.
22. **Ирина Кудрявцева.** Создание и стабилизация дефектов в кристаллах KBr, KCl, RbCl при облучении ВУФ-радиацией. Тарту, 1997.
23. **Andres Osvet.** Photochromic properties of radiation-induced defects in diamond. Tartu, 1998.
24. **Jüri Örd.** Classical and quantum aspects of geodesic multiplication. Tartu, 1998.
25. **Priit Sarv.** High resolution solid-state NMR studies of zeolites. Tartu, 1998.
26. **Сергей Долгов.** Электронные возбуждения и дефектообразование в некоторых оксидах металлов. Тарту, 1998.
27. **Kaupo Kukli.** Atomic layer deposition of artificially structured dielectric materials. Tartu, 1999.
28. **Ivo Heinmaa.** Nuclear resonance studies of local structure in $RBa_2Cu_3O_{6+x}$ compounds. Tartu, 1999.
29. **Aleksander Shelkan.** Hole states in CuO_2 planes of high temperature superconducting materials. Tartu, 1999.
30. **Dmitri Nevedrov.** Nonlinear effects in quantum lattices. Tartu, 1999.
31. **Rein Ruus.** Collapse of 3d (4f) orbitals in 2p (3d) excited configurations and its effect on the x-ray and electron spectra. Tartu, 1999.
32. **Valter Zazubovich.** Local relaxation in incommensurate and glassy solids studied by Spectral Hole Burning. Tartu, 1999.
33. **Indrek Reimand.** Picosecond dynamics of optical excitations in GaAs and other excitonic systems. Tartu, 2000.
34. **Vladimir Babin.** Spectroscopy of exciton states in some halide macro- and nanocrystals. Tartu, 2001.
35. **Toomas Plank.** Positive corona at combined DC and AC voltage. Tartu, 2001.
36. **Kristjan Leiger.** Pressure-induced effects in inhomogeneous spectra of doped solids. Tartu, 2002.
37. **Helle Kaasik.** Nonperturbative theory of multiphonon vibrational relaxation and nonradiative transitions. Tartu, 2002.
38. **Tõnu Laas.** Propagation of waves in curved spacetimes. Tartu, 2002.
39. **Rünno Lõhmus.** Application of novel hybrid methods in SPM studies of nanostructural materials. Tartu, 2002.
40. **Kaido Reivelt.** Optical implementation of propagation-invariant pulsed free-space wave fields. Tartu, 2003.
41. **Heiki Kasemägi.** The effect of nanoparticle additives on lithium-ion mobility in a polymer electrolyte. Tartu, 2003.
42. **Villu Repän.** Low current mode of negative corona. Tartu, 2004.
43. **Алексей Котлов.** Оксианионные диэлектрические кристаллы: зонная структура и электронные возбуждения. Tartu, 2004.

44. **Jaak Talts.** Continuous non-invasive blood pressure measurement: comparative and methodological studies of the differential servo-oscillometric method. Tartu, 2004.
45. **Margus Saal.** Studies of pre-big bang and braneworld cosmology. Tartu, 2004.
46. **Eduard Gerškevitš.** Dose to bone marrow and leukaemia risk in external beam radiotherapy of prostate cancer. Tartu, 2005.
47. **Sergey Shchemelyov.** Sum-frequency generation and multiphoton ionization in xenon under excitation by conical laser beams. Tartu, 2006.
48. **Valter Kiisk.** Optical investigation of metal-oxide thin films. Tartu, 2006.
49. **Jaan Aarik.** Atomic layer deposition of titanium, zirconium and hafnium dioxides: growth mechanisms and properties of thin films. Tartu, 2007.
50. **Astrid Rekker.** Colored-noise-controlled anomalous transport and phase transitions in complex systems. Tartu, 2007.
51. **Andres Punning.** Electromechanical characterization of ionic polymer-metal composite sensing actuators. Tartu, 2007.
52. **Indrek Jõgi.** Conduction mechanisms in thin atomic layer deposited films containing TiO_2. Tartu, 2007.
53. **Aleksei Krasnikov.** Luminescence and defects creation processes in lead tungstate crystals. Tartu, 2007.
54. **Küllike Rägo.** Superconducting properties of MgB_2 in a scenario with intra- and interband pairing channels. Tartu, 2008.